PROCESSING AND CHARACTERIZATION OF MECHANICALLY ALLOYED NiAl-BASED ALLOYS

July 1994

Final Report

By: Dr. Marek Dollar — Principal Investigator
Dr. Phil Nash — Co-principal Investigator
Dr. Stanislaw Dymek — Research Associate
Dr. Seung-Joon Hwang — Research Assistant
Dr. Sung-Jae Suh — Research Assistant

Metallurgical and Materials Engineering Department
Illinois Institute of Technology
IIT Center
Chicago, IL.60616
phone # (312) 567 3032
FAX # (312) 567 8875

Prepared for:

DEPARTMENT OF THE AIR FORCE
AIR FORCE OFFICE OF SCIENTIFIC RESEARCH
BOLLING AIR FORCE BASE, DC 20332 - 6448

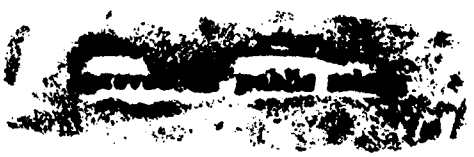

REPORT DOCUMENTATION PAGE

Dist: A

Form Approved
OMB No. 0704-0188

1. AGENCY USE ONLY (Leave blank)	2. REPORT DATE	3. REPORT TYPE AND DATES COVERED
	July 20, 1994	Final Report, 2/15/90-6/30/94

4. TITLE AND SUBTITLE

Processing and Characterization of Mechanically Alloyed NiAl-Based Alloys

5. FUNDING NUMBERS

Grant AFOSR-90-0152B

6. AUTHOR(S)

Dr. Marek Dollar — Principle Investigator
Dr. Philip Nash — Co-Principle Investigator
Dr. Stanislaw Dymek — Research Associate
Dr. Seung-Joon Hwang — Research Assistant
Dr. Sung-Jae Suh — Research Assistant

7. PERFORMING ORGANIZATION NAME(S) AND ADDRESS(ES)

Metallurgical and Materials Engineering Department
Illinois Institute of Technology
IIT Center
Chicago, IL 60616

8. PERFORMING ORGANIZATION REPORT NUMBER

5-54718-1

AFOSR-TR- 94 0545

9. SPONSORING/MONITORING AGENCY NAME(S) AND ADDRESS(ES)

Department of the Air Force
Air Force Office of Scientific Research
Bolling Air Force Base, DC 20332-6448

10. SPONSORING/MONITORING AGENCY REPORT NUMBER

11. SUPPLEMENTARY NOTES

12a. DISTRIBUTION/AVAILABILITY STATEMENT

Unlimited

A

12b. DISTRIBUTION CODE

13. ABSTRACT *(Maximum 200 words)*

Mechanical alloying of powders followed by hot extrusion has been used to produce NiAl-based materials. The technique is capable of producing fully dense, free of cracks, fine grained materials containing a bimodal distribution of aluminum oxide dispersoids. The mechanically alloyed materials produced in our laboratory are much stronger at both ambient and elevated temperatures and significantly more ductile than their cast counterparts. Minimum creep rates in the MA NiAl are on average three orders of magnitude lower than that in their cast counterparts. The creep resistance of the MA NiAl is better than that of solid solution- and other dispersion-strengthened NiAl and comparable to the creep resistance of precipitation-strengthened NiAl. Improved mechanical properties of the present materials result from their unique microstructure.

14. SUBJECT TERMS

Mechanical Alloying, NiAl-Aluminides, Intermetallics
Strength, Ductility and Creep in NiAl

15. NUMBER OF PAGES

16. PRICE CODE

17. SECURITY CLASSIFICATION OF REPORT	18. SECURITY CLASSIFICATION OF THIS PAGE	19. SECURITY CLASSIFICATION OF ABSTRACT	20. LIMITATION OF ABSTRACT
			Unlimited

CONTENTS

I. INTRODUCTION

The present report constitutes the final report summarizing the results of our studies on microstructure, plastic deformation and mechanical properties of mechanically alloyed NiAl and NiAl-based alloys. The research work, supported by AFOSR Grant # 90 - 0152 B, was initiated on February 15, 1990 and concluded on June 30, 1994.

In the following sections an attempt is made to highlight our approach to processing and characterization of NiAl and to outline the most important results and their discussion. The detailed results of our studies were presented in three previous reports, submitted to AFOSR in, respectively, April 1991, March 1992 and July 1993.

Based on the results of our studies, we published a series of papers, the list of which appears in Appendix I. The copies of the refereed archival publications appear in Appendix II.

During the duration of the program, we have graduated two Ph.D. and one M.S. students. The title pages of their theses are presented in Appendix III. A post-doctoral research associate, S. Dymek, was also part of the research team.

The focus of the reported research has been on NiAl. This intermetallic compound is a possible high temperature structural material, either in monolithic form or as a matrix phase in a composite, because of its low density, high melting temperature, good thermal conductivity and excellent oxidation resistance [1]. However, before this material can be of practical use a number of technical problems must be overcome including lack of ductility at room temperature and poor strength at high temperatures.

Several attempts to resolve the problem of room temperature brittleness through modification of slip systems [2,3], grain refinement [4-6], grain boundary elimination [7], and microalloying with boron [8], have been made. The successes were at the best incomplete [8,9]. The approaches used to improve high temperature strength included addition of dispersoids and/or precipitates [10,11] and production of composites [12,13].

As far as processing is concerned, two developments, representing two extremes of microstructural control, have emerged as potential solutions to the problems mentioned above. One is the production of single crystals, pioneered by GE, which clearly has potential for the production of turbine blades, as it is the case in currently produced turbine blades made out of nickel-base, single crystal superalloys. Such processing, however, has limitations both in geometry and microstructure.

An alternative method is to use grain refinement. Mechanical alloying of NiAl - a processing technique adopted and modified at the Illinois Institute of Technology by our research group, used to produce dispersion strengthened fine grained materials, analogous to oxide dispersion strengthened superalloys - belongs to this category. The advantages of this powder metallurgy route are: flexible control of alloy composition and microstructure, possible near net shape processing for complex parts and ease of use for intermetallic matrix composites.

II. GENERAL APPROACH

The flow chart, presented in Fig.1, summarizes our general approach to explore mechanical alloying (MA) as a processing route for NiAl-based intermetallics and to study microstructure, plastic deformation and mechanical properties of mechanically alloyed (MA)

OVERALL RESEARCH APPROACH

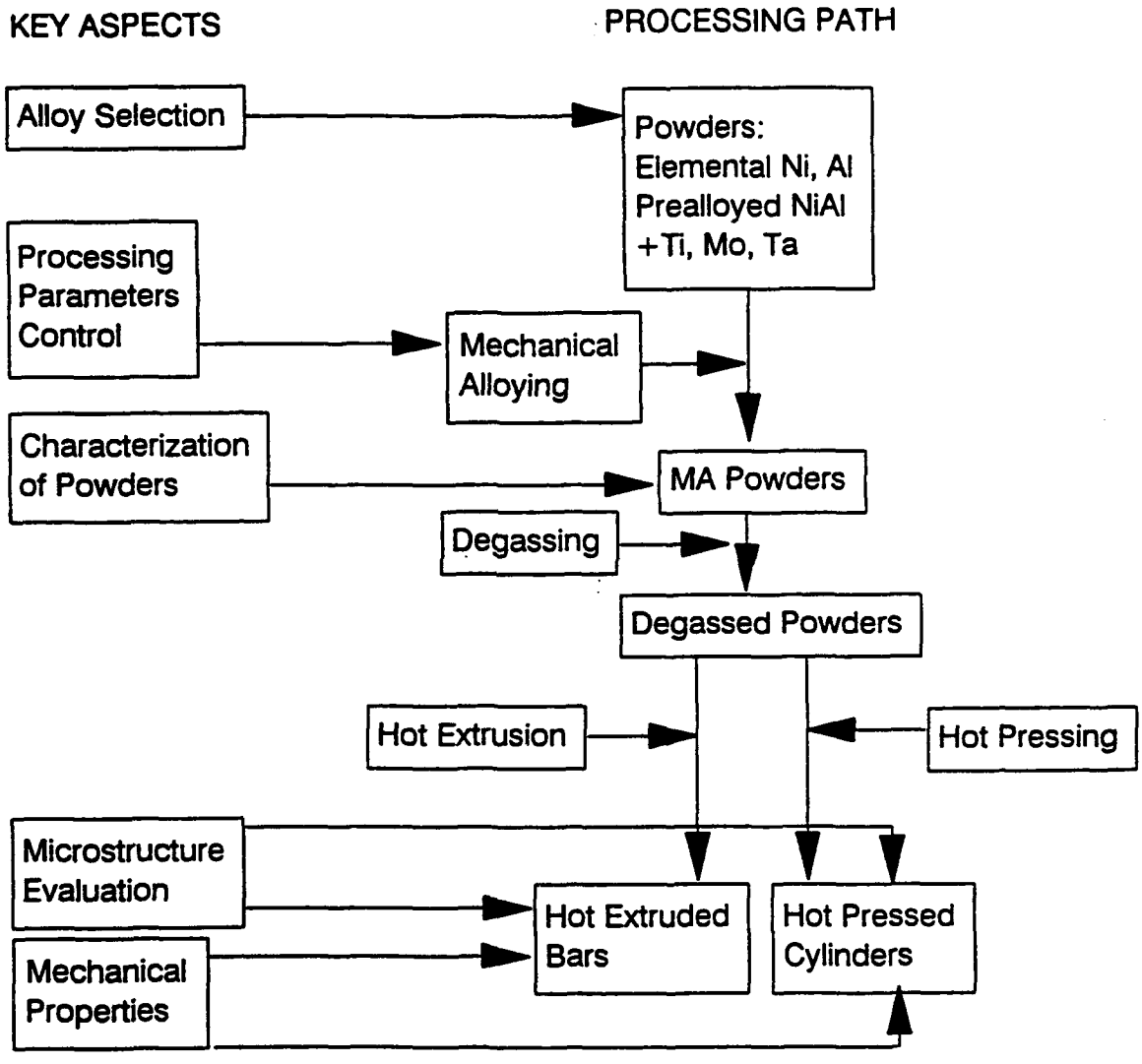

Figure 1. Flow Chart for Overall Research Approach

NiAl and NiAl-based alloys.

We have been using elemental powders of Ni and Al. In selecting the alloys, our design philosophy has been to use a number of elements, such as Ti, Ta, Mo, as solution strengtheners or precipitate formers. The powders were mechanically alloyed with a strict control of processing parameters. The physical, chemical and microstructural characterization of the as-milled powders was carried out. The powders collected after milling were degassed and encapsulated under vacuum in stainless steel cans. The cans were hot extruded. Alternative consolidation route, hot pressing, was also used. The evolution of microstructure in the materials during consolidation and during deformation of consolidated materials was examined and mechanical properties were evaluated.

Our final product is in the form of hot extruded bars or hot pressed cylinders. The technique allows us to produce quality powders, which when consolidated, have high strength at both ambient and elevated temperatures and good compressive ductility.

III. MECHANICAL ALLOYING

Mechanical alloying was first developed in 1968 by the INCO Company to produce oxide dispersion strengthened nickel-base superalloys. Over the years, MA and following consolidation have been shown to be quite a general process for producing alloys that are either difficult or impossible to produce by conventional ingot metallurgy. However, MA can be used not only when conventional methods fail. Mechanically alloyed powders, consolidated typically by hot extrusion or hot pressing, exhibit unique microstructures with very fine grains, containing controlled amount and distribution of dispersoids and/or precipitates; this frequently results in improved mechanical properties compared to conventional counterparts, and the process may be a viable alternative to conventional methods [14].

This notion led to our research. We hoped that by using MA to produce dispersion strengthened, fine-grained intermetallics, in particular B2 nickel aluminide, NiAl, we would address both the lack of ductility at room temperature NiAl and high temperature strength.

MA is a high energy ball milling process [14]. Starting materials may be a mixture of pure elemental or prealloyed powders, poured into an attritor mill, in which small balls are activated by impellers radiating from a rotating central shaft. MA intimately mixes the constituents which, given a sufficiently long attrition time, form a true alloy. When the powder particles are trapped between the colliding balls, two competing processes occur, that of fracture and that of cold welding. In a dry, highly energetic ball charge the rates of welding and fracturing are typically in balance and the average powder particle size remains coarse, about 50 μm. If there is a need to refine the particle size, which is typically the case, one uses milling liquids (process control agents) to minimize welding and the powder particle reach sizes as small as one micron.

The schematic diagram of the attritor mill used in the present work is shown in Fig.2. Our milling is a dry process, however, the role of the process control agent plays milling atmosphere: argon -oxygen mixture. The importance of oxygen is twofold and cannot be overestimated. Oxygen is known to decrease cold welding, thus refining final powders, and it forms fine oxides dispersed throughout the final product. In order to isolate the process from the outside atmosphere, a sealed chamber was added. Liquid nitrogen was used to promote the initial cold fracture through a cryogenic milling. Again, the key issue during MA is to control the

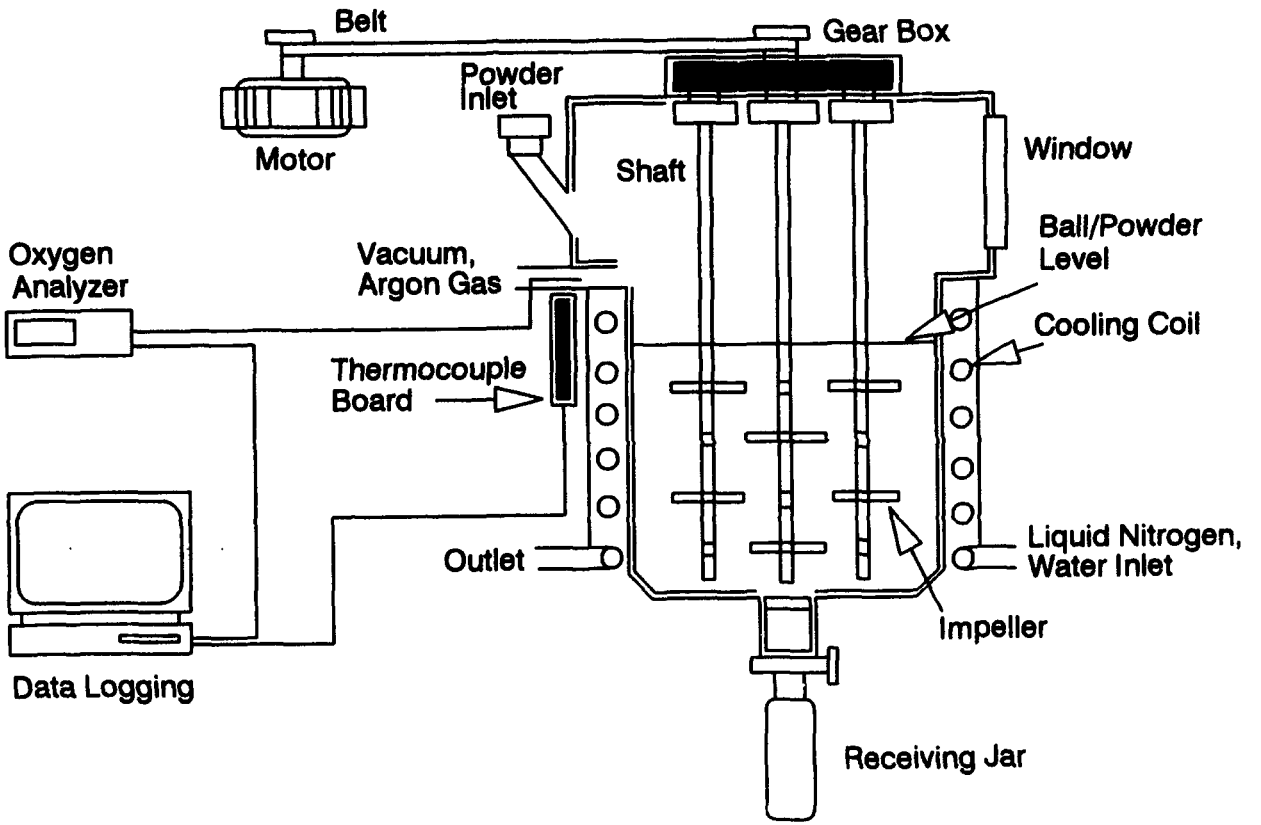

Figure 2. Schematic Diagram of Szegvari Attritor Mill

desirable balance between cold welding and fracture. Any variable which affects the balance will have a drastic effect on the product and has to be optimized. Among the processing parameters of MA which were kept under control are: process control agent - argon-oxygen mixture, in particular oxygen content, milling temperature and time, mill speed, grinding media size, powder/grinding media weight ratio.

IV. CONSOLIDATION OF MECHANICALLY ALLOYED POWDERS

The mechanically alloyed powders were consolidated by hot extrusion and hot pressing. The hot extrusion was carried out at NASA Lewis Center. Approximately 200 grams of powder was sealed in a steel can and extruded at 1127°C at the reduction ratio of 16:1. Finally, consolidated materials with core diameter of 5 to 9 mm were obtained. For the hot pressing, high strength graphite die was prepared. To prevent oxidation of graphite at high temperature, the die, plunger, spacers and die support were coated with silicon carbide. Boron nitride was applied to lubricate the contacting surface between each coated component. Typically, 45 grams of powder with -325 mesh size was put into the die hole and pressed at 10 MPa for about 2 hours until the hot pressing temperature of 1050°C was reached. After reaching up the temperature, pressure was increased to 40 MPa and kept constant until no displacement (no further densification of powders) was detected by linear variable differential transformer (LVDT) connected to the data acquisition system. Argon gas was supplied into the heating chamber throughout the pressing. The schematic diagram of the hot press used in the present study is illustrated in Figure 3.

V. ALLOY SELECTION

Over the last 4 years, about twenty MA NiAl-based alloys have been produced in our laboratory. Elemental powders of Ni and Al and prealloyed NiAl powders were used. In selecting the alloys, our design philosophy was to employ a number of elements, such as Ti, Ta, Mo, as solution strengtheners or precipitate formers.

The chemical and phase composition of five selected MA NiAl-based materials are shown in Table 1.

Table 1. Chemical and Phase Composition of Selected MA NiAl-based Materials and Cast NiAl.

Alloy	Powders	Phases	Ni	Al	Ti	Ta	Mo	O
MA 1	Elemental	NiAl/Ni_2TiAl	38.0	46.3	6.7	1.2	-	6.7
MA 2	Elemental	NiAl/α-Mo	45.3	42.2	2.7	-	5.0	2.6
MA 3	Prealloyed	NiAl	52.0	42.3	1.4	-	-	3.6
MA 4	Elemental	NiAl	41.9	43.9	6.7	-	-	5.8
MA 5	Elemental	NiAl	47.0	47.4	1.4	-	-	1.7
cast	-	NiAl	50.1	49.9	-	-	-	0.007

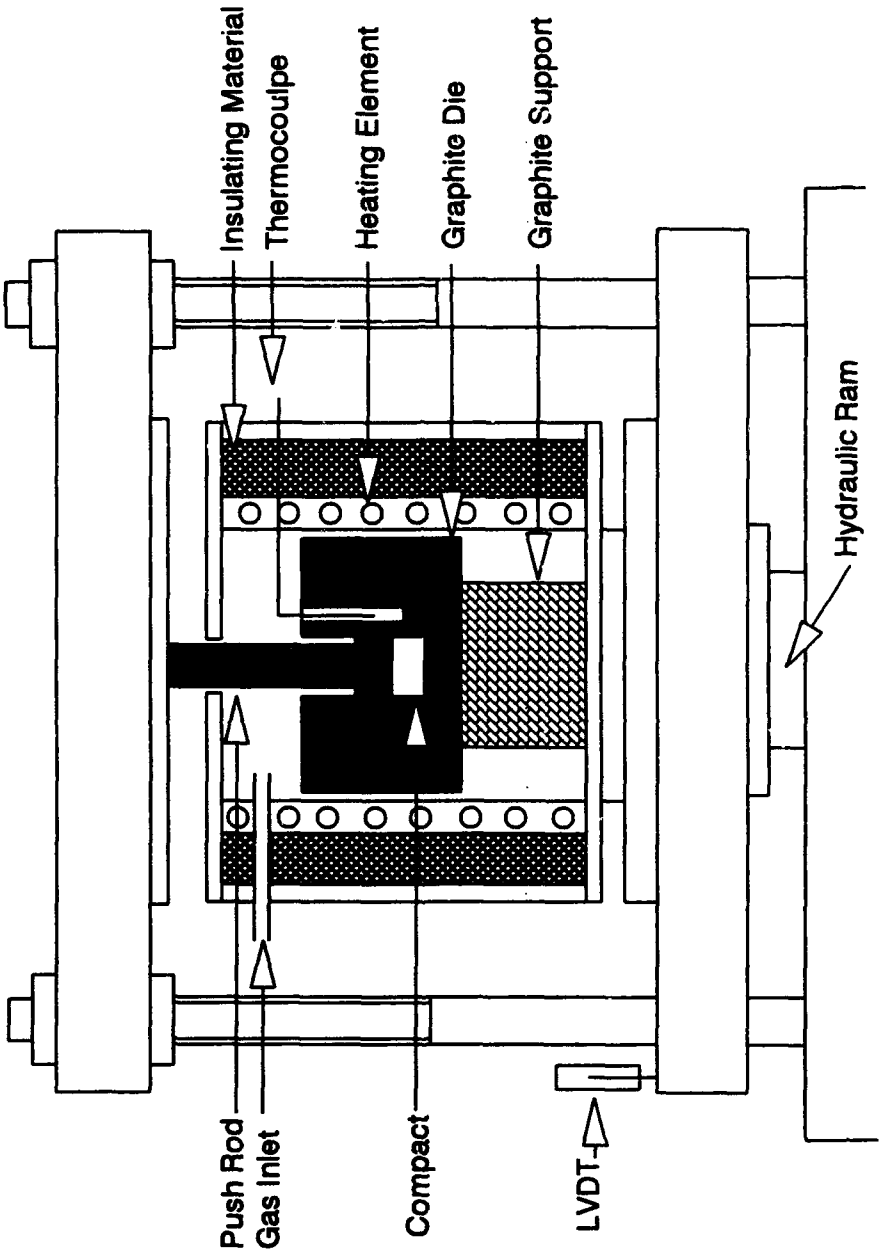

Figure 3. Schematic Diagram of Hot Press Used in This Study

Three types of alloys were produced, NiAl with a brittle, Heusler type, second phase, typified by Alloy 1, NiAl with a ductile second phase (Alloy 2), and single phase NiAl (Alloys 3, 4, 5). The content of Ti in Alloy 4 was unintentionally high, and Alloy 3 was synthesized using prealloyed powders.

The results of our studies of microstructures and mechanical properties indicate that the presence of the hard phase is unacceptable, and the presence of the ductile phase not justified. There is no advantage of using excessive amounts of Ti, and the use of prealloyed powders has a slightly deteriorating effect on the microstructure homogeneity. As a result, the most comprehensive studies of microstructure and properties were carried out on alloy MA 5, single phase NiAl, containing nearly equal amounts of Ni and Al, moderate amounts of solid solution strengtheners, Ti and Mo, and 1.7at.% of oxygen. The microstructure and properties of the material, described and summarized in the following section, typify those of other MA NiAl-based alloys produced in our laboratory.

VI. CHARACTERIZATION OF THE MA NiAl

VI.1. MATERIALS, MICROSTRUCTURES, TEXTURES, AND SLIP SYSTEMS

The MA NiAl was obtained from elemental Ni and Al powders. MA powder collected after milling, was sieved to -325#, degassed at 973K for 1.5 hours in a vacuum furnace, encapsulated under vacuum in a stainless steel can and hot extruded at 1400K at a ratio of 16:1. For comparison with the MA alloy, a near-stoichiometric NiAl, with the chemical composition given in Table I, was prepared from a cast ingot and hot extruded under the same conditions.

The optical microscopy observations showed that the hot extruded MA material is fully dense and free from cracks. TEM studies revealed fine, equiaxed grains with an average size of about 0.5μm, separated typically by low angle grain boundaries, and a homogeneous distribution of aluminum oxides with bimodal sizes of 10 and 100nm (Fig.4). The coarse oxides are preferentially distributed on grain boundaries and the small ones are dispersed uniformly throughout the grains. The optical and transmission electron microscopy observations showed that the cast NiAl is a single phase material with an average grain size of about 50 μm fully recrystallized during hot extrusion.

The extrusion texture has been determined on transverse sections by the Schulz back reflection method using copper K_α radiation. The analysis indicates that the MA alloy exhibits a strong <110> fiber texture parallel to the extrusion axis while the hot extruded cast material has a <111> fiber texture (for details see [15]).

The <110> fiber texture is a common texture produced by drawing or extrusion in b.c.c. materials. Since the texture of MA powders is essentially random and featureless, the <110> texture in MA NiAl is a direct consequence of the deformation during extrusion. This deformation texture was postulated to be retained in MA NiAl alloys due to the presence of dispersoids, above all the coarser ones, and the predominant occurrence of low mobility, low angle grain boundaries. The <111> texture observed in cast NiAl is a common recrystallization texture observed in NiAl by others as well (for further discussion and references see [15]).

Several studies have been undertaken to determine the operative slip systems at ambient temperatures in NiAl. The consensus of these investigations is that this compound deforms predominantly by {110} <100> slip. As reported elsewhere [16], the occurrence of <100>

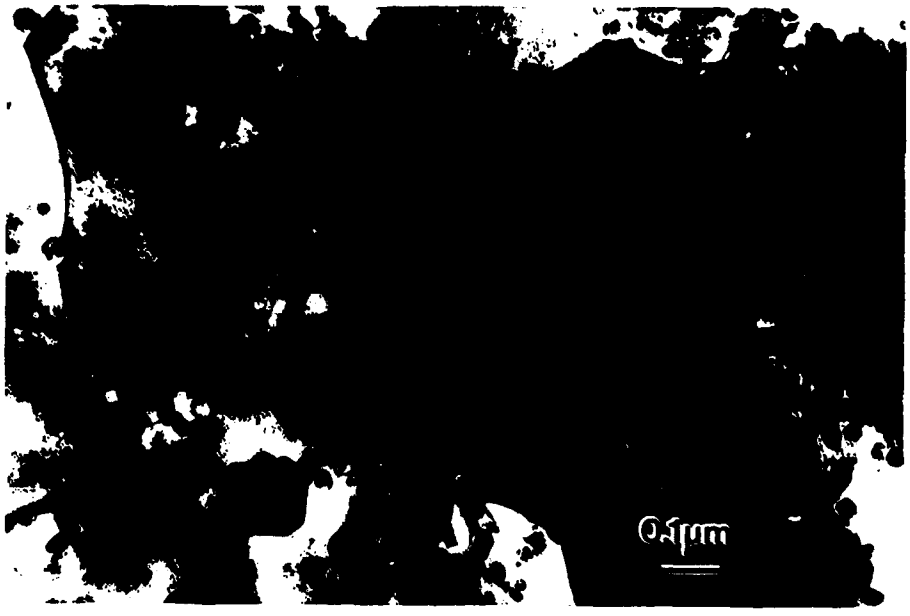

Figure 4. Typical TEM Microstructure of Hot-Extruded MA Alloys

slip was confirmed in both MA and cast NiAl, and a strong, unequivocal evidence for <110> slip in the compressed specimens of the MA NiAl was gathered.

The different slip systems activated in the cast and MA NiAl were postulated to be a result of distinct textures exhibited by these differently processed materials [16,17]. Using a generalized Schmid law, one can calculate resolved shear stresses in potentially active slip systems in a grain of given orientation [17]. The results of the calculations of resolved shear stresses in potentially active slip systems in <110> and <111> oriented grains, do actually indicate that the strong <110> texture of the MA material enables the activation of {110}<100> and {110}<110> slip systems while the <111> texture allows only {110}<100> slip systems to operate (for further discussion and references see [16-18]).

VI.2. MECHANICAL PROPERTIES

Mechanical properties of the as-extruded MA and cast NiAl have been examined in compression tests. The compression tests were performed in air from room temperature to 1100K at a nominal strain rate of $8.5 \times 10^{-4} s^{-1}$ using SiC push rods. Selected results, relevant for further discussion, are shown in Table II. Room temperature compression test of the MA material was stopped when the load on the specimen reached the limit of the Instron load cell. The 1100K test was stopped as well since the compressive ductilities at high temperatures exceed typically 30%.

Table 2. Yield stress and strain till failure of MA and cast NiAl.

Alloy	Deformation Temperature (K)	Yield Stress (MPa)	Strain to Failure (%)
MA	300	1275	>11.5
MA	800	950	6.8
MA	1100	234	>13.7
cast	300	303	2.8

Room temperature compressive ductility

The {110} <100> slip, typically observed in NiAl compound at ambient temperature, provides only three independent slip systems. Thus, the number of independent slip systems available for general deformation is insufficient because the von Mises criterion for plasticity - at least five independent slip systems in a grain - is not fulfilled, and NiAl polycrystals are predicted to be brittle. In our study [16], only <100> slip vectors were observed in cast NiAl at room temperature, in accordance with previous observations, and this material exhibited very limited compressive ductility.

In MA NiAl, the occurrence of {110}<001> slip in NiAl was confirmed and, more importantly, strong evidence for <110> slip was obtained [16]. It was proven that when the

<001> and <011> slip vectors are encountered, five independent slip systems operate and the von Mises requirement for general plasticity is satisfied [16]. The operation of five independent slip systems is suggested to contribute to a notable room temperature compressive ductility of the MA NiAl. Another factors postulated to contribute tc the improved compressive ductility is the predominance of low angle grain boundaries, facilitating the transmission of slip between neighboring grains and likely not allowing large elastic incompatibility stresses to develop in their vicinity. The differences in compressive ductility between cast and MA NiAl could also be attributed to the difference in grain size (for further discussion and references see [17]).

Room temperature strength

The MA NiAl is much stronger than the cast NiAl (Table 2). Several factors may be postulated to contribute to the high strength of the MA material: grain refinement, texture, deviations from stoichiometry, the presence of dispersoids as well as interstitial and/or substitutional solute atoms. It was shown that the significant strengthening factors in MA NiAl are grain refinement and the presence of dispersoids and interstitials. It was estimated that the increase in yield stress due to grain refinement in the MA NiAl is between about 200 MPa and 650 MPa and due to dispersoids about 200 MPA. Because of the complex chemistry of the MA materials it was not possible to quantify the strengthening contributions of interstitial atoms (for further discussion and references see [17]).

Elevated temperature mechanical properties

The strength at the intermediate temperature of 800K ($\approx 0.4T_M$) is only about 10% lower than at room temperature, indicating that thermally activated climb does not yet occur. At 1100K ($\approx 0.55T_M$), thermally activated processes facilitate the dislocation motion, resulting in significantly decreased yield stress and work hardening and improved ductility.

At 800K, MA NiAl exhibited considerably lower compressive ductility than that measured in specimens deformed at lower and higher temperature (Table 2). The ductility trough was in fact observed in all MA NiAl-based materials processed in our laboratory, but not in cast NiAl.

Typically, a loss of ductility at elevated temperatures is a result of dynamic strain aging (DSA). However, the results of strain rate change tests disproved any role of DSA. The drop in compressive ductility at 800K was shown to be associated with pronounced, attractive dislocation - dispersoid interactions revealed by TEM studies (for further discussion and references see [17]).

At elevated temperatures, the MA NiAl-based materials produced in our laboratories are much stronger and significantly more ductile than their cast counterpart.

VII. CREEP OF MA NiAl

As discussed in preceding sections, MA allowed us to produce quality powders, which,

when consolidated, have high strength at both ambient and elevated temperatures and good compressive ductility. One of the major issues which needed to be addressed in the course of our studies was creep resistance. In this section, results of our studies on creep in MA NiAl materials are presented and contrasted with the results of analogous studies of their conventionally processed counterparts.

A nominally stoichiometric, NiAl based-material, produced by mechanical alloying of elemental Ni and Al powders and consolidated by either hot extrusion or hot pressing, has been investigated. For comparison with the MA NiAl, a near-stoichiometric, hot extruded cast NiAl has been examined as well. The chemical composition of consolidated materials are presented in Table 3.

Table. 3. Chemical Composition of Examined Alloys (Atomic Percent)

Alloy	Ni	Al	C	O	N	H
MA NiAl	48.32	49.74	0.56	0.63	0.12	0.63
Cast	50.1	49.9	0.06	0.007	0.003	0.12

VII.1. CREEP TESTS

SATEC M-3 creep machine has been used in the present study. The machine is equipped with a tubular furnace with maximum operating temperature of 1000°C. A K-type thermocouple is connected to the specimen and the test temperature is kept within +/-1.5°C tolerance at all test temperatures. The compression creep fixtures were designed for testing of MA materials. Linear variable differential transformer was used to obtain displacement-voltage responses. The voltage change associated with the sample displacement was recorded every 3 minutes and translated into strain and finally into creep curves. The constant load tests were conducted on 5 mm diameter, 10 mm long cylindrical specimens which had been electro-discharge machined from the consolidated materials, parallel to the directions of hot extrusion or hot pressing.

The apparent activation energy for creep, Q, was determined from the simple Arrhenius type plot of temperature dependence of creep rate at constant stress:

$$Q = -R\left[\frac{\partial \ln \dot{\varepsilon}}{\partial (1/T)}\right]_{\sigma} \quad (1)$$

Similarly, the apparent stress exponent, n, was obtained from the plot of minimum creep rate against applied stress at a constant temperature. The exponent n is defined as:

$$n = \left[\frac{\partial \ln \dot{\varepsilon}}{\partial \ln \sigma}\right]_{T} \quad (2)$$

VII.2. CREEP BEHAVIOR

Creep of MA NiAl

The creep properties of HE and HP MA NiAl were investigated at 800, 850 and 900°C, and at 40, 110 and 180MPa. For HE material, additional tests at a lower stress and temperature (20MPa and 750°C) were carried out. Normalized temperatures and stresses ranged from 0.46 to $0.55T_M$ and from $2\times10G^{-4}$ to $2\times10^{-3}G$, respectively. Creep curves obtained in the present study are typified by the creep curve for HP MA NiAl deformed at 800°C and 110MPa (Fig.5). Figure 6 illustrates the relationship between creep rate and time derived from Figure 5. As can be seen, the primary creep with a high creep rate is followed by the steady state creep which begins after about 5 - 10 hours. The tertiary creep was not observed, primarily because of the crack closure during compression creep testing. Incidentally, the tertiary creep region has rarely been investigated in NiAl-based materials [19] because most testing to date has been in compression [20, 21, 22].

The steady state creep rates for HP MA NiAl are shown in Table 4. The effects of temperature and stress on the creep rate are illustrated in Figures 7 and 8, respectively. The analysis of the data allowed us to determine the average apparent values of activation energy for creep and stress exponent which equal, respectively, 204kJ/mol and 3.5.

Table 4. The Steady State Creep Rates (s^{-1}) of HP MA NiAl

Stress(MPa)	800°C	850°C	900°C
40	2.19×10^{-9}	5.43×10^{-9}	1.04×10^{-8}
110	4.27×10^{-8}	1.42×10^{-7}	6.97×10^{-7}
180	3.91×10^{-7}	1.26×10^{-6}	1.68×10^{-6}

As mentioned before, the creep performance of HE MA NiAl was characterized as well. The minimum creep rates in HE MA NiAL are always higher (2 - 10 times) than those in HP MA NiAl; the activation energy for creep and stress exponent were found to be 175kJ/mol and 2, respectively.

The higher creep rates observed in HE MA NiAl may be attributed to:

i) the development of a strong, <110> fiber texture along the extrusion direction [15], and the lack of a measurable texture in HP MA NiAl; the predominant, <110> orientation of grains in hot-extruded MA NiAl is a soft orientation and may be postulated to result in a stronger creep response and higher creep rates;

ii) the presence of somewhat coarser oxides in HE material; hot extrusion was carried out at higher temperature than hot pressing what led to slight, but noticeable coarsening of dispersoids likely deteriorating creep resistance;

iii) the lower level of interstitial carbon and nitrogen in HE material; during hot pressing coating materials containing carbon and nitrogen were used, increasing the content of these interstitials in hot-pressed materials, as evidenced in another study [23].

Several other MA NiAl-based materials, with and without ternary additions, were synthesized and processed in our laboratory and their creep properties were investigated. The

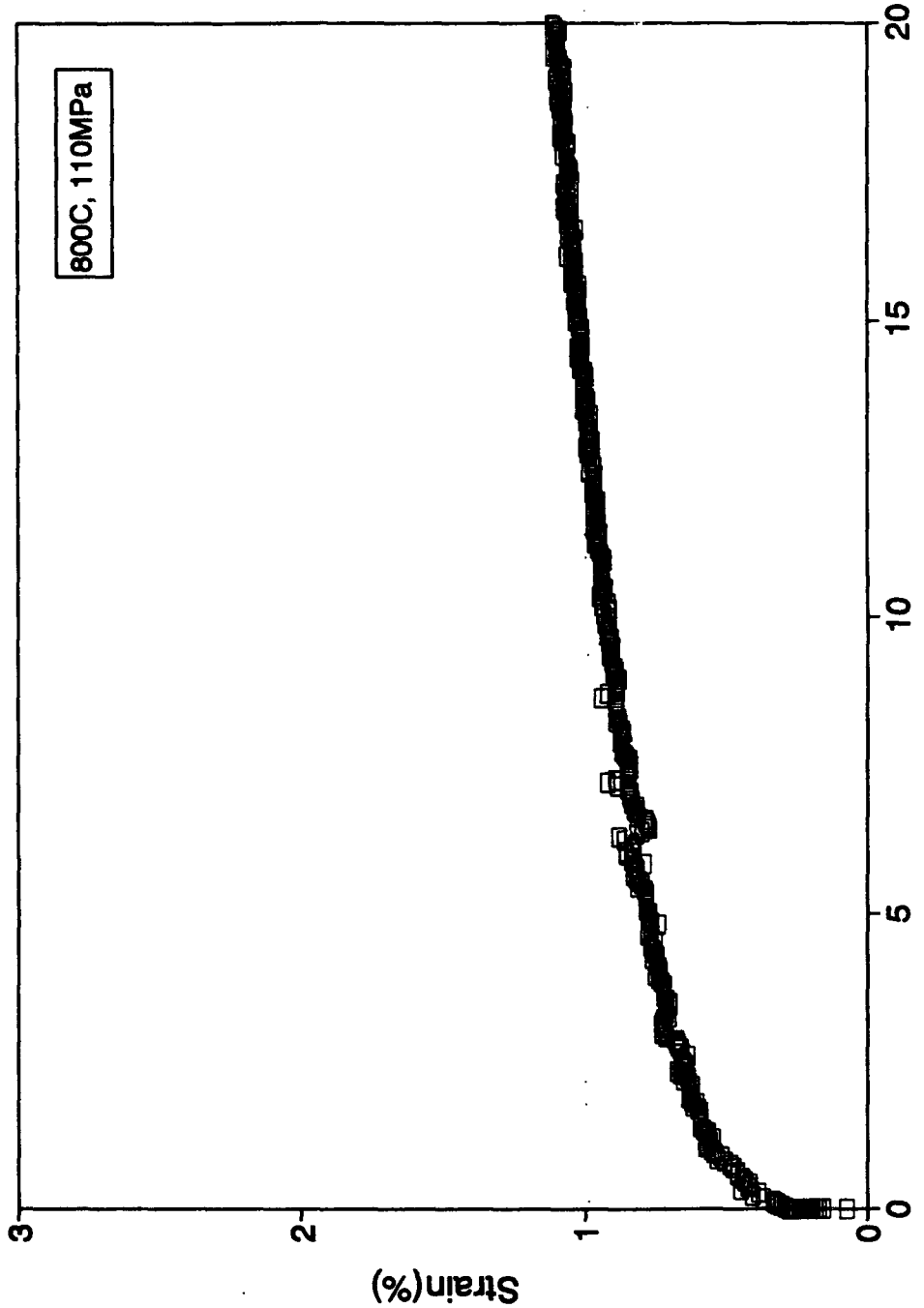

Figure 5. Creep Curve for Hot-Pressed MA NiAl Deformed at 800°C and 110MPa

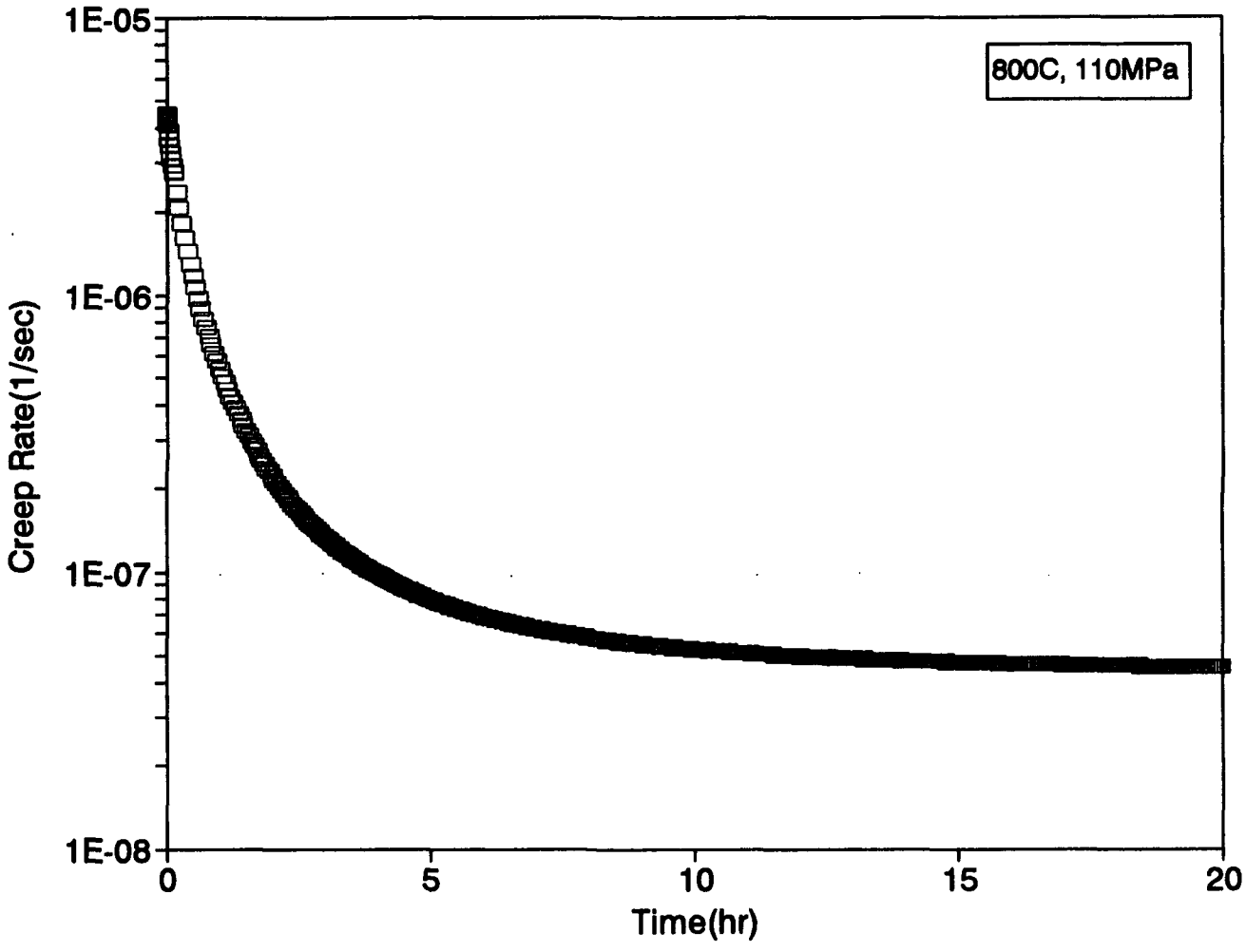

Figure 6. The Creep Rate as a Function of Time for Hot-Pressed MA NiAl at 800°C and 110MPa

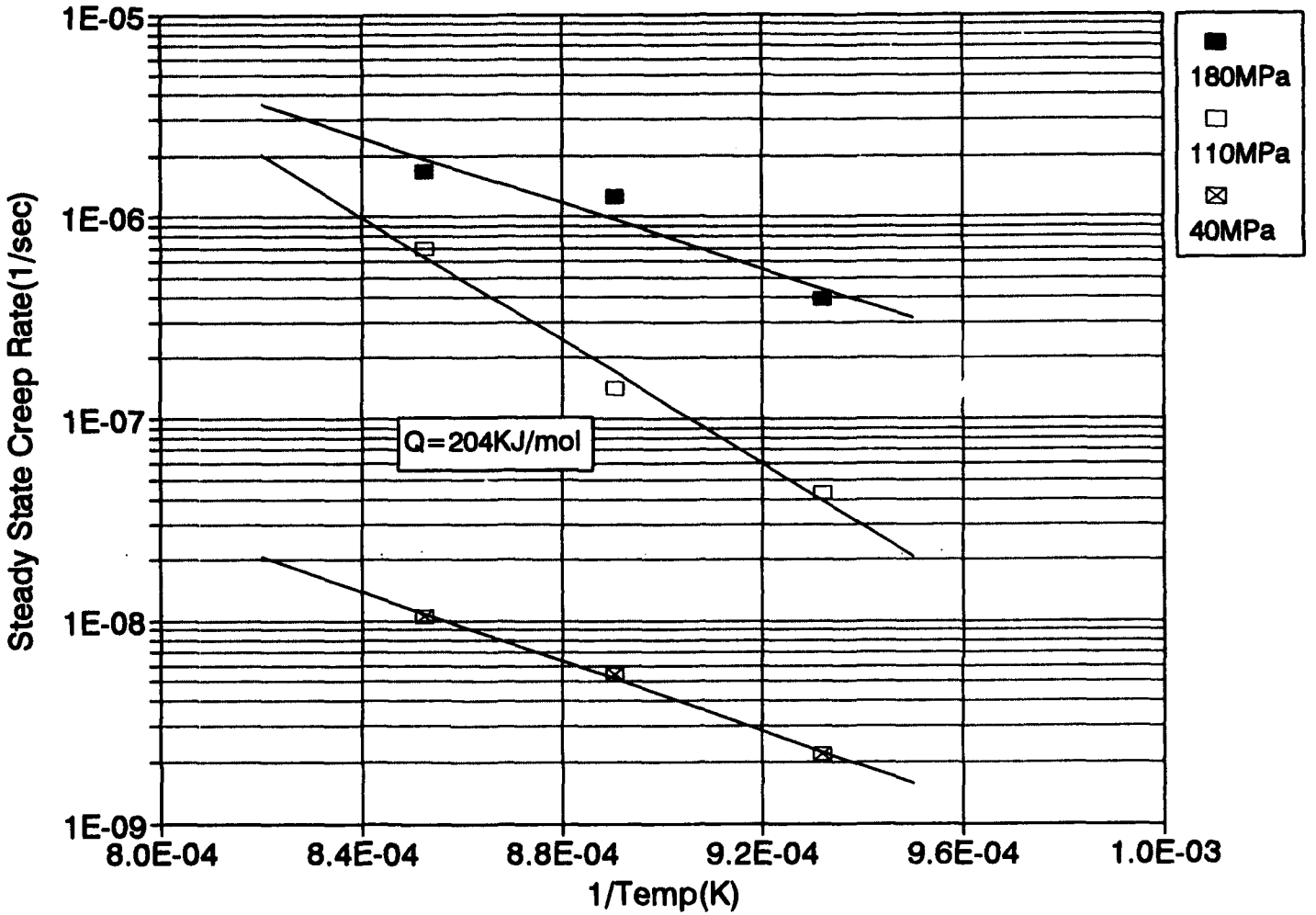

Figure 7. Temperature Dependence of Creep Rate for Hot-Pressed MA NiAl

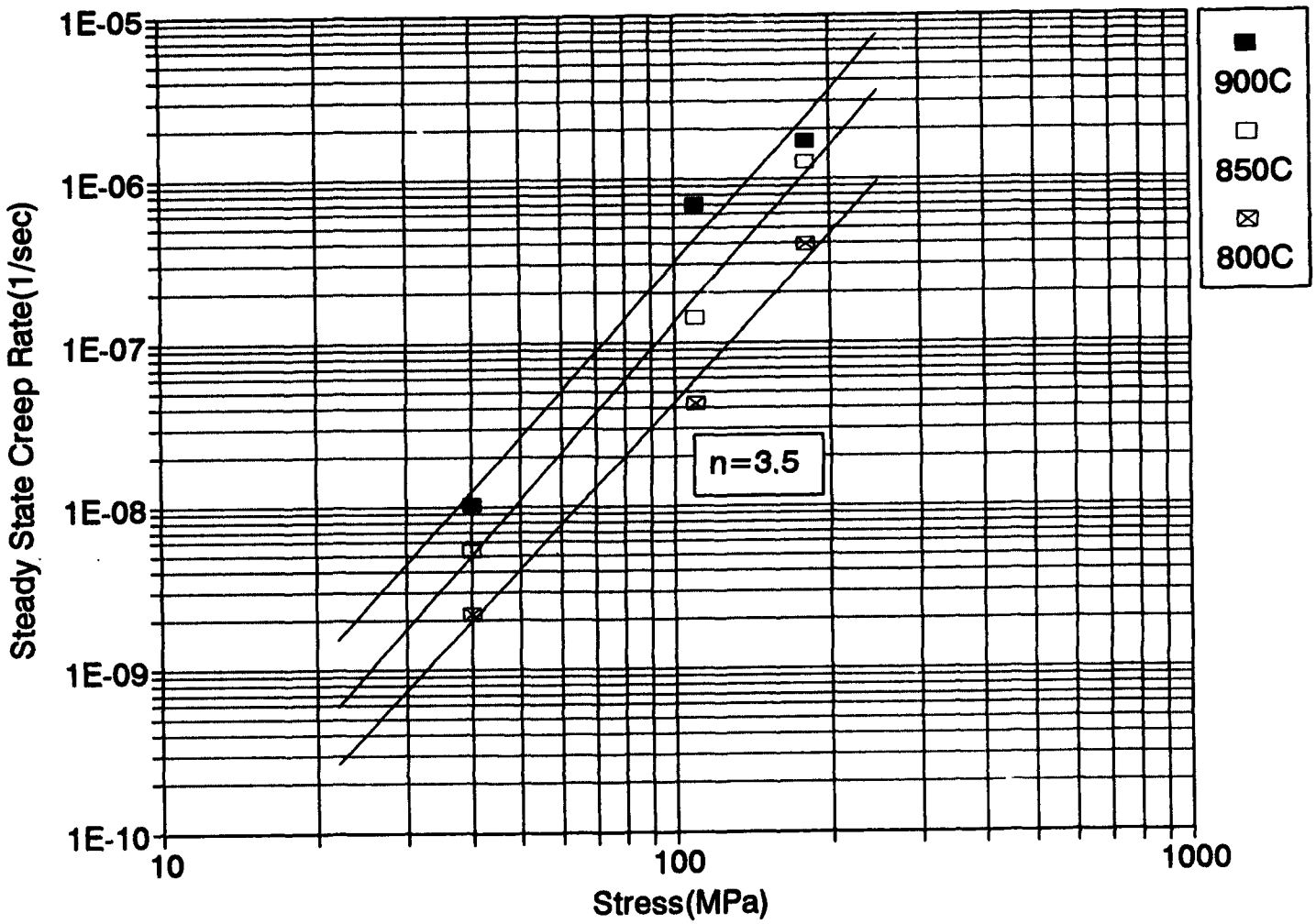

Figure 8. Stress Dependence of Creep Rate for Hot-Pressed MA NiAl

stress exponent in all the MA materials, including the present alloy, ranged from 1.75 to 3.8 while the activation energy for creep varied from 175 to 225 kJ/mol. The values of n and Q are indicative of creep mechanisms and their significance is discussed in the following section.

Creep of MA *versus* Cast NiAl

Creep behavior of the stoichiometric, cast NiAl was investigated under the same experimental conditions - characterized earlier - for comparison with the MA NiAl. The steady state creep rates at different temperatures and stresses are shown in Table 5 and compared with that in HP NiAl. As can be noted there, the creep rate is on average three orders of magnitude lower in MA NiAl than in its cast counterpart tested under the same experimental conditions.

Compressive creep properties of single phase NiAl, both in polycrystalline and single crystal forms, were investigated by many authors [24, 25, 26, 27]. The creep rates measured in these studies at 900°C have been plotted as a function of stress in Fig.9, along with the creep rates for HP MA NiAl. The plot shows that the present material exhibits significantly lower creep rates (on average one to four orders of magnitude) than its single phase counterparts.

Table 5. The Minimum Creep Rates (s^{-1}) of HP MA NiAl and Cast NiAl at 800°C

Stress(MPa)	HP MA NiAl	Cast NiAl
20		9.4×10^{-8}
40	2.19×10^{-9}	1.5×10^{-6}
110	4.27×10^{-8}	1.0×10^{-5}
180	3.91×10^{-7}	

Many authors characterized creep parameters, the activation energy for creep, Q, and the stress exponent, n, of single phase NiAl. As recently summarized by Nathal [19], the best choice for the activation energy is about 310 kJ/mol and for stress exponent about 6. This activation energy is reasonably close to the activation energies determined in diffusion experiments which cluster between 150 and 250 kJ/mol [28, 29, 30]. The relatively high value of the stress exponent is close to the values of n characteristic for pure metal type, or so called Class M, creep (see criteria for classifying dislocation creep behavior, Table 6 [31, 32]).

Table 6. Criteria for Classifying Dislocation Creep Behavior

	Class M	Class A
Controlling Mechanism	Climb	Viscous Glide
Stress Exponent	5	3
Activation Energy	Diffusion	Diffusion
Dislocation Structure	Subgrains	Homogeneous

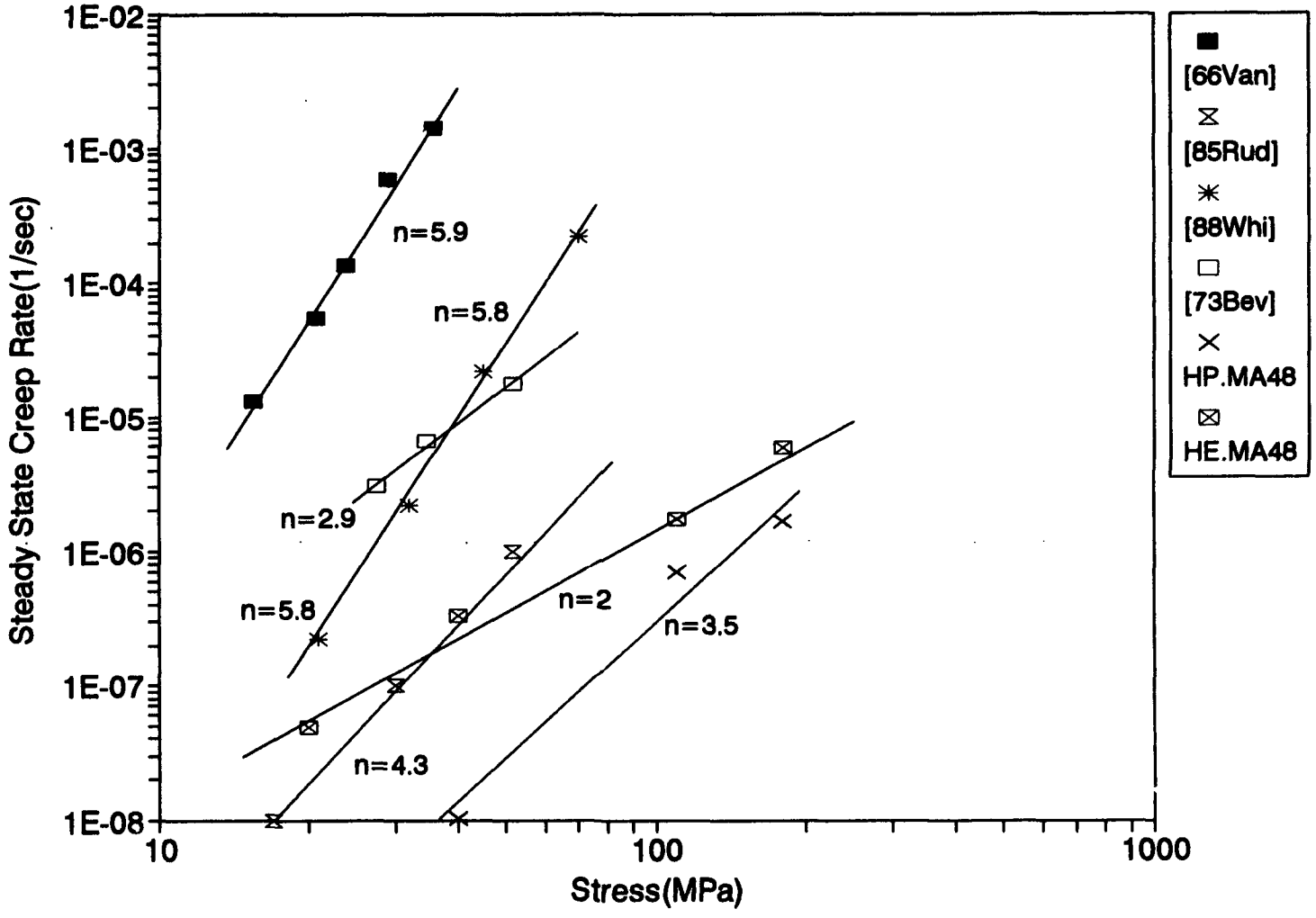

Figure 9. Comparison of Creep Rates for Stoichiometric NiAl and MA NiAl at about 900°C

In addition, subgrain formation after high temperature deformation of NiAl was observed by many authors (for review see [19]). In sum, a strong experimental evidence has been accumulated indicating that dislocation creep is responsible for high temperature creep (700 - 1000°C) of single phase NiAl and that the rate of the process is controlled by dislocation climb.

As far as the MA NiAl alloys are concerned, the activation energies for creep (175 - 225 kJ/mol) are clearly within the range of the activation energies determined in diffusion experiments and the stress exponents (1.75 - 3.8) are significantly lower than that in single phase NiAl. Such the drop of n is typically attributed to the change of the mechanism controlling creep [31].

The values of n close to 3 are characteristic for alloy-type, or so called class A, creep [32] (see Table 6). In solid solutions of pure metals, Class A creep is controlled by the movement of dislocations restricted by the drag of solutes, aided by vacancy diffusion [31]. The effects of solute additions on creep rate of NiAl have been summarized by Nathal [19]: the solid solution NiAl alloys exhibit lower creep rates, and the values of n near 3 - 4. Thus, the creep mechanism likely changes in the presence of solute atoms from climb controlled in pure NiAl to viscous drag in solution-hardened NiAl, as is the case in solid solutions of pure metals. However, such a simple explanation of the low value of n and low creep rates in the present materials cannot be adopted because MA NiAl is strengthened not only by foreign atoms, but also by oxide dispersoids and small grain size [17, 18]. The same factors are postulated to contribute to improved creep resistance of MA NiAl and are discussed in the following sections.

MA *versus* other NiAl-based alloys with improved creep resistance

Many attempts have been undertaken to improve creep resistance of NiAl. The improvements were observed in solid solution- [26], precipitation- [33, 34], and dispersion-strengthened NiAl [34], and in discontinuously and continuously reinforced composites [35]. Figs. 10, 11 and 12, generated based on original references, illustrate 1200 K creep resistance improvements in, respectively, solution-, precipitation-, and dispersion-strengthened NiAl compared to the stoichiometric, single phase NiAl. The creep rates of the present hot-extruded and hot- pressed MA NiAl are also plotted. As can be seen,

i) significant improvements in creep resistance have been achieved in all three classes of NiAl materials, and

ii) the creep resistance of the present MA NiAl, in particular that of the hot-pressed material, is better than the creep resistance of solution- and other dispersion-strengthened NiAl and comparable to the creep resistance of precipitation-strengthened NiAl.

The Role of Dispersoids in Controlling Creep

A unique feature of the present MA NiAl is the presence and a bimodal distribution of aluminum oxide dispersoids. As summarized elsewhere [15], the coarse oxides, residing at grain boundaries, prevent grain growth, affect the progress of recrystallization and play an indirect role in providing the material with a notable room temperature compressive ductility. The fine oxides, dispersed throughout the grains, contribute significantly to the material's high strength at both ambient and elevated temperature. The present materials are not only strong at high

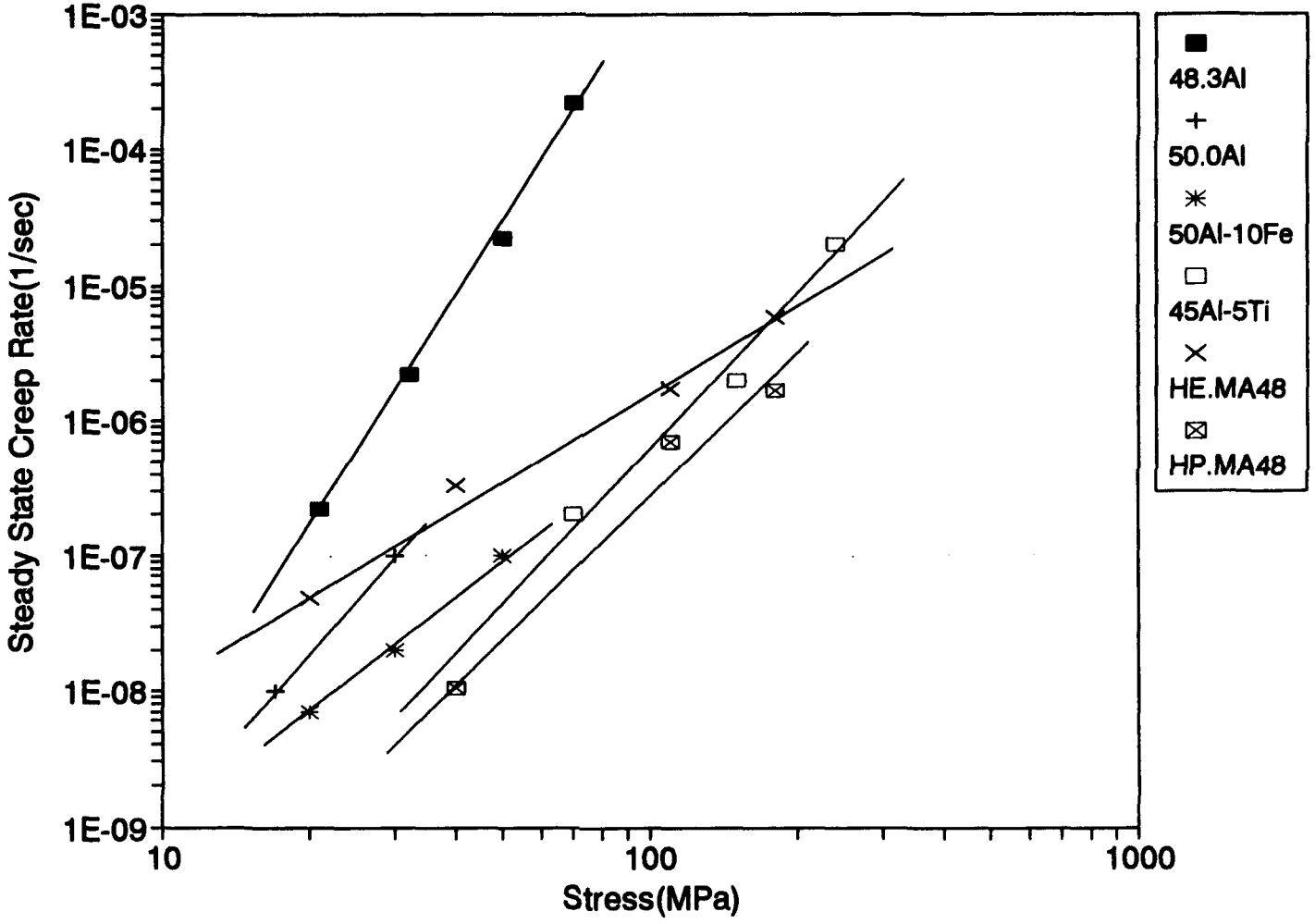

Figure 10. Creep Rates of Solid Solution Hardened NiAl and MA NiAl at about 900°C [26, 34, 41].

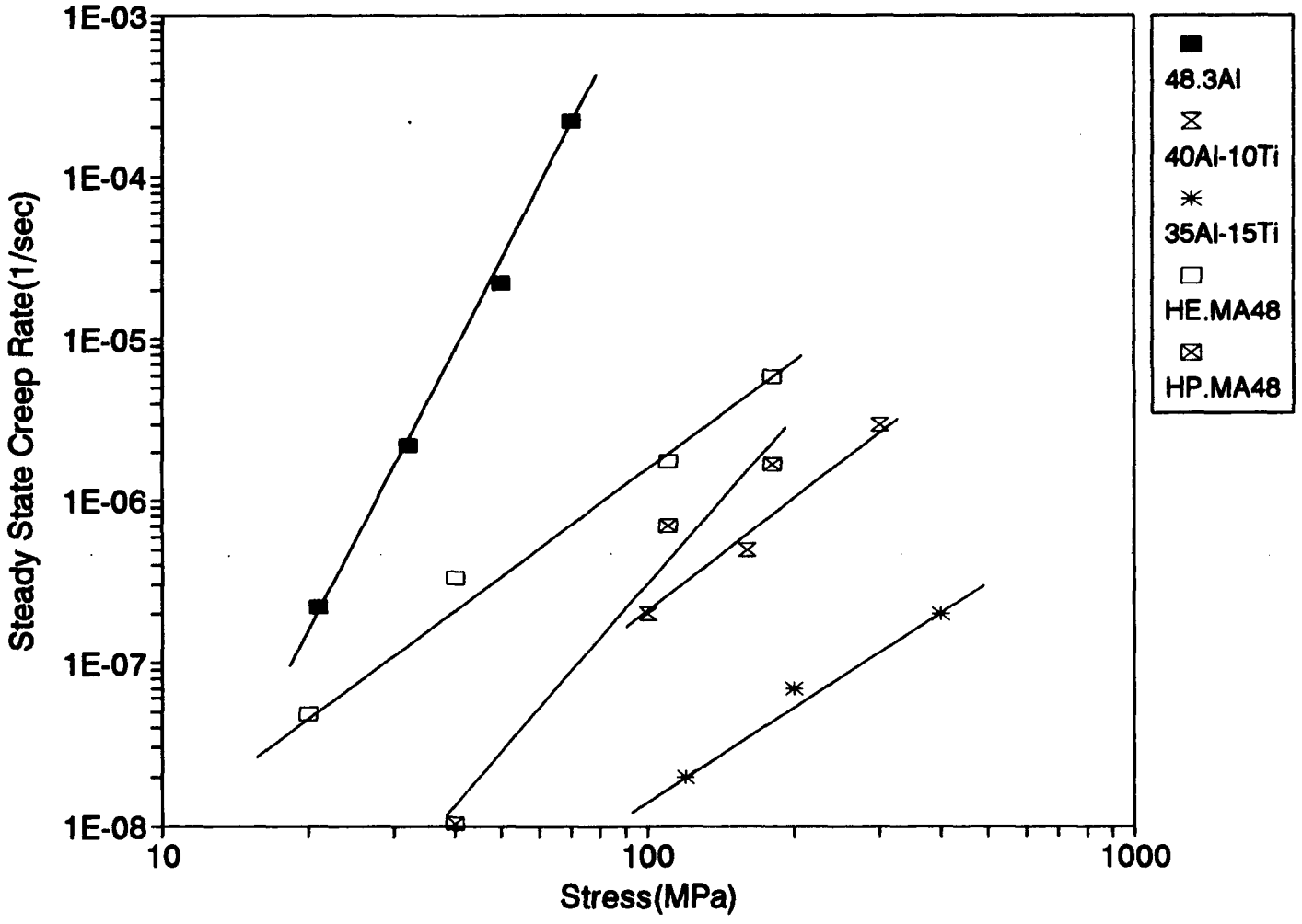

Figure 11. Creep Rates of Precipitation Hardened NiAl and MA NiAl at about 900°C [34, 41].

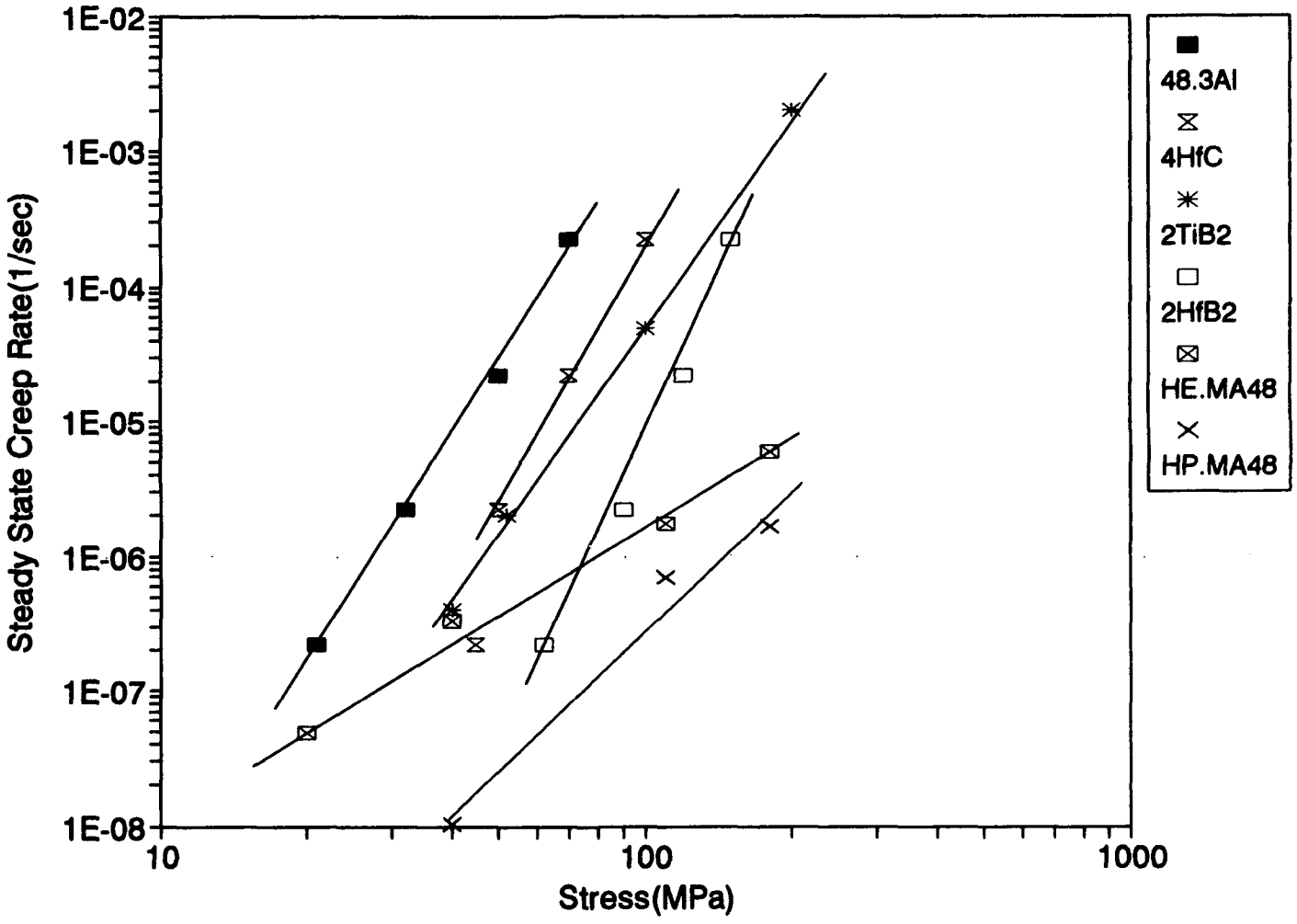

Figure 12. Creep Rates of Dispersion Strengthened NiAl and MA NiAl at about 900°C [34, 35, 41].

temperatures but also microstructurally stable up to 1375°C [36] and these two features are believed to contribute to the much lower creep rates in MA NiAl compared to those in single phase NiAl.

Due to lack of space, a detailed discussion of the role of dispersoids in the present materials will have to be presented elsewhere [37]. In short, however, we can state here that we have gathered TEM evidence indicating that the motion of dislocations during creep deformation is hindered by dispersoids. In addition, our studies have proved that there exists a threshold stress of about 15-20 MPa below which no detectable creep occurs and a model assuming equilibrium climb over non-interacting particles has provided us with the best estimate of the threshold stress [38].

The Role of Grain Size

Dislocation creep mechanisms are generally considered to be independent of grain size. A review of relevant references indicates that, as a first approximation, this is true in NiAl [19]. However, in some cases, creep strength can be somewhat improved by decreasing the grain size [27, 39]. It can be speculated that since NiAl is a Class M material - in which subgrain boundaries act as obstacles for dislocations - the improved creep resistance is to be expected when the grain size is finer than the equilibrium subgrain size. Possible, beneficial effects of decreasing grain size are limited to low temperatures and high stresses, where diffusional creep is of secondary importance.

The present MA NiAl materials are notably more creep resistant than their cast counterparts. It is believed to be above all due to the presence of dispersed particles and solute atoms, but, based on the above comments on the role of grain size, the fine grain size may be postulated to contribute somewhat to the improved creep resistance in MA NiAl rather than deteriorate it. In the present study, creep properties have been investigated at the temperatures 0.5 - 0.6 T_M and the stresses 10^{-3} - $5x\ 10^{-3}$ G, thus clearly within the predominance of the dislocation creep mechanism. The small grain size of about 0.5μm is likely less than a critical subgrain size.

More on Creep of MA NiAl

As discussed above, creep of MA NiAl is controlled by diffusion. However, creep does not occur as a result of diffusional flow, but rather is controlled by resistance to dislocation motion dragged above all by dispersoid and aided by vacancy diffusion. It is so because:
a) in the present study, creep was investigated in the stress range between 5×10^{-4}G and $5x10^{-3}$G (diffusional flow is believed to predominate at $< 10^{-4}$G [40]);
b) the values of the stress exponent n are low, but much higher than that believed to be responsible for diffusional flow [31];
c) test temperatures are between 0.5 and 0.6 T_M (diffusion flow is believed to predominate at above $0.7T_M$);
d) the alloys exhibit the threshold behavior, due to dislocation - dispersoid interactions.

VIII. CONCLUSIONS

1. Ni and Al elemental and prealloyed powders have been mechanically alloyed and consolidated by hot extrusion resulting in fine grained NiAl-based alloys, containing a bimodal distribution of aluminum oxide dispersoids.
2. The dispersoids affect the progress of recrystallization and contribute to the preservation of the <110> deformation texture. The <110> texture enables the activation of {110}<100> and {110}<110> slip systems. The occurrence of <100> and <110> slip dislocations satisfies the von Mises criterion for general plasticity and is postulated to contribute to notable compressive ductility of the MA materials. Another factor likely affecting the compressive ductility is the predominant occurrence of low angle grain boundaries.
3. The MA materials are very strong at room temperature and 800K due to fine grains, the presence of dispersoids and interstitial atoms. At 800K, they exhibit compressive ductility significantly lower than that at lower and higher temperatures, resulting from the attractive dislocation-dispersoid interactions. At 1100K, the strength decreases but remains quite high (>200 MPa).
4. The MA NiAl-based materials produced in our laboratory are much stronger at both ambient and elevated temperatures and significantly more ductile than their cast counterpart.
5. Creep behavior of MA NiAl, consolidated by hot extrusion or hot pressing, has been also examined. Creep tests were carried out at temperatures between 750 and 900°C and over a wide range of stresses between 20 and 180 MPa. The apparent activation energies varied from 175 kJ/mol to 204 kJ/mol, and the values are within the range of activation energies determined in diffusion experiments. The apparent stress exponent ranged from 2 to 3.5.
6. Hot extruded MA NiAl exhibited higher creep rates due to the development of a strong <110> texture along the extrusion direction, the presence of somewhat coarser oxides and the lower level of interstitial atoms.
7. Minimum creep rates in MA NiAl were on average three orders of magnitude lower than that in their cast counterpart tested under the same experimental conditions, and significantly lower (1-4 orders of magnitude) than that measured by others in single phase NiAl. Improved creep resistance of NiAl may be postulated to result from the presence of oxide dipersoids and interstitial atoms and, to a limited extent, from its fine grain size.
8. The creep resistance of MA NiAl was found to be better than the creep resistance of solution- and other dispersion-strengthened NiAl and comparable to the creep resistance of precipitation-strengthened NiAl.
9. Taking into consideration the temperature and stress ranges in the present study, the measured values of the stress exponent and the activation energies for creep, and the occurrence of the threshold stress below which creep does not occur, one can conclude that creep in the MA NiAl materials is controlled by climb of dislocations over dispersoids.

IX. REFERENCES

1. R. Darolia, J. of Metals, 1991, vol. 43, #3, pp. 44-49.
2. D. B. Miracle, S. Russell and C. C. Law, in: High Temperature Ordered Intermetallic Alloys III, eds., C.T.Liu et al., MRS Symp. Proc., Pittsburgh 1989, vol. 133, pp. 225-230.
3. R. D. Field, D. F. Lahrman and R. Darolia, Acta Met. Mater., 1991, vol. 39, pp. 2961-2969.
4. E. M. Schulson and D. R. Baker, Scripta Met., 1983, vol. 17, pp. 519-522.
5. K. S. Chan, Scripta Met., 1990, vol. 24, pp. 1725- 1730.
6. I. Baker, P. Nagpal, F. Liu and P. R. Munroe, Acta Met. Mater., 1991, vol. 36, pp. 1637-1644.
7. K. Vedula and P. S. Khadkikar, in: High Temperature Aluminades and Intermetallics, eds., S. H Whang et al., TMS Publication, Warrendale PA, 1990, pp. 197-217.
8. I. Baker and P. R. Munroe, J. of Metals, 1988, vol. 40, #2, pp. 28-31.
9. I. Baker and P. R. Munroe, Ref. [7], pp. 425-452.
10. C. C. Koch, in: High Temperature Ordered Intermetallic Alloys II, eds., N. S. Stoloff et al., MRS Symp. Proc., Pittsburgh 1987, vol. 81, pp. 369-380.
11. J. D. Whittenberger, G. J. Gaydosh and K. S. Kumar, J. Mat. Sci., 1990, vol. 25, pp. 2771-2776.
12. J. D. Whittenberger, R. K. Viswanadham, S. K. Mannan and B. Sprissler, J. of Mat. Sci., 1990, vol. 25, pp. 35-44.
13. R. D. Noebe, R. R. Bowman and J. I. Eldridge, in: Intermetallic Matrix Composites, eds., D. L. Anton et al., MRS Proc. Symp., Pittsburgh 1990, vol. 194, pp. 323-331.
14. P. S. Gilman and J. S. Benjamin, Mechanical Alloying, Ann. Rev. Mater. Sci., 1983, vol. 13, pp. 279-300.
15. S. Dymek, S. J. Hwang, M. Dollar, J. Kallend, and P. Nash, Scripta Metall. & Mater., 1992, vol. 27, pp. 161-166.
16. M. Dollar, S. Dymek, S. J. Hwang, and P. Nash, Scripta Metall. & Mater., 1992, vol. 26, pp. 29-32.
17. M. Dollar, S. Dymek, S. J. Hwang, and P. Nash, Metall. Trans., 1993, vol. 24A, pp. 1993-2000
18. S. Dymek, S. J. Hwang, M. Dollar, and P. Nash, Mat. Sci. & Eng., 1992, vol. A152, pp. 160-165.
19. M. V. Nathal, Ordered Intermetallics - Physical Metallurgy and Mechanical Behavior, eds., C. T. Liu et al., Kluwer Academic Publishers, 1992, pp. 541-563
20. J. D. Whittenbeger, R. Ray, and S. C. Jha, Mater. Sci. Eng., 1992, vol A151, pp. 137-146
21. S. V. Raj and S. C. Farmer, High Temperature Ordered Intermetallic Alloys V, MRS Symp. Proc., eds., I. Baker, R. Darolia, J. D. Whittenberger, and M. H. Yoo, 1993, pp. 647-652
22. E. Artz, E. Göhring, and P. Grahle, Ref.[21], pp. 861-866
23. M. Dollar, P. Nash, S. Dymek, S. J. Hwang, and S. J. Suh, Annual Report, AROSR-90-015B, 1992
24. R. R. Vandervoort, A. K. Mukherjee, and J. E. Dorn, Trans. ASM, 1966, vol. 59, pp. 931-944

25. J. Bevk, R. A. Dodd, and P. R. Strutt, Metall. Trans., 1973, vol. 4, pp. 159-166
26. M. Rudy, G. Sauthoff, High Temperature Ordered Intermetallic Alloys, eds., C. C. Koch, C. T. Liu, and N. S. Stoloff, 1985, vol. 39, pp. 327-333
27. J. D. Whittenberger, J. Mater. Sci., 1988, vol. 23, pp. 235-240
28. G. F. Hancock and B. R. McDonnell, Phys. Status Solidi, 1971, vol. 4, pp. 143-150
29. A. Lutze-Birk and H. Jacobi, Scripta Met., 1975, vol. 9, pp. 761-765
30. S. Shankar and L. L. Seigle, Metall. Trans., 1978, vol. 9A, pp. 1467-1476
31. O. D. Sherby and P. M. Burke, Prog. Mater. Sci., 1968, vol. 13, pp. 325-390
32. F. A. Mohamed and T. G. Langdon, Acta Metall., 1974, vol. 22, pp. 779-788
33. R. S. Polvani, W. Tzeng, and P. R. Strutt, Metall. Trans., 1976, vol. 7A, pp. 33-40
34. J. D. Whittenberger, R. K. Viswanadam, S. K. Mannan, and K. S. Kumar, J. Mater. Res., 1989, vol. 4, pp. 1164-1171
35. J. D. Whittenberger, R. Ray, S. C. Jha, and S. Draper, Mater. Sci. Eng., 1991, vol. A138, pp. 83-93
36. S. C. Ur, personal communication, 1994
37. S. J. Suh and M. Dollar, to be submitted to Metall. Trans.
38. M. Dollar, P. Nash, and S. J. Suh, Annual Report, AFOSR-90-015B, 1993
39. D. L. Yaney, J. C. Gibeling, and W. D. Nix, Acta Metall., 1987, vol. 35, pp. 1391-1400
40. C. M. Sellars and R. A. Petkovic-Luton, Mater. Sci. Eng., 1980, vol. 46, pp. 75-87
41. J. D. Whittenberger, J. Mater. Sci., 1987, vol. 22, pp. 394-402

X. APPENDIX I

ARTICLES PUBLISHED BASED ON THE PRESENT RESEARCH

REFERRED ARCHIVAL PUBLICATIONS

1. S. Dymek, M. Dollar, P. Nash, and S. J. Hwang, "Deformation Mechanisms and Ductility of Mechanically Alloyed NiAl", Mater. Sci. & Eng., A152 (1992) 160
2. M. Dollar, S. Dymek, P. Nash, and S. J. Hwang, "The Occurrence of <110> Slip in NiAl", Scripta Metall. & Mat., 26 (1992) 29
3. S. Dymek, S. J. Hwang, M. Dollar, J. S. Kallend, and P. Nash, "Microstructure and Texture in Hot-extruded NiAl", Scripta Metall. & Mat., 27 (1992) 161
4. M. Dollar, S. Dymek, P. Nash, and S. J. Hwang, "The Role of Microstructure in Mechanically Alloyed NiAl", Metall. Trans., 24A (1993) 1993
5. S. Suh, M. Dollar, P. Nash, "Creep in Mechanically Alloyed NiAl", Mater. Sci. & Eng., accepted for publication
6. M. Dollar, S. Dymek, Reply to Discussion of "The Role of Microstructure in Mechanically Alloyed NiAl", Metall. Trans., accepted for publication
7. S. Suh and M. Dollar, "On The Threshold Stress in Mechanically Alloyed NiAl", submitted to Scripta Metall. & Mat.

ARTICLES IN REFEREED CONFERENCE PROCEEDINGS

8. S. J. Hwang, P. Nash, M. Dollar, and S. Dymek, "Microstructure and Mechanical Properties of Mechanically Alloyed NiAl", in: High-Temperature Ordered Intermetallic Alloys IV, L. A. Johnson et al. eds., Materials Research Society Proceedings Vol.213, Materials Research Society 1991, p.661
9. S. J. Hwang, P. Nash, M. Dollar, and S. Dymek, "The Production of Intermetallics Based on NiAl by Mechanical Alloying", Proc. of International Symposium on Mechanical Alloying, Kyoto, Japan 1991, Materials Science Forum Vols. 88-90, 1992, p.611
10. S. Dymek, M. Dollar, S. J. Hwang, and P. Nash, "The Role of Dispersoids in Mechanically Alloyed NiAl", in: High-Temperature Ordered Intermetallic Alloys V, I. Baker et al. eds., Materials Research Society Proceedings Vol. 288, Materials Research Society 1993, p.1117
11. S. Dymek and M. Dollar, "Slip in the Ordered B2 Alloys", Proc. of the 8th Conference on Electron Microscopy of Solids, S. Gorczyca et al. eds., Metallurgy and Materials Science Committee of the Polish Academy of Sciences, Wroclaw, 1993, p. 280
12. S. Dymek and M. Dollar, "The Effect of a Dispersed, Ordered Phase on Deformation Structure of a Ni-25%Mo- 8%Cr Alloy", Proc. of the 8th Conference on Electron Microscopy of Solids, S. Gorczyca et al. eds., Metallurgy and Materials Science Committee of the Polish Academy of Sciences, Wroclaw, 1993, p. 290
13. M. Dollar and P. Nash, "Mechanical Alloying as a Processing Route for NiAl-based Intermetallics", Processing of the 1st International Conference on Processing Materials for Properties, Honolulu, November 1993, p.663

XI. APPENDIX II

Materials Science and Engineering, A152 (1992) 160–165

Deformation mechanisms and ductility of mechanically alloyed NiAl

S. Dymek, M. Dollar, S. J. Hwang and P. Nash

Illinois Institute of Technology, Department of Metallurgical and Materials Engineering, Chicago, IL 60616 (USA)

Abstract

An NiAl-based alloy has been produced by mechanical alloying and hot extrusion, resulting in material which is fully dense, with a homogeneous distribution of oxide particles and with a fine grain size of less than 1 μm. Mechanical properties of the mechanically alloyed (MA) NiAl were studied by compression testing from room temperature to 1300 K. At room temperature, the alloy exhibited high yield strength (1380 MPa) and considerable compressive ductility (greater than 11.5%). Transmission electron microscopy of the compressed specimens was carried out. In order to determine the Burgers-vectors of slip dislocations a rigorous procedure was followed. The ⟨100⟩ slip was found to be predominant but strong evidence of ⟨110⟩ slip was also gathered. The occurrence of the slip vectors satisfies the general requirement for plasticity and contributes to the notable compressive ductility. Cast and hot extruded NiAl has been also investigated for comparison with the MA material. At room temperature, it exhibited a poor ductility (2.3%), low yield strength (400 MPa) and only ⟨100⟩ slip dislocations were observed. The ⟨100⟩ slip provides three independent slip systems, an insufficient number for general plasticity. The different behavior of cast and MA NiAl is believed to be a result of distinct textures, ⟨111⟩ and ⟨110⟩ respectively, exhibited by these differently processed materials.

1. Introduction

NiAl is a potential structural material, either in monolithic form or as a matrix phase in a composite, for high temperature applications such as gas turbine engines. A number of technological issues must be addressed before this material can be of practical use including ambient temperature brittleness. As reviewed in the discussion, several attempts to resolve the problem of ductility through alloying, grain refinement and grain boundary elimination have been made.

Our design philosophy has been to use mechanical alloying to produce very fine grained material containing dispersoids to address both the ductility and high temperature strength problems. In this work we present and discuss the results of our studies of deformation mechanisms and mechanical properties in an NiAl-based alloy, with the emphasis on the factors controlling slip systems and ductility of the alloy. For comparison with the mechanically alloyed (MA) material, the results of analogous studies on cast and extruded NiAl are also presented.

2. Experimental details

An NiAl-based alloy has been produced by mechanical alloying in a Szegvari-type attritor mill using elemental powders. The as-milled chemical composition of the alloy is given in Table 1. The MA powders were sieved and then degassed at 973 K for 1.5 h in a vacuum furnace prior to encapsulation under vacuum in a stainless steel can. The can was hot extruded at 1400 K at a ratio of 16:1 and air cooled to room temperature. A cast NiAl ingot, hot extruded at 1400 K at a ratio of 16:1, and air cooled to room temperature, was also investigated for comparison with the MA NiAl. The chemical composition of the cast material is given in Table 1.

Mechanical properties of the as-extruded MA and cast NiAl have been examined by compression tests. The compression test specimens were electrodischarge machined cylinders 10 mm in length (parallel to the extrusion direction) and 5 mm in diameter. The compression tests were performed in air from room temperature to 1300 K at a nominal strain rate of $8.5 \times 10^{-4}\ s^{-1}$ using SiC push rods.

Transmission electron microscopy (TEM) of the as-extruded MA and cast NiAl has been carried out. Thin foils for TEM were prepared from both hot extruded and compressed specimens. In order to determine the Burgers vectors of slip dislocations the procedure described by us in detail elsewhere has been followed [1]. The "near invisibility" criterion $\mathbf{g} \times \mathbf{b} = 0$ developed for anisotropic crystals by Loretto and Smallman [2] and Edington [3] was applied. During imaging of dislocations under two-beam conditions the deviation from the Bragg equation s_g was kept small and positive. Changing of s_g was used to verify whether the observed weak contrast might correspond to the condition

0921-5093/92/$5.00

TABLE 1. Chemical composition of MA and cast NiAl

Alloy	Ni	Al	Ti	Mo	C	H	N	O
MA	46.9	47.4	1.37	0.56	0.13	0.42	1.38	1.72
Cast	45.5	54.3	—	—	0.05	0.12	0.003	0.007

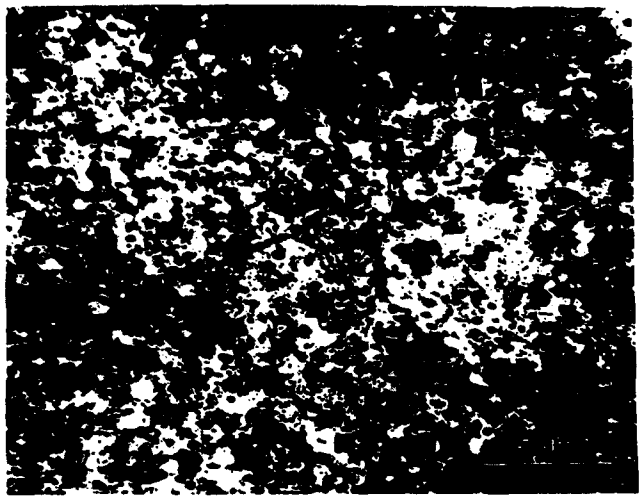

Fig. 1. Microstructure of as-extruded MA NiAl.

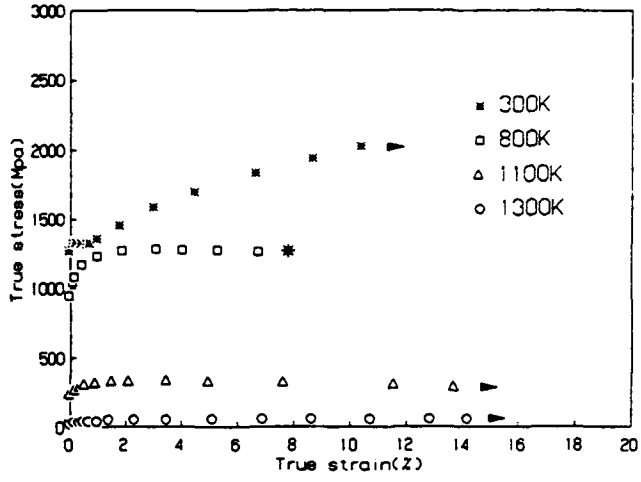

Fig. 2. Compression test results of MA NiAl from 300 to 1300 K (*, specimen fractured; ▶, test stopped).

$\mathbf{g} \times \mathbf{b} = 0$. Changing the sense of the vector $\mathbf{g}$ was also exercised.

3. Results

The microstructure of as-extruded MA NiAl can be best illustrated by a TEM image taken at a low magnification (Fig. 1). Hot extrusion resulted in material which is fully dense, with a homogeneous distribution of dispersoid particles with bimodal sizes of 10 and 100 nm and with a fine grain size of less than 1 μm. The alloy contains no titanium or molybdenum precipitates since the small amounts of titanium and molybdenum do not exceed the solubility limit [4, 5]. The cast NiAl was found to be a single phase alloy with an average grain size of about 30 μm.

Compression stress–strain curves of MA and cast NiAl at selected temperatures are shown in Figs. 2 and 3 respectively. At room temperature, MA NiAl exhibits greater than 11.5% compression ductility without cracking (the specimens were tested to load cell limits and the tests were halted before fracture occurred). However, the cast material shows poor compressive ductility, failing after 2.3% strain with evidence of many microcracks. The cast material becomes much more ductile at higher temperatures. The ductility of the MA material decreases at 800 K and again increases at higher temperatures. Figure 4

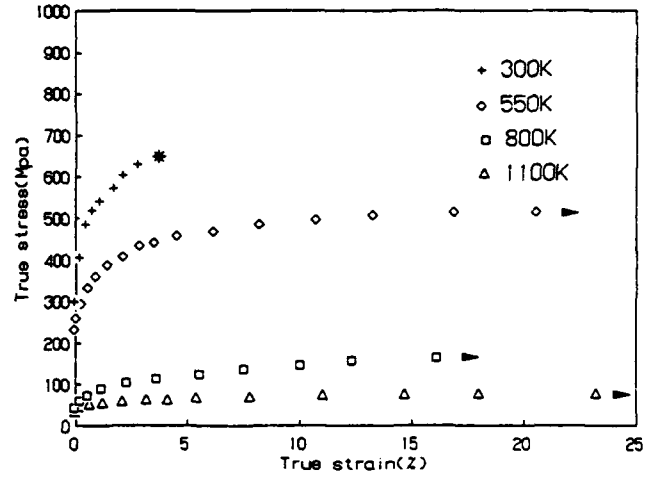

Fig. 3. Compression test results of cast NiAl from 300 to 1100 K (*, specimen fractured; ▶, test stopped).

shows the yield strength as a function of temperature for MA and cast NiAl. At all the temperatures, the MA material is at least three times stronger than its cast counterpart.

Comprehensive TEM studies of the MA material, deformed to 2% at 300, 800 and 1100 K, have been carried out. At 300 K, relatively high dislocation density was observed (Fig. 5). Dislocations are often arranged in networks but many single dislocations are observed as well. Dislocations are usually short and

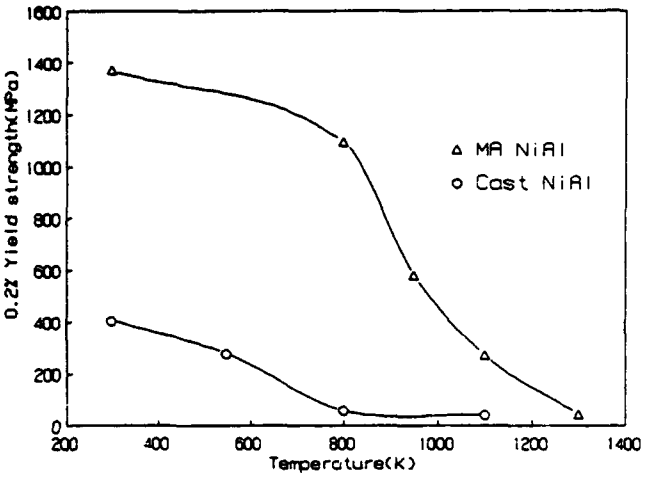

Fig. 4. The 0.2% yield strength as a function of temperature for the MA and cast NiAl.

curved, and long, straight dislocations occur very seldom. The analysis of the Burgers vectors indicates that ⟨100⟩ slip predominates. Strong evidence of ⟨110⟩ slip has also been gathered [1]. Figure 5 conclusively illustrates the occurrence of ⟨110⟩ dislocations.

Specimens tested at 1100 K exhibit much lower dislocation density than those tested at room temperature after the same amount of deformation. As in the specimens tested at room temperature, ⟨100⟩ and ⟨110⟩ slip vectors has been found.

No classical Orowan or cutting mechanisms have been observed. Instead of Orowan-type looping around particles, the dislocations are pinned on the oxides. This mechanism was found to be particularly pronounced in specimens deformed at 800 K (Fig. 6).

TEM observations of deformation structures in cast NiAl have been also conducted. Only ⟨100⟩ slip was identified at room temperature.

4. Discussion

NiAl is an equiatomic B2 aluminide with the ordered CsCl cubic structure. Several studies have been undertaken to determine the operative slip systems in NiAl. The consensus of these investigations is that this compound deforms predominantly by {110}⟨100⟩ slip at ambient temperature [6–8], hence providing only three independent slip systems, as first predicted by Copley [9]. No additional slip systems are provided by cross-slip, since the three operative slip directions are mutually at right angles [10]. Thus, the number of independent slip systems available for general deformation is insufficient because the von Mises criterion for plasticity [11]—at least five independent slip systems in a grain—is not fulfilled, and NiAl polycrystals are expected to be brittle. In fact, polycrystalline NiAl intermetallics exhibit a brittle to ductile transition in the temperature range 300–600 °C, with the exact temperature depending on composition, grain size and processing [12, 13]. This transition is believed to be the result of activation of new slip systems with vectors ⟨110⟩ and ⟨111⟩ at elevated temperature [14].

To address this shortcoming, there have been numerous attempts to change the slip vector from ⟨100⟩ to ⟨111⟩, as recently reviewed by Miracle *et al.* [15], since the {110}⟨111⟩ slip satisfies the general requirements for plasticity. The impetus for such attempts was the observation that another B2 aluminide, FeAl, deforms by {110}⟨111⟩ slip [16]. In an attempt to achieve similar results in NiAl, alloying with chromium and manganese was used, but with only partial success. Even though the ⟨111⟩ slip was successfully promoted [15], near-stoichiometric NiAl remained brittle.

In the present study, only ⟨100⟩ slip vectors were observed in cast NiAl at room temperature, in accordance with previous observations and, not surprisingly, this material exhibited very limited compressive ductility. In MA NiAl, the occurrence of {110}⟨001⟩ slip in NiAl was confirmed and, more importantly, strong evidence for ⟨110⟩ slip was obtained. To determine the number of independent slip systems in the present situation the method proposed by Groves and Kelly [17] was followed [1]. It was proven that when the ⟨001⟩ and ⟨011⟩ slip vectors are encountered, five independent slip systems operate and the von Mises requirement for general plasticity is satisfied. The operation of five independent slip systems is suggested to contribute to the notable compressive ductility of the present MA NiAl. However, it should be noted that the substantial ductility of the present MA NiAl was observed in compression tests during which fracture initiation and propagation might have been delayed compared with tensile deformation.

The present study has provided unequivocal evidence of {110}⟨110⟩ slip in NiAl. The ⟨110⟩ slip vector was noted in NiAl at ambient temperature by Pascoe and Newey [14], but it is believed that junction, not slip, dislocations were actually observed [8, 18]. Miracle [19] has recently reported that the glide of ⟨110⟩ dislocations on {110} planes is the primary mode of deformation in the vicinity of NiAl bicrystal interfaces [19].

The different behavior of cast and MA NiAl is postulated to be, above all, a result of distinct textures, ⟨111⟩ and ⟨110⟩ [20] respectively, exhibited by these differently processed materials. The predominant occurrence of grains of given orientation affects slip patterns in these grains by imposing Schmid factors. In

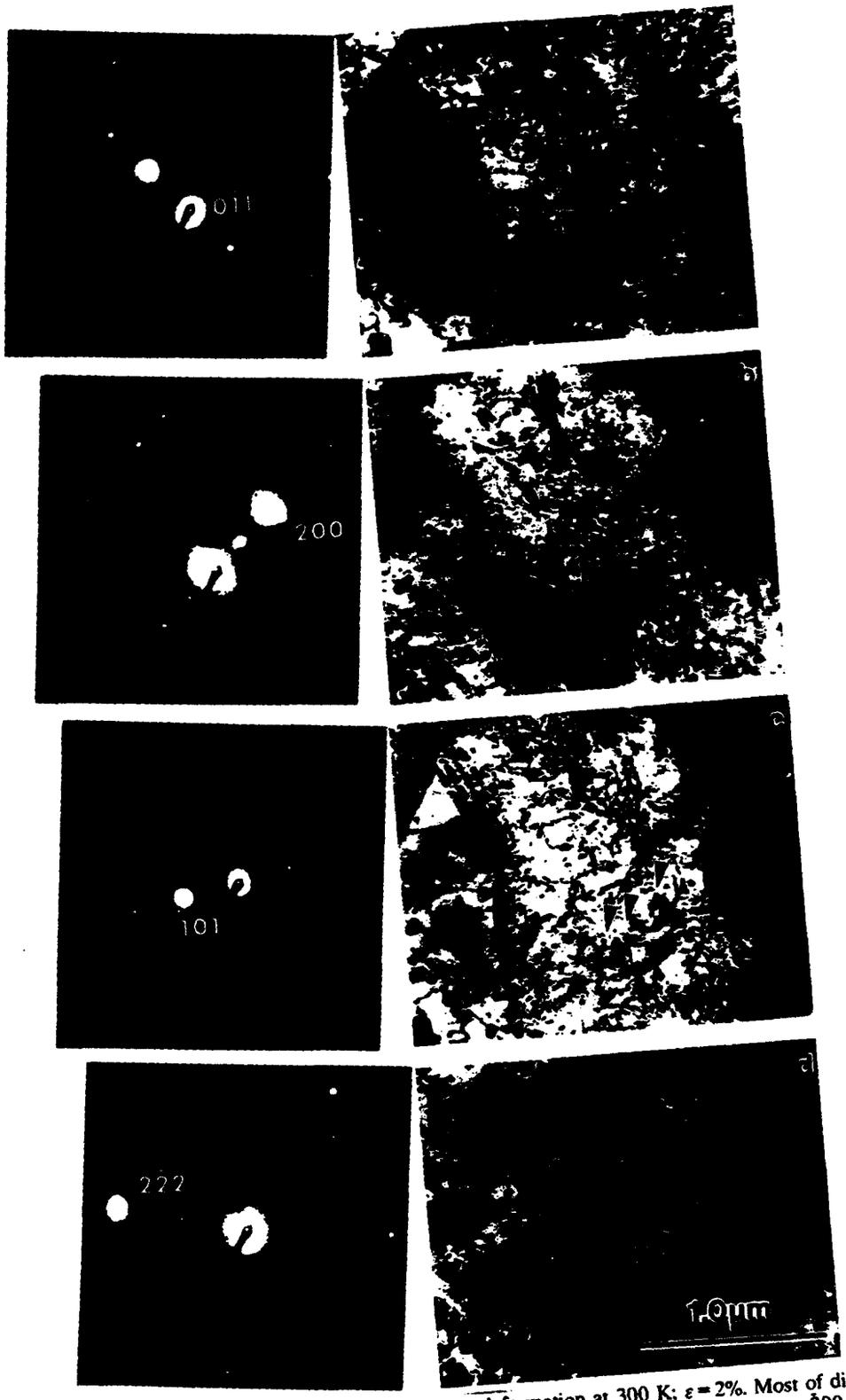

Fig. 5. Typical dislocation microstructure after deformation at 300 K; $\varepsilon = 2\%$. Most of dislocations have the ⟨100⟩ Burgers vector. Arrows indicate ⟨110⟩ dislocations exhibiting strong contrast for $g = 0\bar{1}1$ (a) and for $g = \bar{2}00$ (b), and the lack of contrast for $g = 101$ (c) and $g = 2\bar{2}2$ (d).

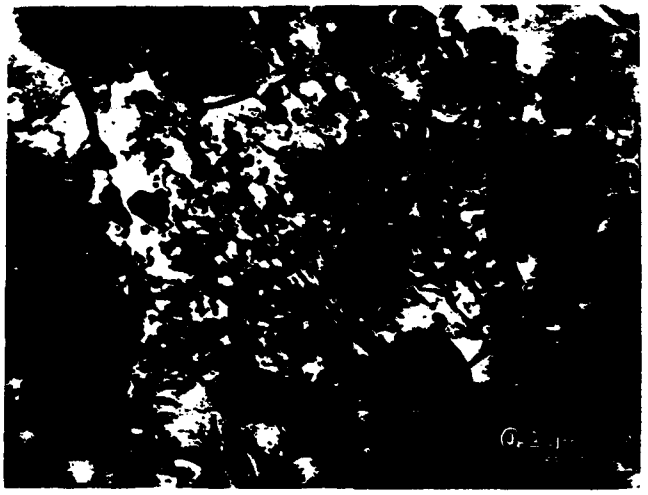

Fig. 6. Dislocations pinned on oxides after deformation at 800 K.

fact, by using Schmid's law one can calculate the imposed shear stresses in potentially active slip systems [20] and prove that the strong ⟨110⟩ texture of the MA material enables the activation of five independent slip systems (*e.g.* [100](011), [100](01$\bar{1}$), [010](101), [$\bar{1}$01](101), [0$\bar{1}$1](011)), while the ⟨111⟩ texture reduces to three the number of potentially active slip systems in the cast material (*e.g.* [100](011), [010](101), [001](110)).

The differences in ductility between cast and MA NiAl can also be attributed to the difference in grain size. Grain refinement has been suggested to be a way of obtaining ductility in NiAl [13]. Limited evidence indicates that grain size effects on ductility can be quite significant. For example, it was reported that while the ductility of NiAl at 400 °C is very low (about 2% tensile elongation) and independent of grain size for $d > 20$ μm, at finer sizes the ductility increases with decreasing grain size [13]. NiAl thus appears, at least at 400 °C, to exhibit a critical grain size below which it becomes ductile in tension. Cottrell's concept [21] that a critical grain size exists below which the stress to nucleate cracks is less than the stress to propagate them may help to explain this behavior. In fine-grained polycrystals, in terms of Cottrell's notion, crack propagation proceeds only after plastic flow has occurred. However, the adaptation of this concept in the present case would oversimplify the problem since it does not account for the different deformation mechanisms in fine-grained MA NiAl.

Owing to the very fine grain size and the presence of small, uniformly distributed oxides MA NiAl is much stronger than its cast counterpart. The higher strength is suggested to play an important role in activating additional slip systems in the MA material. The results of Ball and Smallman's approximate calculations have shown that screw dislocations of $b = \langle 110 \rangle$ have elastic energies only about 10% higher than ⟨100⟩ dislocations and are reasonably mobile at room temperature [10]. At room temperature, however, stresses required for the activation of ⟨110⟩ slip are much higher than those for the activation of ⟨100⟩ slip [12]. Thus, the fine-grained structure of MA alloys increases the stress to propagate cracks, whereas the high yield strength is sufficient to activate ⟨110⟩ slip.

In the MA NiAl the deformation structures in specimens compressed at 300 and 1100 K have been observed to be similar. The general requirement for plasticity is apparently fulfilled at both temperatures. Thus, it is not surprising that these fine-grained materials exhibit notable compression ductility in the whole range of temperatures investigated. The yield strength decreases significantly above 800 K, or 0.45 of the melting temperature. This implies a role of diffusion. It is suggested that climb of edge components of slip dislocations contributes to the decreasing strength and somewhat increasing ductility accompanying the increase in deformation temperature.

The drop of ductility observed in MA NiAl (but not in the cast material) at 800 K may be attributed to the interaction between solute atoms, such as carbon or nitrogen, and moving dislocations (dynamic strain aging) or to pinning dislocations on dispersoid particles (Fig. 6). This phenomenon, pronounced at 800 K, is under investigation.

5. Conclusions

The occurrence of ⟨100⟩ and ⟨110⟩ slip dislocations, observed in the present MA alloyed NiAl, satisfies the von Mises criterion of five independent slip systems and is suggested to contribute to substantial compressive ductility of this material.

Owing to very fine grain and the presence of dispersoid particles the MA NiAl exhibits high yield strength. The high strength, as well as the ⟨110⟩ fibre texture of the material, enable activation of the additional slip in the ⟨110⟩ direction.

Acknowledgments

This research was supported by Air Force Office of Scientific Research, under the technical direction of Dr. Alan H. Rosenstein (grant No. 90-0152B). The authors wish to thank Dr. Rosenstein, Dr. S. Copley (IIT), Dr. J. D. Whittenberger (NASA Lewis) and Dr. D. B. Miracle (AFWAL/MLLM) for helpful discussions, and Captain Chuck Ward of AFWAL/MLLM for extruding the material. We wish to thank GE Aircraft Engines for supplying the cast ingot.

References

1 M. Dollar, S. Dymek, S. J. Hwang and P. Nash, *Scr. Metall.*, *26* (1992) 29.
2 M. H. Leretto and R. E. Smallman, *Defect Analysis in Electron Microscopy*, Chapman and Hall, London, 1975.
3 J. W. Edington, *Practical Electron Microscopy in Materials Science*, Van Nostrand Reinhold, New York, 1976.
4 P. Nash, S. Fielding and D. R. F. West, *Met. Sci.*, *17* (1983) 192.
5 P. Nash and W. W. Liang, *Metall. Trans. A*, *16* (1985) 319.
6 K. Vedula and P. S. Khadkikar, in S. H. Whang, C. T. Liu, D. P. Pope and J. O. Stiegler (eds), *High Temperature Aluminides and Intermetallics*, TMS, Warrendale, PA, 1990, p. 197.
7 R. D. Noebe, R. R. Bowman, J. T. Kim, M. Larsen and R. Gibala, in S. H. Whang, C. T. Liu, D. P. Pope and J. O. Stiegler (eds), *High Temperature Aluminides and Intermetallics*, TMS, Warrendale, PA, 1990, p. 271.
8 I. Baker and P. R. Monroe, in S. H. Whang, C. T. Liu, D. P. Pope and J. O. Stiegler (eds), *High Temperature Aluminides and Intermetallics*, TMS, Warrendale, PA, 1990, p. 425.
9 S. M. Copley, *Philos. Mag.*, *93* (1963) 1599.
10 A. Ball and R. E. Smallman, *Acta Metall.*, *14* (1966) 1517.
11 R. von Mises, *Z. Angew. Math.*, *8* (1928) 161.
12 R. T. Pascoe and C. W. A. Newey, *Met. Sci. J.*, *2* (1968) 138.
13 E. M. Schulson and D. R. Barker, *Scr. Metall.*, *17* (1983) 519.
14 R. T. Pascoe and C. W. A. Newey, *Phys. Stat. Solidi*, *29* (1968) 357.
15 D. B. Miracle, S. Russell and C. C. Law, *Mater. Res. Soc. Symp. Proc.*, *133* (1989) 225.
16 I. Baker and P. R. Munroe, *J. Met.*, *40* (1988) 28.
17 G. W. Groves and A. Kelly, *Philos. Mag.*, *89* (1963) 877.
18 H. L. Fraser, R. E. Smallman and M. H. Loretto, *Philos. Mag.*, *28* (1973) 657.
19 D. B. Miracle, *Acta Metall.*, *39* (1991) 1457.
20 S. J. Huang, S. Dymek, M. Dollar, P. Nash and J. S. Kallend, submitted for publication.
21 A. H. Cottrell, *Trans. AIME*, *212* (1958) 192.

Scripta METALLURGICA et MATERIALIA
Vol. 26, pp. 29-34, 1992
Printed in the U.S.A.

THE OCCURRENCE OF <110> SLIP IN NiAl

M.Dollar, S.Dymek, S.J.Hwang and P.Nash
Metallurgical and Materials Engineering Department
Illinois Institute of Technology, Chicago Il 60616

(Received July 19, 1991)
(Revised October 15, 1991)

Introduction

As part of a broader study on microstructure, plastic deformation and mechanical properties of mechanically alloyed (MA) NiAl and NiAl-based alloys, transmission electron microscopy (TEM) investigations were carried out in order to characterize the deformation substructure after room temperature compression tests. In MA NiAl, {110} <100> slip was found to be predominant, but unequivocal evidence of <110> slip was also obtained.

This is the first observation of <110> slip in polycrystalline NiAl and the purpose of this paper is to present the evidence for its occurrence. <110> slip vectors were noted in NiAl at ambient temperatures by Pascoe and Newey (1), but it is believed that junction, not slip dislocations were actually observed (2). Miracle has recently reported that the glide of <110> dislocations on {110} planes is the primary mode of deformation in the vicinity of NiAl bicrystal interfaces (3).

The occurrence of <100> and <110> slip vectors is indeed significant since, as shown in discussion, the activity of both the <100> and <110> slip vectors satisfies the von Mises criterion of five independent slip systems for polycrystalline ductility. This contributes to the notable room temperature compressive ductility (>11.5%) of the present MA NiAl and NiAl-based alloys, which have been reported recently (4).

Experimental Details

Nickel aluminide (NiAl) with the composition: 46.9% Ni, 47.4% Al, 1.37% Ti, 0.56% Mo, 0.13% C, 0.42% H, 1.38% N and 0.72% O (at. %) has been produced by mechanical alloying in a Szegvari type attritor mill using elemental powders. The MA powders were hot extruded at 1400K at a ratio of 16:1 and cooled to room temperature, resulting in material which was fully dense, with a homogeneous distribution of oxide particles with bimodal sizes of 10 and 100 nm and with a fine grain size of less than 1 μm (Fig.1). Specimens for compression tests were electro-discharge machined from the consolidated material.

Specimens after 2% compressive deformation, chosen arbitrarily in order to establish slip vectors, have been examined. Discs for TEM were prepared from both hot extruded and compressed specimens. The discs were electrolytically thinned by a jet technique, using a solution of composition 90 ml $HClO_4$, 885 ml CH_3OH and 525 ml butyl cellosolve. Thin foils were examined at 100 kV using a JEOL 100CX microscope.

In order to determine the Burgers vectors of slip dislocations, the invisibility criterion $\mathbf{g}\cdot\mathbf{b}=0$ developed by Hirsch et al. (5) has been applied. If a crystal is isotropic and contains pure screw or edge dislocations the determination of Burgers vector is straightforward by imaging the dislocations under two-beam conditions with successively different diffracting vectors. In the case of the present MA NiAl, however, dislocations are neither purely edge nor purely screw. Also, NiAl is elastically anisotropic; the Zener anisotropy factor A of stoichiometric NiAl is 3.28 (6). For this reason a "near invisibility" criterion has been applied, i.e. very weak contrast has been interpreted on the basis that $\mathbf{g}\cdot\mathbf{b}=0$.

To ensure the correct assignment of b, some appropriate precautions, described by Loretto and Smallman (7) and Edington (8) have been also undertaken. First and foremost, the deviation from the Bragg equation s_g was kept small and positive. In practice, the position of the bright Kikuchi line in the selected area diffraction pattern (SADP) was always very close to the strongly diffracting spot. Changing of s_g was used to verify whether the observed weak contrast might correspond to the condition $\mathbf{g}\cdot\mathbf{b}=0$: if very strong contrast was observed on slightly changing the value of s_g, the previously observed weak contrast was not treated as fulfillment of the invisibility criterion. Changing of the sense of the vector g was also exercised; if $\mathbf{g}\cdot\mathbf{b}=0$ the image of the dislocation coincides with the actual position

0036-9748/92 $5.00 + .00

of the dislocation core and thus, if the sign of g is reversed, there should be no image shift. The double contrast of a dislocation observed when $\mathbf{g}\cdot\mathbf{b}=2$ and $s_g=0$, and in general, broad images observed when $\mathbf{g}\cdot\mathbf{b}=2$ or 3, were very helpful in the determination of Burgers vectors.

The above analysis was supplemented by the use of selected diffracted beams producing dark field images. If a particularly intense spot is selected the image due to this spot is then magnified without tilting the specimen so as to allow observation of the dislocation pattern. Those dislocations having their Burgers vectors lying in this reflecting plane are invisible. This method was developed by Delavignette and Amelinckx (9).

Results

TEM examination has revealed that, after 2% deformation of the present MA NiAl at room temperature, dislocation density increases significantly compared to the hot extruded material. Dislocations are often arranged in a network but many single dislocations are observed as well (Fig.2). Dislocations are usually short and curved, and long, straight dislocations occur very seldom. It is worth noting that no classical Orowan or cutting mechanism was observed. Instead of the Orowan-type looping around particles, the dislocations are pinned on the oxides.

The analysis of the Burgers vectors indicates that {110} <100> slip predominates, but an unequivocal evidence of <110> slip was also obtained. The composite figure 3 conclusively illustrates the occurrence of <110> dislocations. It is characteristic that in many grains only one type of slip vector has been found. In some grains, though, both <100> and <110> slip vectors have been observed and in such cases it is often difficult to establish whether <110> dislocations are slip or junction dislocations resulting from the interactions between <100> dislocations.

Discussion

Several studies have been undertaken to determine the operative slip systems in NiAl. The consensus of these investigations is that this compound deforms predominantly by {110} <100> slip at ambient temperatures (10-12), hence providing only three independent slip systems, as first predicted by Copley (13). No additional slip systems are provided by cross-slip, since the three operative slip directions are mutually at right angles (14). Thus, the number of independent slip systems available for general deformation is insufficient because the von Mises criterion for plasticity (15) - at least five independent slip systems in a grain - is not fulfilled, and NiAl polycrystals are expected to be brittle. In fact, polycrystalline NiAl intermetallics exhibit a brittle to ductile transition in the temperature range 300 to 600°C (16). To address this shortcoming, there have been numerous attempts to change the slip vector from <100> to <111>, as recently reviewed by Miracle et al. (17), since {110} <111> slip satisfies the general requirements for plasticity. Alloying with Cr and Mn was used, but with only partial success. Even though the <111> slip was successfully promoted (17), near-stoichiometric NiAl remained brittle.

In the present study, the occurrence of {110} <100> slip in NiAl has been confirmed and, more importantly, strong evidence for <110> slip has been obtained. To determine the number of independent slip systems in the present situation, the method proposed by Groves and Kelly (18) will be followed. The procedure requires:

a) determination of slip systems defined by:

unit vector normal to the slip plane $\mathbf{n}\ (n_x, n_y, n_z)$,
and unit vector in the slip direction $\mathbf{b}\ (b_x, b_y, b_z)$;

b) calculation of the components of the strain tensor produced by an arbitrary amount of glide on a given slip system:

$\epsilon_x = \alpha\, n_x\, b_x$, $\epsilon_y = \alpha\, n_y\, b_y$, $\epsilon_z = \alpha\, n_z\, b_z$,
$\epsilon_{ij} = \alpha/2\ (n_i\, b_j + n_j\, b_i)$, for $i, j = x,y,z$ and $i \neq j$, α = const.;

c) arbitrary choice of 5 slip systems and formation of the 5 x 5 determinant of the quantities:

$\epsilon_x^i - \epsilon_x^i$, $\epsilon_y^i - \epsilon_z^i$, ϵ_{xy}^i, ϵ_{xz}^i, ϵ_{yz}^i, for $i = 1 - 5$;

d) calculation of the value of the determinant.

If the value is other than zero, the five slip systems are independent and the general requirement for plasticity is fulfilled.

Following Groves' and Kelly's method, Ball and Smallman considered the operation of the {110} <100> slip system in NiAl and concluded, as Copley had previously done (13), that three independent slip systems, e.g. [010] (10$\bar{1}$), [001] (110) and [001] (1$\bar{1}$0) are activated and that no additional slip systems are provided by cross-slip (14).

For {110} <110> slip, we obtain strain tensors representing three possible, non-trivial slip systems (for $\alpha = 2$):

1)	2)	3)
[$\bar{1}$01](101)	[0$\bar{1}$1](011)	[$\bar{1}$10](110)
$\bar{1}$ 0 0	0 0 0	$\bar{1}$ 0 0
0 0 0	0 $\bar{1}$ 0	0 1 0
0 0 1	0 0 1	0 0 0

Since: 1) - 2) = 3), two independent slip systems are provided.

Let us consider now three {110} <100> slip systems, suggested by Ball and Smallman and two {110} <110> slip systems, 1) and 3),
and form an appropriate determinant:

$$\begin{vmatrix} 0 & 0 & 1 & 0 & \bar{1} \\ 0 & 0 & 0 & 1 & 1 \\ 0 & 0 & 0 & 1 & \bar{1} \\ \bar{2} & \bar{1} & 0 & 0 & 0 \\ \bar{2} & 1 & 0 & 0 & 0 \end{vmatrix}$$

Since no row (or column) can be expressed as a linear combination of other rows (or columns), the value of the determinant D = 0 (actually D = 12) and the five slip systems are independent.

More general analysis of {hk0} <100> and {kk0} <110> slip systems yields:

$$\begin{vmatrix} 0 & 0 & C_1 & 0 & C_2 \\ 0 & 0 & 0 & C_3 & C_4 \\ 0 & 0 & 0 & C_5 & C_6 \\ C_7 & C_8 & 0 & 0 & 0 \\ C_9 & C_{10} & 0 & 0 & 0 \end{vmatrix}$$

where C_i = const. The value of the determinant D $\neq$ 0 as well.

Thus, when the <100> and <110> slip vectors are encountered, five independent slip will operate and the von Mises requirement for general plasticity will be satisfied. This contributes to the notable compressive ductility of the present MA NiAl. The mechanism by which the slip systems are activated is under detailed investigation. The <110> texture exhibited by the present material is concluded to be of primary importance to the mechanism [19]. In addition, due to the very fine grain size and the presence of oxide dispersoids the material is very strong (σ_y = 1380 MPa). The high strength is needed to activate the <110> slip during room temperature plastic deformation. Our considerations will be published shortly (19,20).

Acknowledgements

This research was supported by Air Force Office of Scientific Research, under the technical direction of Dr. Alan H. Rosenstein (grant no. 90-0152). Dr. Rosenstein's guidance and helpful comments and discussions are strongly appreciated. The authors wish to thank Dr. S. Copley, IIT, Dr. J. D. Whittenberger, NASA Lewis and Dr. D. B. Miracle, AFWAL/MLLM for helpful discussions, and Captain Chuck Ward of AFWAL/MLLM for extruding the material.

References

1. R.T. Pascoe and C.W.A. Newey, Phys. Stat. Sol., 29, 357 (1968).
2. H.L. Fraser, R.E. Smallman and M.H. Loretto, Phil. Mag., 28, 657 (1973).
3. D.B. Miracle, Acta Met., 39, 1457 (1991).
4. S.J.Hwang, P.Nash, M.Dollar and S.Dymek, in: Materials Research Society Symposium Proceedings (Boston '89), "*High-Temperature Ordered Intermetallic Alloys IV*", L.A.Johnson et al., eds., Vol. 213, p.661. Pittsburgh (1991).
5. P.B. Hirsch, A. Howie and M.J. Whelan, Phil. Trans. R. Soc. 252A, 499 (1960).
6. R.J. Wasilewski, Trans. A.I.M.E., 236, 455 (1969).
7. M.H. Loretto and R.E. Smallman, "*Defect Analysis in Electron Microscopy*" p. 63. ed. Chapman and Hall, London, (1975).
8. J.W. Edington, "*Practical Electron Microscopy in Materials Science*" ed. Van Nostrand Reinhold Company, (1976).
9. P. Delavignette and S. Amelinckx, Phil. Mag., 5, 729 (1960).
10. K. Vedula and P.S. Khadkikar, *High Temperature Aluminides and Intermetallics*, p.197, S.H. Whang et al., eds., The Minerals, Metals and Materials Society, (1990).
11. R.D. Noebe, R.R. Bowman, J.T. Kim, M. Larsen, and R. Gibala, ibid, p.271.
12. I. Baker and P.R. Monroe, ibid, p.425.
13. S.M. Copley, Phil. Mag., 93, 1599 (1963).
14. A. Ball and R.E. Smallman, Acta Met. 14, 1517 (1966)
15. R.von Mises, Z.Angew.Math., 8, 161 (1928).
16. E.M. Schulson and D.R. Barker, Scripta Met., 17, 519 (1983).
17. D.B. Miracle, S. Russell and C.C. Law, in: "*High-Temperature Ordered Intermetallic Alloys III*", MRS Symposium Proceedings, Vol. 133, p.225 C.T.Liu et al. eds., Boston, (1989).
18. G.W. Groves and A. Kelly, Phil. Mag., 89, 877 (1963).
19. S. Dymek, M. Dollar, S.J. Hwang and P. Nash, Mat. Sci. Eng., accepted for publication.
20. J.S. Kallend, M. Wróbel, S. Dymek, M. Dollar, S.J. Hwang and P. Nash, in preparation.

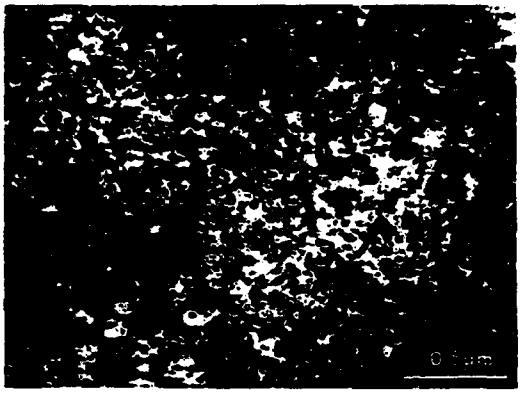

Fig:1. Transmision Electron Micrograph of as-extruded MA NiAl.

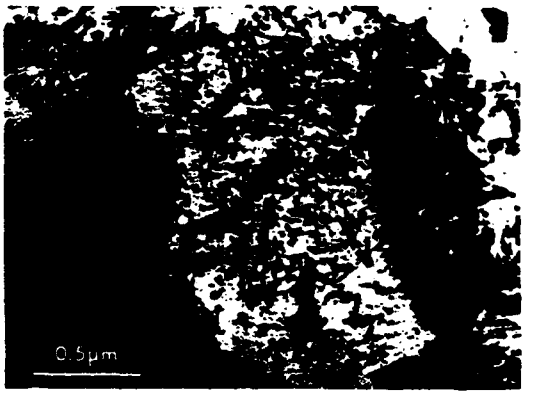

Fig.2. Typical dislocation structure of MA NiAl after 2% deformation at room temperature.

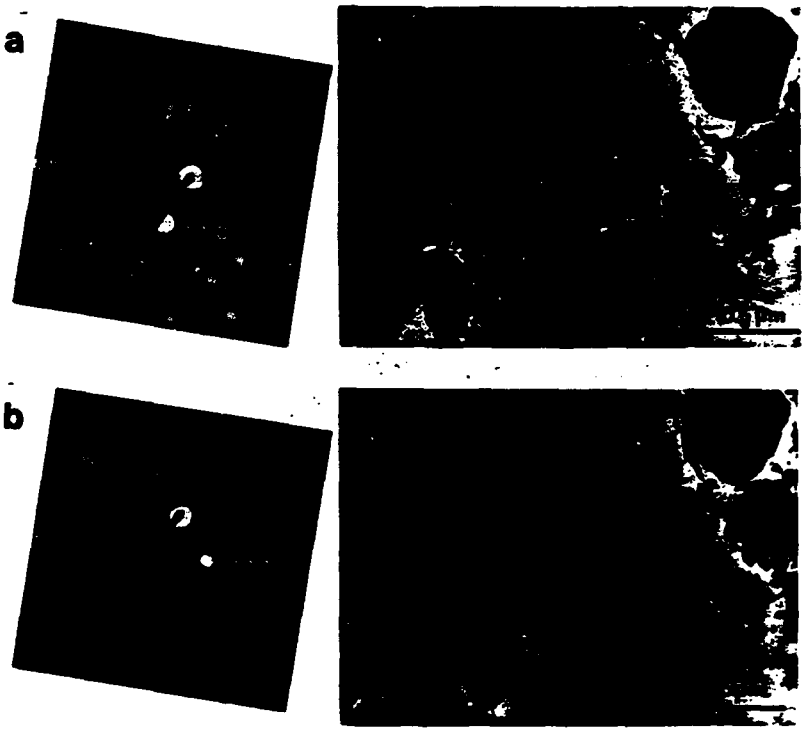

Fig.3. An analysis of the Burgers vector of the dislocations indicated by arrows. The dislocation contrast analysis of a), b) and c) eliminates the possible Burgers vector <100>, and of e) and f) - <111>. The Burgers vector of the dislocations is [10$\bar{1}$].

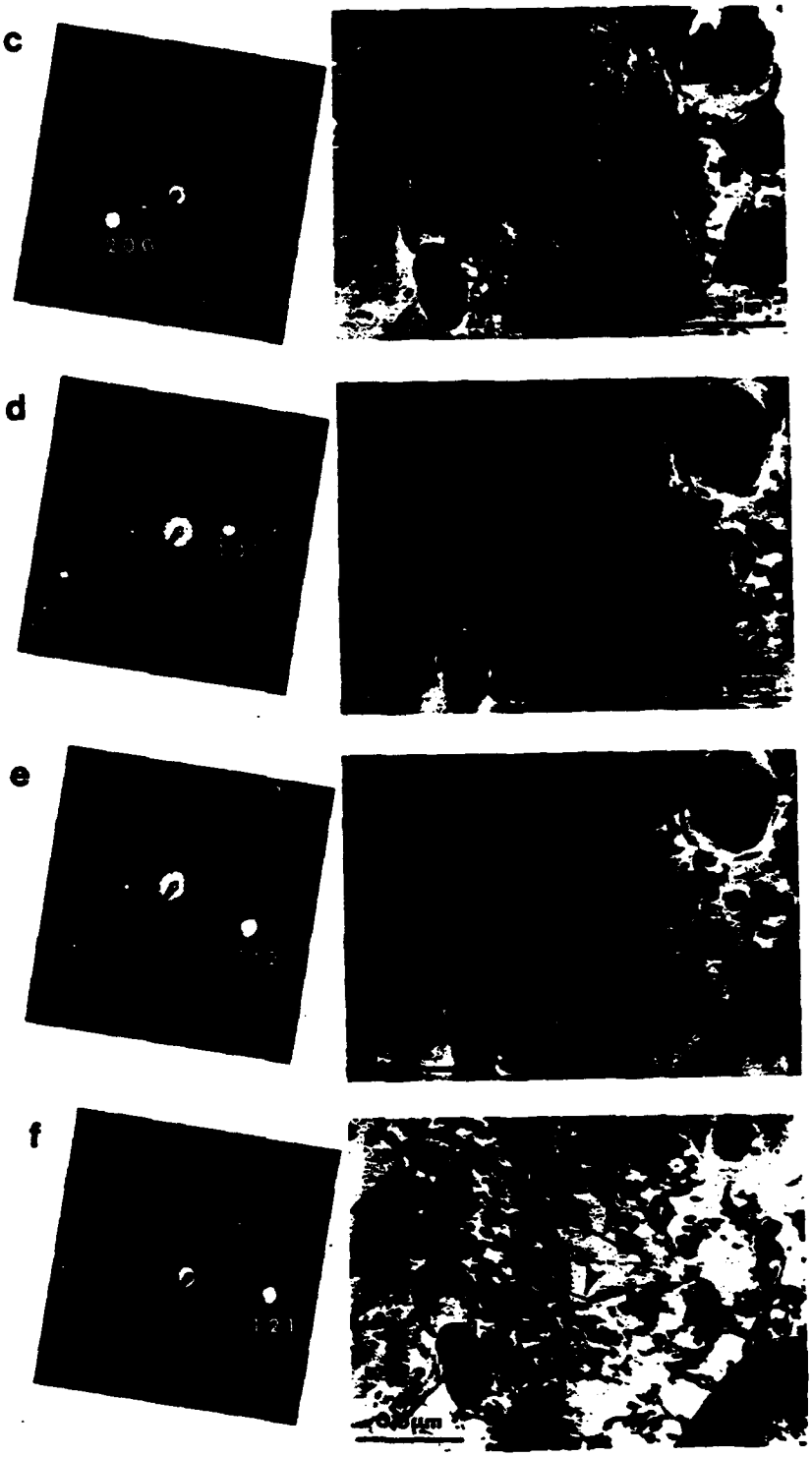
c
d
e
f

Scripta METALLURGICA et MATERIALIA
Vol. 27, pp. 161-166, 1992
Printed in the U.S.A.

MICROSTRUCTURE AND TEXTURE IN HOT-EXTRUDED NiAl

S. Dymek*, S.J. Hwang, M. Dollar, J.S. Kallend and P. Nash
Illinois Institute of Technology, Chicago, Il. 60616
*On leave from Academy of Mining and Metallurgy, Kraków, Poland

(Received May 11, 1992)

Introduction

NiAl, an ordered B2 intermetallic, is a potential structural material for high-temperature applications such as gas turbine engines. A number of technological issues must be addressed before this material can be of practical use including ambient temperature brittleness. Recently, it was shown that MA NiAl alloys exhibit an order of magnitude higher compressive ductilities than their cast counterpart (>13% vs. 2.3%, respectively) (1) and that the occurrence of <100> and <110> slip dislocations in MA materials, satisfying the von Mises criterion of five independent slip systems, contributes to the substantial compressive ductility (2). (Only {110}<100> slip systems were identified in cast NiAl). It was suggested that the different slip patterns may be a result of different textures developing in these differently processed NiAl-based materials[1].

To test this idea, texture analysis has been carried out. This paper describes the results of our studies of preferred orientations observed along the extrusion direction in both MA NiAl-based alloys and cast NiAl. The most important observation reported here is that during hot extrusion of MA and cast NiAl distinct textures, <110> and <111> respectively, develop.

The texture determination is presented along with a characterization of microstructures of hot-extruded MA and cast NiAl, since a unique microstructure of the MA materials, in particular the presence of small oxide particles, is believed to control recrystallization and ultimately texture. The present discussion is also hoped to shed light on the development of microstructure and texture during hot deformation of particle-containing polycrystals.

Experimental

In the present investigation, two NiAl-based alloys were studied, with the chemical compositions shown in Table I. One of the alloys was obtained from prealloyed NiAl powders, mechanically alloyed in an attritor mill, sieved, degassed and encapsulated under vacuum in a stainless steel can and hot extruded at 1400 K at a ratio of 16:1. The other, near-stoichiometric NiAl, was prepared from a cast ingot, hot extruded under the same conditions. The microstructure and texture of this material typifies those of other MA NiAl-based materials, including near stoichiometric alloys (4).

Table I

Alloy	Ni	Al	Ti	C	H	N	O
MA	51.96	42.26	1.38	0.14	0.1	0.5	3.62
Cast	45.5	47.4	-	0.05	0.12	0.003	0.007

Optical and transmission electron microscopy studies of longitudinal and transverse sections of the hot extruded rods were carried out to characterize the microstructure of the alloys.

[1]A likely role of texture on low temperature mechanical properties of B2 NiAl alloys was recently suggested by Hahn and Vedula (3).

0956-716X/92 $5.00 + .00

Supplementary X-ray diffraction and energy dispersive spectroscopy (EDS) examinations were conducted to determine the phase and chemical composition of the MA NiAl.

The texture was determined on transverse sections by the Schulz back reflection method using Copper K_α radiation. <110> and <200> pole figures were measured to a maximum tilt of 80°. The pole figure data were further analyzed to give orientation distribution functions and inverse pole figures using a modified WIMV algorithm (5,6).

Results

The optical microscopy observations show that the MA material is fully dense and free from cracks. The optical microstructure reveals a fairly homogenous distribution of dispersoids throughout the matrix with average particle size of about 0.1 μm (Fig.1). The particles were identified by the X-ray diffraction and EDS as alumina oxides α-Al_2O_3. The volume fraction of the dispersion phase is about 10%. The optical microscopy observations show that the cast NiAl is a single phase material with the average grain size of about 30 μm (Fig.2). The equiaxed grains observed on both longitudinal and transverse sections indicate that the material was fully recrystallized during hot extrusion.

Transmission Electron Microscopy (TEM) studies of the hot-extruded MA NiAl reveal fine, equiaxed grains with an average size of less than 1μm (Fig.3). Selected area diffraction analysis indicates that low angle grain boundaries predominate. Moreover, many grains exhibited the same contrast even after tilting the specimen over several degrees. The other important feature of an as-extruded microstructure is a bimodal distribution of alumina oxides. There are two types of oxides: coarser, with diameter of about 100nm (revealed also by optical microscopy), preferentially distributed on grain boundaries and much smaller with mean size of about 10nm, dispersed uniformly throughout the grains.

The <110> and <200> pole figures were analyzed to give orientation distribution functions and inverse pole figures. The analysis indicates that the hot extruded MA alloys have a strong <110> fiber texture parallel to the extrusion axis (Fig.4) while the hot extruded cast material has a <111> fiber texture with a minor component <331> (Fig.5). Little variation is seen around the azimuth in the pole figures. This is expected from the symmetry of the processing operation.

Discussion

The present analysis of the pole figures and the orientation distribution functions has revealed a strong <111> fiber texture along the extrusion direction in the cast and hot extruded NiAl (Fig.5). This result is consistent with the results of others: The preferred orientation, <111>, characterized by plotting inverse pole figures, was also observed along the extrusion direction in cast and extruded NiAl by Khadkakir et al. (7). TEM observations of Raj et al. revealed that 80% of grains in an as-extruded NiAl powders had a <111> texture (8).

During hot extrusion, the cast material is subjected to stress and high temperature simultaneously and dynamic recrystallization takes place. As a result, the microstructure of the as-extruded cast NiAl consists of recrystallized and equiaxed grains (Fig.2). The recrystallized microstructure in the as-extruded condition, observed in the present and other studies (7,8), as well as the observation that the <111> preferred orientation was preserved after annealing for 24 hours at the temperature of extrusion (7) indicate that the <111> texture develops as a result of recrystallization.

On the other hand, mechanically-alloyed and hot extruded NiAl-based alloys investigated in the present study show a strong <110> fiber texture. This is a common texture produced by cold drawing or extrusion in b.c.c. materials (9,10). The <110> texture was also observed in oxide dispersion strengthened ferritic alloys produced by mechanical alloying (11). Since the texture of MA powders is essentially random and featureless, the <110> texture in MA NiAl is a direct consequence of the deformation during extrusion. The development of similar deformation texture is understandable when one recalls that during high-temperature deformation of the NiAl alloys <110> and <111> Burgers vectors in addition to <100> slip are activated (12,13). The <100> and <110> dislocations slip on {110} planes (12,14). This coplanar slip as well as slip along <111> may produce similar lattice rotations as <111> pencil glide in b.c.c. metals and in consequence the same type of texture. This deformation texture is retained in MA NiAl alloys likely due to the presence of dispersoids, preventing the formation of the usual <111> texture observed in recrystallized single phase NiAl.

It is well established that the recrystallization process involves the nucleation of strain-free regions with at least one high-angle boundary capable of migration and of a size bigger than the critical one (15). Such a recrystallization process is called discontinuous or heterogeneous. The influence of dispersed second phase on the progress of

recrystallization is known to depend on the size of dispersoids and on the average distance between them (15,16). Fine ($<1\mu m$) particles are established to have a strong inhibiting effect on the recrystallization and grain growth (17). Such fine dispersoids constrain the motion of subboundaries and when their average spacing is less than a critical nucleus size (typically about 1 μm), nucleation is prevented altogether. In such a case discontinuous recrystallization often gives way to a subgrain coarsening reaction, i.e. continuous or *in situ* recrystallization (15).

In the present MA alloys, continuous recrystallization is postulated to take place. The postulate is strongly supported by TEM observations, revealing very fine equiaxed grains typically separated by low angle boundaries and pinned by the coarser oxide particles. A review of the relevant literature (17,18) indicates that the coarser dispersoids in the present (size about $0.1\mu m$, average spacing about $0.5\mu m$) belong to the class of fine, closely-spaced particles inhib ecrystallization. Pronounced deformation texture also tends to lead to an inhibition of grain growth because grains of preferred orientation are separated by low angle grain boundaries, known to have low mobility (18,19). The other likely factor inhibiting classical recrystallization in MA alloys are solutes not present in the cast alloy. TEM has provided an additional insight into the role of dispersoids on recrystallization processes in MA NiAl alloys. TEM observations revealed that most of the grains exhibited the <110> orientation, not an unexpected result. However, some grains, typically 2 - 3 times coarser than average ones, had the <111> orientation. These grains were occasionally observed in the areas relatively free of dispersoids. They are believed to result from local discontinuous recrystallization.

It is well known that the presence of dispersoids not only affects the progress of recrystallization but may also modify recrystallization texture (20). This was clearly demonstrated e.g. by Leslie (21), who examined the control of annealing texture by copper precipitation in cold-rolled iron and found that the rolling texture was retained on subsequent annealing in the presence of small copper precipitates. Kaneno et al. (22) observed that in an Al-Ge alloy discontinuous recrystallization occurred and the recrystallization texture was formed at higher annealing temperatures in the absence of precipitates, while continuous recrystallization took place and the rolling texture was retained at lower temperatures because precipitation occurred during annealing preceding recrystallization. In a recent study on hot extruded NiAl powders, Whittenberger observed a slight <110> texture after extrusion at 1100K and <111> texture after extrusion at 1400K (23).

In the present study the influence of dispersion phase is believed to be complex because of a bimodal distribution of oxide particles. The role of coarser particles has been already recognized. Smaller oxides, with mean size of about 10nm, have the strongest effect on the yield strength (24), but, as evidenced by our TEM studies, they also pin grain boundaries, contributing to the inhibition of recrystallization.

In sum, the results of our microstructural and texture studies allow us to postulate that the coarser and, to some extent, finer dispersoids in MA NiAl materials control the progress of recrystallization and contribute to the preservation of the <110> deformation texture. More specifically, the dispersoids are believed to prevent subboundaries from moving and becoming recrystallization nuclei.

Acknowledgments

This research was supported by Air Office of Scientific Research, under the technical direction of Dr. Alan H. Rosenstein (grant No. 90-0152B). The authors wish to thank Dr. J. D. Whittenberger, NASA Lewis, and Captain Chuck Ward of AFWAL/MLLM for extruding the material.

References

1. S. Dymek, M. Dollar, S.J. Hwang and P. Nash, *Mat. Sci. Eng.* in print.
2. M. Dollar, S. Dymek, S.J. Hwang and P. Nash, *Scripta Met.* 26, 29 (1992).
3. K.H. Hahn and K. Vedula, *Scripta Met.* 23, 7 (1989).
4. S.J. Hwang, PhD thesis, Illinois Institute of Technology, 1992.
5. S. Matthies and G.W. Vinel, *phys. stat. sol.* (b) 112, K111 (1982).
6. J.S. Kallend, U.F. Kocks, A.D. Rollet and H.-R. Wenk, *Mat. Sci. Eng.* A132, 1 (1991).
7. P.S. Khadkakir, G.M. Michal and K. Vedula, *Metall. Trans.* 21A, 279 (1990).
8. S.V. Raj, R.D. Noebe and R. Bowman, *Scripta Met.* 23, 2049 (1989).
9. M. Hatherly and W.B. Hutchinson, *An Introduction to Textures in Metals*, institution of Metallurgists, London 1979.
10. R.W.K. Honeycombe, *The Plastic Deformation of Metals*, p. 327, Edward Arnold (Publ.), American Society for Metals (1984).

11. A. Alamo, H. Regle, G. Pons and J.L. Bechade, *"Mechanical Alloying"*, Proc. of the Int. Symp. on Mechanical Alloying, p. 183,Kyoto, Japan, ed. P.H. Shingu, Kyoto University (1992).
12. R.T. Pascoe and C.W.A. Newey, *phys. stat. sol.* 29, 357 (1968).
13. C.H. Lloyd and M.H. Loretto, *phys. stat. sol.* 39, 163 (1970).
14. R.D. Noebe, R.R. Bowman, J.T. Kim, M. Larsen and R. Gibala, *High Temperature Aluminides and Intermetallics*, p. 271, ed. by S.H. Whang, C.T. Liu, D.P. Pope and J.O. Stiegler, The Minerals, Metals and Materials Society, (1990).
15. E. Hornbogen and U. Köster, *Recrystallization of Metallic Materials*, Rieder-Verlag GMBH, Stuttgart 1978.
16. F.J. Humphreys, *Metal Sci.* 13, 136 (1979).
17. M.F. Ashby, *Recrystallization and Grain Growth of Multi-phase and Particle Containing Materials*, p. 325, Risø Nat. Lab., Roskilde, Denemark (1980).
18. B. Ralph, *Mat. Sci. Techn.* 6, 1139 (1990).
19. G.S. Grest, D.J. Srolovitz and M.P. Anderson, *Acta Met.* 33, 509 (1985).
20. D.J. Jensen, N. Hansen and F.J. Humphreys, *ICOTOM 8*, p. 431, ed. by J.S. Kallend and G. Gottstein, The Metallurgical Society, (1988).
21. W.C. Leslie, *Metall. Trans.* 221, 752 (1961).
22. Y. Kaneno, H. Inoue and N. Inakazu, *Texture and Microstructure*, 14-18, 709 (1991).
23. J.D. Whittenberger, private communication.
24. S.J. Hwang, P. Nash, M. Dollar and S. Dymek, *Mat. Res. Soc. Symp. Proc. Vol. 213*, p. 661, Materials Research Society (1991).

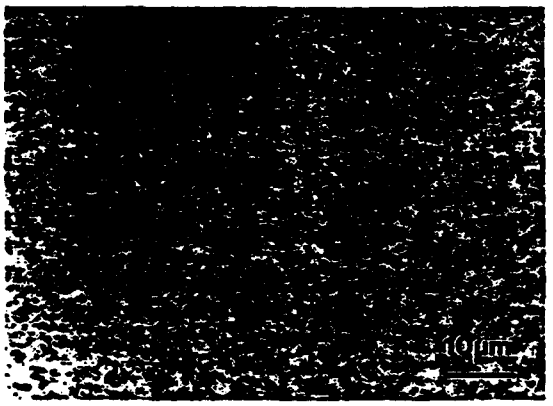

Fig.1. Optical microstructure of the as-extruded MA alloy.

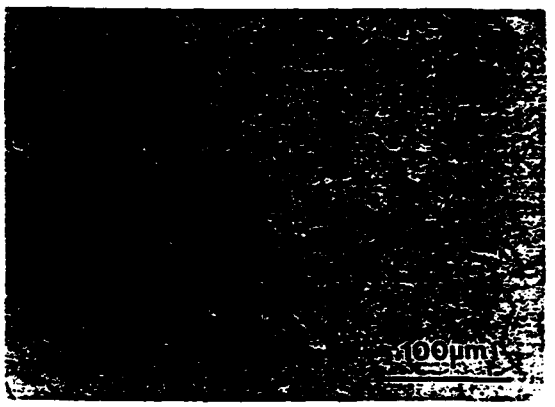

Fig.2. Optical microstructure of the as-extruded cast NiAl

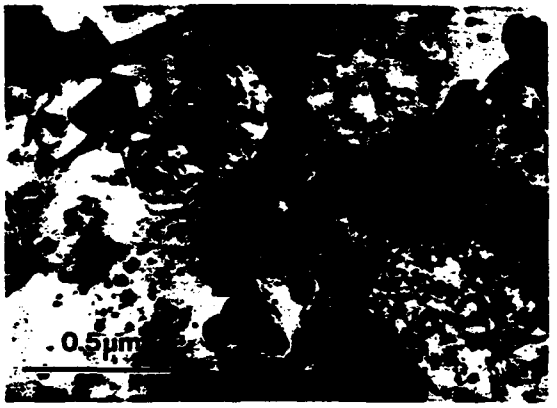

Fig.3. Typical TEM microstructure of the as-extruded alloy.

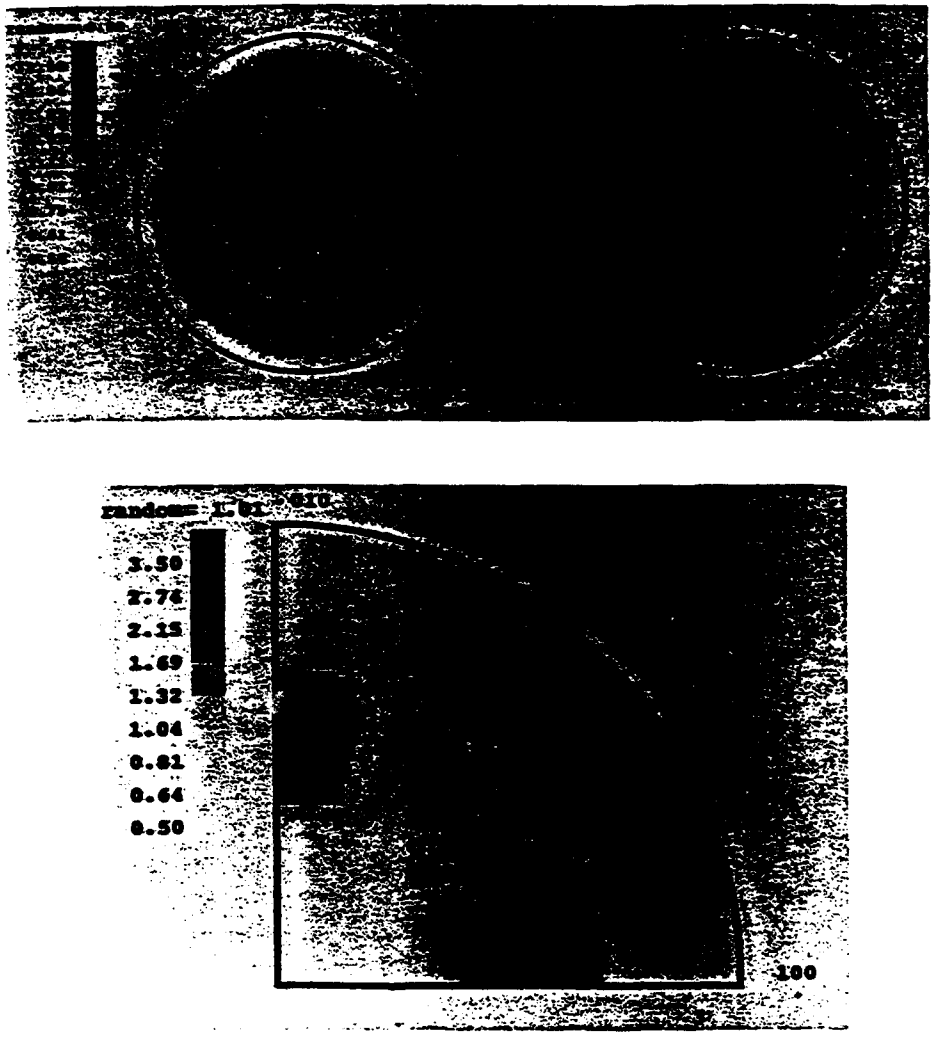

Fig.4. (110) and (200) pole figures (a) and the corresponding inverse pole figure (b) of an MA alloy.

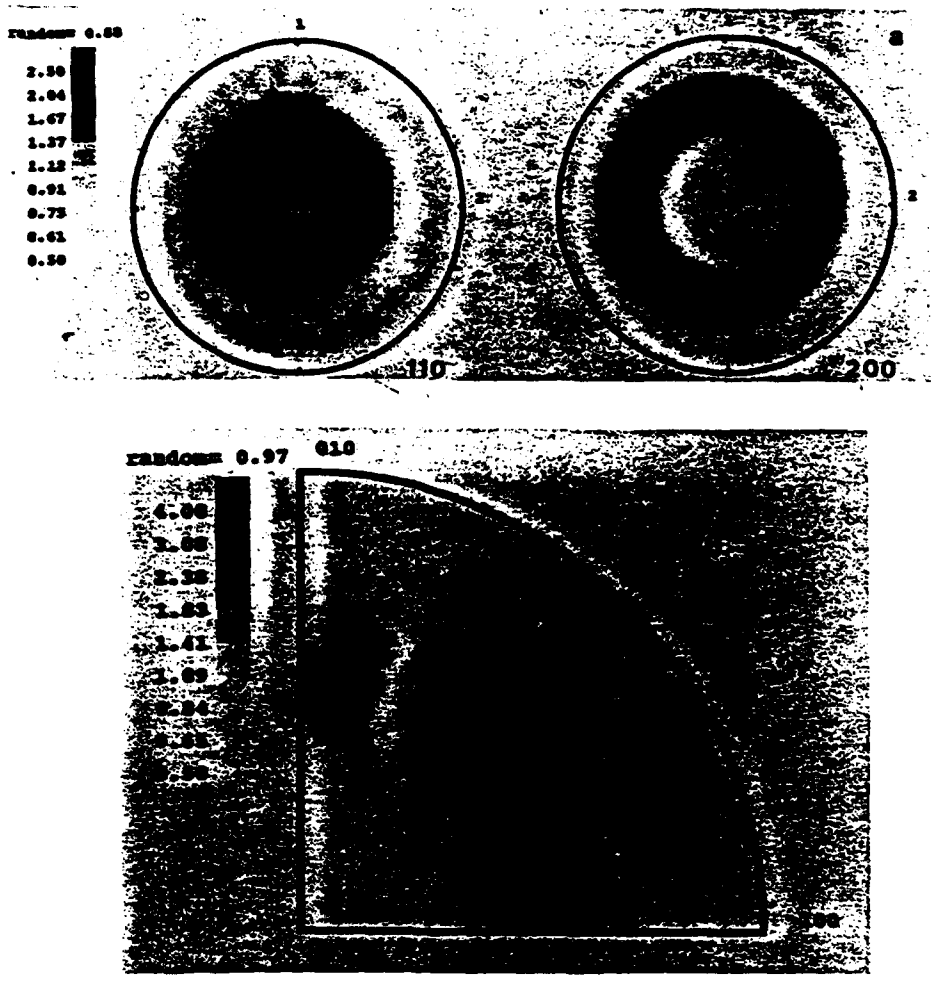

Fig. 5. (110) and (200) pole figures (a) and the corresponding inverse pole figure (b) of the as-extruded cast NiAl.

The Role of Microstructure on Strength and Ductility of Hot-Extruded Mechanically Alloyed NiAl

M. DOLLAR, S. DYMEK, S.J. HWANG, and P. NASH

Mechanical alloying followed by hot extrusion has been used to produce very fine-grained NiAl-based alloys containing oxide dispersoids. The dispersoids affect the progress of recrystallization during hot extrusion and contribute to the preservation of the ⟨110⟩ deformation fiber texture. The ⟨110⟩ texture enables the activation of {110} ⟨100⟩ and {110} ⟨110⟩ slip systems. The occurrence of ⟨100⟩ and ⟨110⟩ slip dislocations satisfies the von Mises criterion for general plasticity and is postulated to contribute to notable room-temperature compressive ductility of the mechanically alloyed (MA) materials. Another factor likely affecting the compressive ductility is the predominant occurrence of low-angle grain boundaries. The attractive dislocation—dispersoid interactions lead to a ductility trough observed at 800 K in the MA materials. The MA NiAl materials are strong at both ambient and elevated temperatures due to fine grain and the presence of dispersoids and interstitial atoms.

I. INTRODUCTION

INTERMETALLIC compounds, such as nickel, iron, and titanium aluminides, have recently emerged as a new class of potential structural materials for high-temperature applications, such as gas turbine engines. Among others, the NiAl compound is a possible high-temperature structural material, either in monolithic form or as a matrix phase in a composite, because of its low density, high melting temperature, good thermal conductivity, and excellent oxidation resistance.[1] However, before this material can be of practical use, a number of technical problems must be overcome, including lack of ductility at room temperature and poor strength at high temperatures. Several attempts to resolve the problem of room-temperature brittleness through modification of slip systems,[2,3] grain refinement,[4,5,6] grain boundary elimination,[7] and microalloying with boron[8] have been made. The successes were, at best, incomplete.[8,9] The approaches used to improve high-temperature strength included addition of dispersoids and/or precipitates[10,11] and production of composites.[12,13]

Our approach has been to use mechanical alloying followed by hot extrusion to produce several very fine-grained materials containing oxide dispersoids to address both the ambient temperature brittleness and high-temperature strength problems.[14,15] In this article, results of our studies on microstructure, texture, deformation mechanisms, and temperature-dependent mechanical properties of two selected mechanically alloyed (MA) NiAl-based materials are presented and contrasted with the analogous observations of their cast counterpart. The following discussion is focused on how the unique microstructure developed in NiAl during mechanical alloying and hot extrusion controls deformation mechanisms and improves mechanical properties. The discussion of present results is supplemented by an analysis of slip systems in MA NiAl based on our studies published recently.[16]

M. DOLLAR, Associate Professor, and P. NASH, Professor, are with the Department of Metallurgical and Materials Engineering, Illinois Institute of Technology, Chicago, IL 60616. S. DYMEK, Assistant Professor, is with the Department of Metallurgy, Academy of Mining and Metallurgy, Kraków, Poland. S.J. HWANG, Research Associate, is with the Institute of Materials Science, University of Tsukuba, Tsukuba, Japan.

Manuscript submitted December 30, 1992.

II. EXPERIMENTAL DETAILS AND RESULTS

A. *Materials*

In the present investigation, two MA NiAl-based alloys, with the chemical compositions shown in Table I, have been studied. One of the alloys, MA1, was obtained from elemental Ni and Al powders, while the other, MA2, was obtained from prealloyed NiAl powders. Both were mechanically alloyed in an attritor mill. Mechanically alloyed powders, collected after milling, were sieved to −325#, degassed at 973 K for 1.5 hours in a vacuum furnace, encapsulated under vacuum in a stainless steel can, and hot extruded at 1400 K at a ratio of 16:1. For comparison with the MA alloys, a near-stoichiometric NiAl, with the chemical composition given in Table I, was prepared from a cast ingot and hot extruded under the same conditions.

Throughout this study, experimental evidence has been gathered, indicating that the microstructure, texture, slip systems, and deformation mechanisms are similar in both MA materials despite the differences in chemical composition, and consequently, these aspects are analyzed jointly.

B. *Microstructure*

Optical microscopy and transmission electron microscopy (TEM) of the hot-extruded MA and cast NiAl have been carried out. Thin foils for TEM were prepared from both the as-extruded and compressed specimens. The optical microscopy observations showed that the hot-extruded MA materials are fully dense and free from cracks. The optical microstructure revealed a fairly homogenous distribution of dispersoids throughout the matrix, with an average particle size of about 0.1 μm (Figure 1). The particles were identified by X-ray diffraction and energy dispersive spectrometry as aluminum oxide α-Al_2O_3. Transmission electron microscopy

Table I. Chemical Composition of Examined Alloys (Atomic Percent)*

Alloy	Ni	Al	Ti	Mo	C	N	H	O
MA1	46.98	47.40	1.36	0.56	0.13	1.38	0.42	1.72
MA2	51.96	42.26	1.38	—	0.14	0.49	0.12	3.62
Cast	50.1	49.9	—	—	0.05	0.003	0.12	0.007

*The content of Ni and Al in cast NiAl sums up to 100 pct, since the analysis was conducted separately for metallic and interstitial elements.

Fig. 1—Typical optical microstructure of the hot-extruded MA alloys.

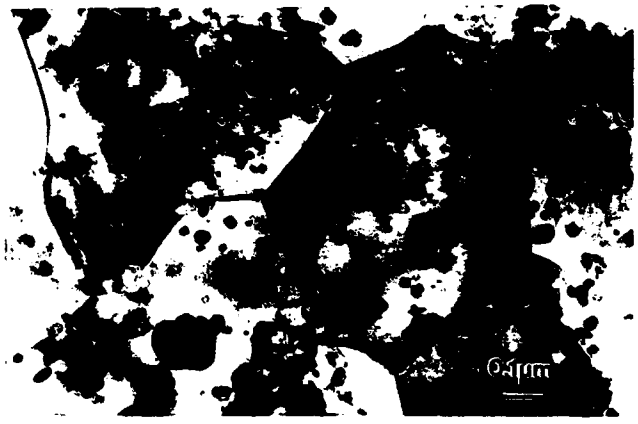

Fig. 2—Typical TEM microstructure of the hot-extruded MA alloys.

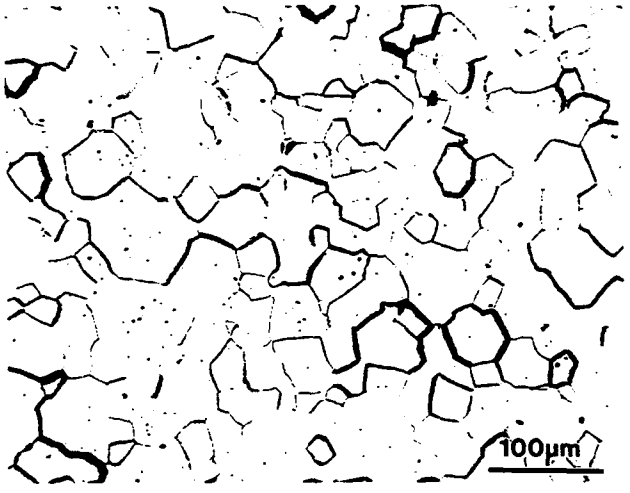

Fig. 3—Optical micrograph of the hot-extruded cast NiAl.

studies of the hot-extruded MA NiAl revealed fine, equiaxed grains with an average size of about 0.5 μm (Figure 2), separated typically by low-angle grain boundaries (the overwhelming majority of grain boundaries analyzed—69 of 76—were found to be low-angle boundaries with misorientation $\theta < 10$ deg). The other important feature of the microstructure of the MA materials is a bimodal distribution of aluminum oxides. There are two types of oxides: coarse, with a diameter of about 100 nm (revealed also by optical microscopy), preferentially distributed on grain boundaries, and much smaller, with a mean size of about 10 nm, dispersed uniformly throughout the grains.

The optical microscopy and TEM observations showed that the cast NiAl is a single-phase material with an average grain size of about 50 μm (Figure 3). The equiaxed grains observed on both longitudinal and transverse sections indicate that the material was fully recrystallized during hot extrusion.

C. *Texture*

The extrusion texture has been determined on transverse sections by the Schulz back reflection method using copper K_α radiation. The (110) and (200) pole figures were measured to a maximum tilt of 80 deg. The pole figure data were further analyzed to give orientation distribution functions and inverse pole figures using a modified Williams-Imhof-Matthies-Vinel algorithm.[17,18]

The analysis indicates that the MA alloys have a strong ⟨110⟩ fiber texture parallel to the extrusion axis (Figure 4), while the hot-extruded cast material has a ⟨111⟩ fiber texture with a minor component ⟨331⟩ (Figure 5). Little variation is seen around the azimuth in the pole figures. This is expected from the symmetry of the processing operation.

D. *Mechanical Properties*

Mechanical properties of the as-extruded MA and cast NiAl have been examined by compression tests. The compression test specimens were electrodischarge machined cylinders 10 mm in length (parallel to the extrusion direction) by 5 mm in diameter. The compression tests were performed in air from room temperature to 1300 K at a nominal strain rate of 8.5×10^{-4} s^{-1} using SiC push rods.

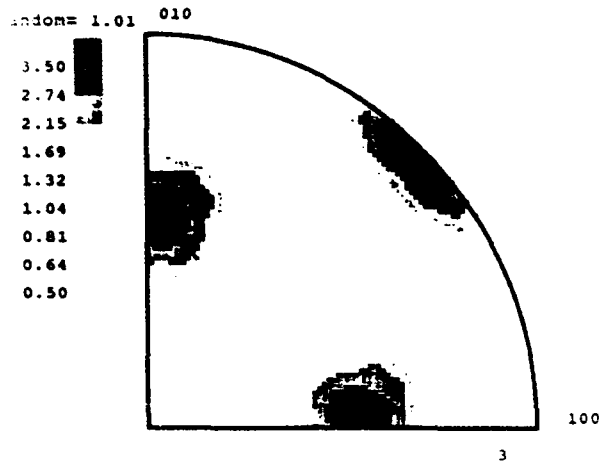

Fig. 4—Typical inverse pole figure of the hot-extruded MA alloys.

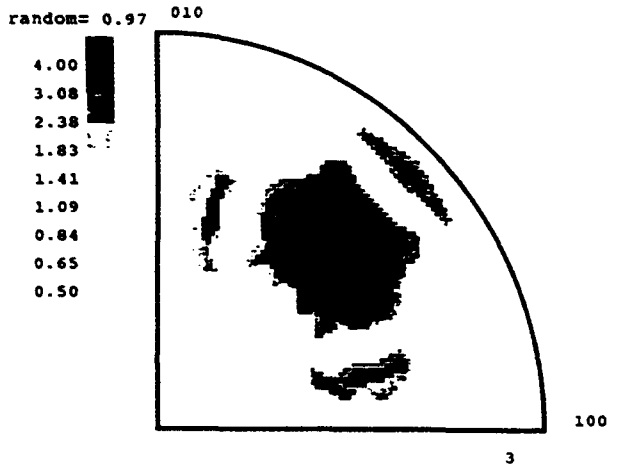

Fig. 5—Inverse pole figure of the hot-extruded cast NiAl.

The true compressive stress-strain curves of MA1, MA2, and cast NiAl at room temperature, 800 K, and 1100 K are presented in Figures 6(a) through (c), respectively. Room-temperature compression tests of the MA materials were stopped when the load on the specimen reached the limit of the Instron cell. The 1100 K tests were stopped as well, since the compressive ductilities at high temperature typically exceeded 30 pct. Selected results are shown in Table II.

Strain-rate change tests were also conducted. Strain-rate changes $\dot{\varepsilon}_2/\dot{\varepsilon}_1 = 10$ were used to measure strain-rate sensitivity, $\beta = \delta\sigma/\delta \ln \dot{\varepsilon}$.[19,20] The results for MA1 are shown in Table III.

E. *Deformation Structures*

Comprehensive TEM studies of the MA material, deformed to 2 pct at 300, 800, and 1100 K, were carried out. At room temperature, a high dislocation density, exceeding that in hot-extruded material by at least one order of magnitude, was observed (Figure 7). The transmission of slip across low-angle grain boundaries was frequently noticed (Figure 8). No classical Orowan or cutting mechanisms were observed. Instead of Orowan-type looping around particles, the dislocations were pinned on the oxides. This mechanism was found to be particularly pronounced in specimens deformed at 800 K, where nearly all dislocations were pinned on the dispersoids (Figure 9). Specimens tested at 1100 K exhibited much lower dislocation densities than those tested at room temperature and at 800 K after the same amount of deformation.

III. DISCUSSION

A. *Microstructure and Texture*

Mechanical alloying of powders followed by hot extrusion was used to produce two NiAl-based alloys, MA1 and MA2, investigated in the present study. The technique is capable of producing fully dense, crack-free, fine-grained materials containing α-Al_2O_3 particles. A unique feature of the MA materials is a bimodal distribution of the aluminum oxides, with coarser (d = 100 nm) residing predominantly at grain boundaries and smaller (d = 10 nm) dispersed uniformly throughout the grains (Figure 2). There is a remarkable contrast between the microstructure of the MA materials and their single-phase, coarse-grained, cast counterpart (Figure 3).

During hot extrusion, the cast material was subjected to stress and high temperature simultaneously and dynamic recrystallization took place. A common recrystallization texture observed in extruded cast NiAl is ⟨111⟩,[21,22] the observation confirmed in our study (Figure 5). On the other hand, the present analysis of the pole figures and the orientation distribution functions revealed a strong ⟨110⟩ fiber texture along the extrusion direction in the MA materials (Figure 4). This is a common texture produced by cold drawing or extrusion in body-centered cubic materials.[23] Since the texture of MA powders is essentially random and featureless, the ⟨110⟩ texture in MA NiAl is a direct consequence of the deformation during extrusion. This deformation texture is postulated to be retained in MA NiAl alloys due to the presence of dispersoids above all the coarser ones. The mean distance between the coarse oxides in the present alloys is much less than a critical nucleus size (typically about 1 μm) and the nucleation is prevented altogether. In such a case, discontinuous recrystallization often gives way to a subgrain coarsening reaction, *i.e.*, continuous or *in situ* recrystallization.[24] In the present MA alloys, continuous recrystallization takes place, as evidenced by TEM observations revealing very fine equiaxed grains typically separated by low-angle boundaries. The grain growth is inhibited because low-angle grain boundaries are known to have low mobility[25,26] and also are pinned by the coarse oxide particles.

B. *Slip Systems at Room Temperature*

NiAl is an equiatomic B2 aluminide with the ordered CsCl cubic structure. Several studies have been undertaken to determine the operative slip systems at ambient temperatures in NiAl. The consensus of these investigations is that this compound deforms predominantly by

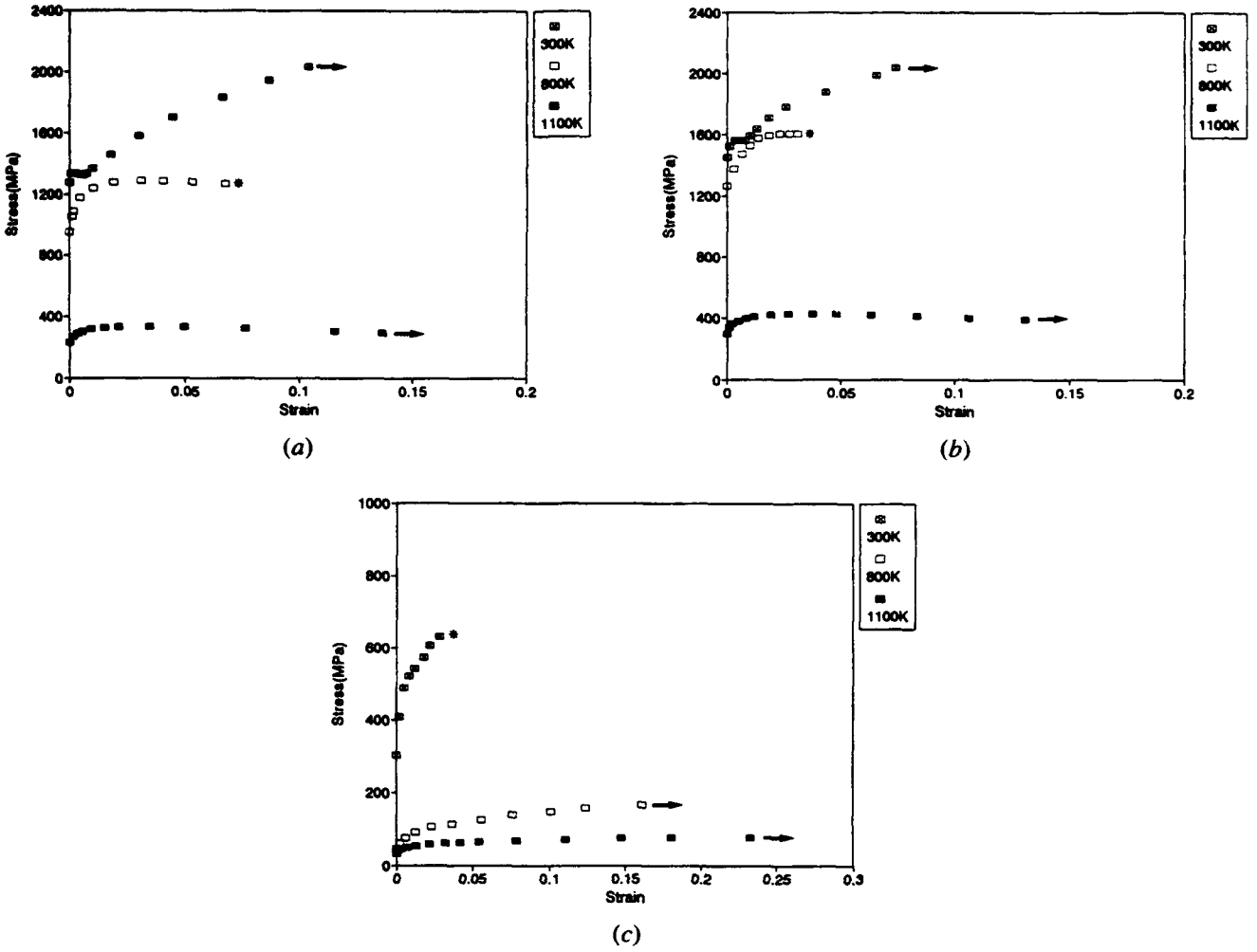

Fig. 6—The compressive stress-strain curves of examined materials (*, specimen fractured; →, test stopped): (*a*) MA1 alloy, (*b*) MA2 alloy, and (*c*) cast NiAl.

Table II. Yield Stress and Strain Untill Failure of MA1 and Cast NiAl

Alloy	Deformation Temperature (K)	Yield Stress (MPA)	Strain to Failure (pct)
MA1	300	1275	>11.5
MA1	800	950	6.8
MA1	1100	234	>13.7
Cast	300	303	2.8

{110} ⟨100⟩ slip.[9,27] As reported elsewhere,[16] the occurrence of ⟨100⟩ slip was confirmed in both MA and cast NiAl, and a strong, unequivocal evidence for ⟨110⟩ slip in the compressed specimens of the MA materials was gathered.

The different slip systems activated in the cast and MA NiAl are postulated to be a result of distinct textures exhibited by these differently processed materials. One can calculate resolved shear stresses in potentially active slip systems in a grain of given orientation by using a generalized Schmid law:[28]

$$\tau_{bn} = a_{bi}a_{nj}\sigma_{ij}$$

Table III. Strain-Rate Sensitivity, β, Measured in the MA1 Alloy at Different Temperatures and Strains

Temperature (K)	$\dot{\varepsilon}$ (cm/cm)	β (MPa)
25	0.058	−26
	0.098	−45
473	0.056	15
	0.081	−5
773	0.01	10
	0.036	10
1073	0.049	76
	0.078	85
	0.096	75

where a_{kl} = transformation coefficients;
σ_{ij} = applied stress tensor; here,

$$\sigma_{ij} = \begin{vmatrix} -1 & 0 & 0 \\ 0 & 0 & 0 \\ 0 & 0 & 0 \end{vmatrix};$$ and

τ_{bn} = resolved shear stress.

The results of calculations of resolved shear stresses in potentially active slip systems in ⟨110⟩ and ⟨111⟩ oriented grains, presented in Table IV, indicate that the strong

Fig. 7—Typical dislocation structure after 2 pct deformation at room temperature in the MA alloys.

Fig. 8—Transmission of slip across a low-angle grain boundary in the MA2 alloy.

⟨110⟩ texture of the MA material enables the activation of {110} ⟨100⟩ and {110} ⟨110⟩ slip systems, while the ⟨111⟩ texture allows only {110} ⟨100⟩ slip systems to operate.

C. *Room-Temperature Compressive Ductility*

The {110} ⟨100⟩ slip, typically observed in NiAl compound at ambient temperature, provides only three independent slip systems, as first predicted by Copley.[29] No additional slip systems are provided by cross slip, since the three operative slip directions are mutually at right angles.[30] Thus, the number of independent slip systems available for general deformation is insufficient, because the von Mises criterion for plasticity[31]—at least five independent slip systems in a grain—is not fulfilled and NiAl polycrystals are expected to be brittle. In fact, polycrystalline NiAl intermetallics exhibit a brittle to ductile transition in the temperature range 300 °C to 600 °C, depending on composition, grain size, and processing.[32] This transition is believed to be the result of activation of new slip systems with vectors ⟨110⟩ and ⟨111⟩ at elevated temperature.[33,34] In our recent study,[16] only ⟨100⟩ slip vectors were observed in cast NiAl at

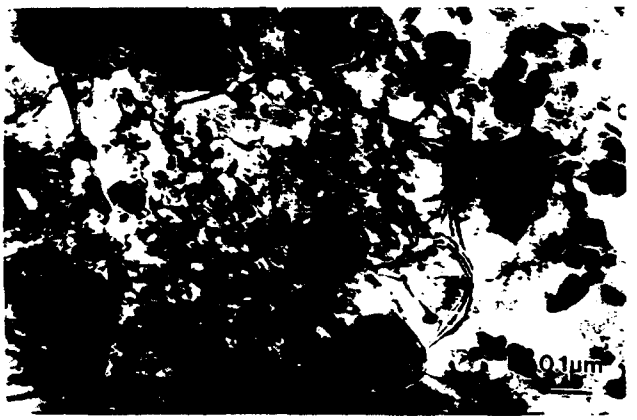

Fig. 9—Typical dislocation structure after deformation at 800 K in the MA alloys.

Table IV. Schmid Factors in Potential Slip Systems for [110] and [111] Compressed Single Crystal

Slip System	[110]	[111]
[100](01$\bar{1}$)	0.35	0.47
[100](011)	0.35	0
[010](10$\bar{1}$)	0.35	0.47
[010](101))	0.35	0
[001](1$\bar{1}$0)	0	0.47
[00$\bar{1}$](110))	0	0
[$\bar{1}$01](101)	−0.25	0
[0$\bar{1}$1](011)	−0.25	0
[110](110)	0	0

room temperature, in accordance with previous observations, and this material exhibited very limited compressive ductility.

In MA NiAl, the occurrence of {110} ⟨001⟩ slip in NiAl was confirmed and, more importantly, strong evidence for ⟨110⟩ slip was obtained.[16] To determine the number of independent slip systems in the present situation, the method proposed by Groves and Kelly[35] was followed.[16] It was proven that when the ⟨001⟩ and ⟨011⟩ slip vectors are encountered, five independent slip systems operate and the von Mises requirement for general plasticity is satisfied. The operation of five independent slip systems is suggested to contribute to a notable room-temperature compressive ductility of the MA NiAl-based materials (Table II).

Another factor postulated to contribute to the improved compressive ductility is the predominance of low-angle grain boundaries, facilitating the transmission of slip between neighboring grains (Figure 8) and likely not allowing large elastic incompatibility stresses to develop in their vicinity.

The differences in compressive ductility between cast and MA NiAl could also be attributed to the difference in grain size. Grain refinement has been suggested to be a way of obtaining ductility in NiAl.[4,5,6] Limited evidence indicates that grain size effects on ductility can be quite significant. For example, it was reported that while the ductility of NiAl at 400 °C was very low (about 2 pct tensile elongation) and independent of grain size for

$d > 20$ μm, at finer sizes, the ductility increased with decreasing grain size.[4] NiAl thus appears, at least at 400 °C, to exhibit a critical grain size below which it becomes ductile in tension. Cottrell's concept[36] that a critical grain size exists below which the stress to nucleate cracks is less than the stress to propagate them may help to explain this behavior. In fine-grained polycrystals, in terms of Cottrell's notion, crack propagation proceeds only after plastic flow has occurred.

In the present case, however, the adaptation of Cottrell's concept would not be justified. No TEM evidence was found that dislocations pile up against predominantly low-angle grain boundaries that would nucleate microcracks. Also, such boundaries would not stop microcracks.

D. *Ductility Trough at 800 K*

At 800 K, present MA NiAl-based alloys exhibited considerably lower compressive ductility than that measured in specimens deformed at lower and higher temperatures (Table II). The ductility trough was in fact observed in all MA NiAl-based materials processed in our laboratory but not in cast NiAl.

Typically, a loss of ductility at elevated temperatures is a result of dynamic strain aging (DSA). It is generally accepted that a negative strain-rate sensitivity, β, is indicative of DSA.[19,20] However, in the present study, a negative β was found at room temperature and 473 K, while at 773 K, β was positive (Table III). Thus, DSA resulting from the interactions between moving dislocations and diffusing interstitial atoms is expected to play a significant role in the present MA materials at ambient temperature rather than at 800 K.

The drop in compressive ductility at 800 K is postulated to be associated with pronounced dislocation-dispersoid interactions revealed by TEM studies. At 800 K, virtually all dislocations were found to be pinned on oxide particles (Figure 9).

Similar dislocation structures have been frequently observed in other dispersion-strengthened materials deformed at elevated temperatures; pinning of dislocations on oxides,[37–40] borides,[41,42] and carbides[43,44] has been reported. Weak beam studies of dislocation configurations in the vicinity of particles revealed that the dislocations were pinned at the departure side of the particles.[39]

The presence of such dislocation configurations implies that there is an attractive force between dislocations and particles. However, the analyses of dislocation-particle elastic interactions predict a repulsive force when the shear modulus of particles exceeds that of the matrix,[44] which is clearly the case in dispersion strengthened systems. To explain the discrepancy, Srolovitz *et al.*[44,45] and Arzt and Wilkinson[46] proposed models predicting that the interaction of dislocations with particles can change from repulsive to attractive as a result of high-temperature relaxation processes. Srolovitz *et al.* considered the effect of diffusion on the elastic interaction between dislocations and oxides and showed that diffusional relaxation of the stress state in the very vicinity of particles causes the interaction to become attractive. Arzt and Wilkinson assumed that dislocation line tension is lower in the vicinity of the particles than in the matrix and also predicted attractive interactions.

The attractive interactions between dislocations and particles are believed to result in a threshold stress for creep[43,46] and an increased creep rate at higher stresses.[47] In the present study, we postulate that the interactions lead to the loss of ductility in MA NiAl at 800 K. This postulate can be rationalized by assuming that if dislocations attach themselves to dispersoids, the recovery processes are strongly inhibited and the dislocation structure established and maintained, which is what limits the capability of the matrix to further accommodate plastic deformation.

E. *Strength*

The MA NiAl-based alloys are much stronger than the cast NiAl. The room-temperature yield strengths of MA1 and MA2 were measured to be 1275 and 1453 MPa, respectively, whereas that of the cast NiAl was 303 MPa. Several factors may be postulated to contribute to the high strength of the MA materials: grain refinement, texture, deviations from stoichiometry, and the presence of dispersoids as well as interstitial and/or substitutional solute atoms.

Off-stoichiometric MA2 is stronger than near-stoichiometric MA1, and the deviation from stoichiometry may contribute to the increase in yield stress, as suggested in Reference 7. Hwang noted that MA NiAl specimens cut parallel and perpendicular to the extrusion direction exhibit essentially the same yield stress;[48] thus, the ⟨110⟩ texture observed in the longitudinal specimens, of primary importance in controlling slip systems and ductility, does not contribute significantly to strengthening. Hwang showed also that the level of substitutional solute atoms does not influence the stress levels in MA NiAl-based materials.[48] Thus, other factors, *i.e.*, grain refinement and the presence of dispersoids and interstitials, are postulated to raise the yield stress of the MA NiAl materials to above 1200 MPa from only about 300 MPa in their cast counterpart. Though meaningful calculations of the various contributions to strength are difficult due to the extremely complex chemistry and microstructure of the MA materials, an attempt to estimate the effects of grain size and dispersoids follows.

Using Hall-Petch plots for NiAl published by Schulson and Barker (k_y = 160 MPa $\mu m^{0.5}$)[49] and by Bowman *et al.* (k_y = 522 MPa $\mu m^{0.5}$),[50] one can estimate that the increase in yield stress due to grain refinement in the MA materials (d = 0.5 μm), compared to that in the cast material (d = 50 μm), is between about 200 and 650 MPa. If an Orowan-type mechanism is assumed, the increment in strength due to dispersoids, $\delta\sigma$, is given by Ashby:[51] $\delta\sigma = (G\mathbf{b}/2\pi L) \times \ln(0.89r/\mathbf{b})$, where G = shear modulus, $\mathbf{b}$ = the Burgers vector, r = particle size, and L = interparticle spacing, using r = 10 nm, $\mathbf{b}$ = 0.29 nm, L = 70 nm, G = 72 GPa, and $\delta\sigma$ = 163 MPa. Since in the present MA materials dislocations are pinned at the departure side of oxides rather than looped around them, the Orowan stress overestimates the actual dispersoids' contributions to overall strength.[46] Because of the complex chemistry of the MA materials, it is not possible to quantify the strengthening contributions of interstitial atoms.

The strength at the intermediate temperature of 800 K

($\approx 0.4T_M$) is only about 10 pct lower than at room temperature, indicating that thermally activated climb does not yet occur. At 1100 K ($\approx 0.55T_M$), thermally activated processes facilitate the dislocation motion, resulting in significantly decreased yield stress and work hardening and improved ductility.

IV. SUMMARY

Nickel and aluminum elemental and prealloyed powders have been MA and consolidated by hot extrusion, resulting in fine-grained NiAl-based alloys containing a bimodal distribution of aluminum oxide dispersoids. The dispersoids affect the progress of recrystallization and contribute to the preservation of the ⟨110⟩ deformation texture. The ⟨110⟩ texture enables the activation of {110} ⟨100⟩ and {110} ⟨110⟩ slip systems. The occurrence of ⟨100⟩ and ⟨110⟩ slip dislocations satisfies the von Mises criterion for general plasticity and is postulated to contribute to notable compressive ductility of the MA materials. Another factor likely affecting the compressive ductility is the predominant occurrence of low-angle grain boundaries. The MA materials are very strong at room temperature and 800 K due to their fine grain and the presence of dispersoids and interstitial atoms. At 800 K, they exhibit compressive ductility significantly lower than that at lower and higher temperatures resulting from the attractive dislocation-dispersoid interactions. At 1100 K, the strength decreases but remains quite high (>200 MPa). The MA NiAl-based materials produced in our laboratory are much stronger at both ambient and elevated temperatures and significantly more ductile than their cast counterparts.

ACKNOWLEDGMENTS

This research was supported by the Air Force Office of Scientific Research, under the technical direction of Dr. Alan H. Rosenstein (Grant No. 90-0152B). The authors wish to thank Dr. Rosenstein, Dr. S.M. Copley, and Dr. J.S. Kallend from IIT; Dr. J.D. Whittenberger (NASA Lewis), Dr. D.B. Miracle (AFWAL/MLLM), and Dr. M. Wróbel from the Academy of Mining and Metallurgy in Kraków, Poland, for helpful discussions; and Dr. Whittenberger and Captain Chuck Ward of AFWAL/MLLM for extruding the material. We wish to thank GE Aircraft Engines for supplying the cast ingot.

REFERENCES

1. R. Darolia: *J. Met.*, 1991, vol. 43, (3), pp. 44-49.
2. D.B. Miracle, S. Russell, and C.C. Law: in *High Temperature Ordered Intermetallic Alloys III*, MRS Symp. Proc., C.T. Liu, A.I. Taub, N.S. Stoloff, and C.C. Koch, eds., Materials Research Society, Pittsburgh, PA, 1989, vol. 133, pp. 225-30.
3. R.D. Field, D.F. Lahrman, and R. Darolia: *Acta Metall. Mater.*, 1991, vol. 39, pp. 2961-69.
4. E.M. Schulson and D.R. Barker: *Scripta Metall.*, 1983, vol. 17, pp. 519-22.
5. K.S. Chan: *Scripta Metall.*, 1990, vol. 24, pp. 1725-30.
6. I. Baker, P. Nagpal, F. Liu, and P.R. Munroe: *Acta Metall. Mater.*, 1991, vol. 36, pp. 1637-44.
7. K. Vedula and P.S. Khadkikar: in *High Temperature Aluminides and Intermetallics*, S.H. Whang, C.T. Liu, D.P. Pope, and J.O. Stiegler, eds., TMS, Warrendale, PA, 1990, pp. 197-217.
8. I. Baker and P.R. Munroe: *J. Met.*, 1988, vol. 40 (2), pp. 28-31.
9. I. Baker and P.R. Munroe: in *High Temperature Aluminides and Intermetallics*, S.H. Whang, C.T. Liu, D.P. Pope, and J.O. Stiegler, eds., TMS, Warrendale, PA, 1990, pp. 425-52.
10. C.C. Koch: in *High Temperature Ordered Intermetallic Alloys II*, MRS Symp. Proc., N.S. Stoloff, C.C. Koch, C.T. Liu, and O. Izumi, eds., Materials Research Society, Pittsburgh, PA, 1987, vol. 81, pp. 369-80.
11. J.D. Whittenberger, G.J. Gaydosh, and K.S. Kumar: *J. Mater. Sci.*, 1990, vol. 25, pp. 2771-76.
12. J.D. Whittenberger, R.K. Viswanadham, S.K. Mannan, and B. Sprissler: *J. Mater. Sci.*, 1990, vol. 25, pp. 35-44.
13. R.D. Noebe, R.R. Bowman, and J.I. Eldridge: in *Intermetallic Matrix Composites*, MRS Proc. Symp., D.L. Anton, P.L. Martin, D.B. Miracle, and R. McMeeking, eds., Materials Research Society, Pittsburgh, PA, 1990, vol. 194, pp. 323-31.
14. S.J. Hwang, P. Nash, M. Dollar, and S. Dymek: in *High Temperature Ordered Intermetallic Alloys IV*, MRS Symp. Proc., L.A. Johnson, D.P. Pope, and J.O. Stiegler, eds., Materials Research Society, PA, 1991, vol. 213, pp. 661-66.
15. S.J. Hwang, P. Nash, M. Dollar, and S. Dymek: in *Proc. Int. Symp. on Mechanical Alloying*, Kyoto University, Kyoto, Japan, 1991, P.H. Shingu, ed., Trans. Tech. Publications, Aedermannsdorf, Switzerland, pp. 611-18.
16. M. Dollar, S. Dymek, S.J. Hwang, and P. Nash: *Scripta Metall. Mater.*, 1992, vol. 26, pp. 29-32.
17. J.S. Kallend, U.F. Kocks, A.D. Rollet, and H.-R. Wenk: *Mater. Sci. Eng. A*, 1991, vol. 132, pp. 1-11.
18. S. Matthies and G.W. Vinel: *Phys. Status Solidi B*, 1982, vol. 112, pp. 111-14.
19. A. Van Den Beukel: *Acta Metall.*, 1980, vol. 28, pp. 965-69.
20. P. Wycliffe, U.F. Kocks, and J.D. Embury: *Scripta Metall.*, 1980, vol. 14, pp. 1349-54.
21. P.S. Khadkakir, G.M. Michal, and K. Vedula: *Metall. Trans. A*, 1990, vol. 21A, pp. 279-88.
22. S.V. Raj, R.D. Noebe, and R. Bowman: *Scripta Metall.*, 1989, vol. 23, pp. 2049-54.
23. M. Hatherly and W.B. Hutchinson: *An Introduction to Textures in Metals*, Institution of Metallurgists, London, 1979.
24. E Hornbogen and U. Köster: *Recrystallization of Metallic Materials*, Rieder-Verlag GMBH, Stuttgart, 1978.
25. B. Ralph: *Mater. Sci. Technol.*, 1990, vol. 6, pp. 1139-44.
26. G.S. Grest, D.J. Srolovitz, and M.P. Anderson: *Acta Metall.*, 1985, vol. 3, pp. 509-20.
27. R.D. Noebe, R.R. Bowman, J.T. Kim, M. Larsen, and R. Gibala: in *High Temperature Aluminides and Intermetallics*, S.H. Whang, C.T. Liu, D.P. Pope, and J.O. Stiegler, eds., TMS, Warrendale, PA, 1990, pp. 271-300.
28. A. Kelly and G.W. Groves: *Crystallography and Crystal Defects*, Longman, London, 1970.
29. S.M. Copley: *Phil. Mag.*, 1963, vol. 93, pp. 1599-60.
30. A. Ball and R.E. Smallman: *Acta Metall.*, 1966, vol. 14, pp. 1517-26.
31. R. von Mises: *Z. Angew. Math.*, 1928, vol. 8, pp. 161-72.
32. J.R. Stephens and M.V. Nathal: in *Superalloys 1988*, D.N. Duhl, G. Maurer, S. Antolovich, C. Lund, and S. Reichman, eds., TMS, Warrandale, PA, 1988, pp. 183-92.
33. R.T. Pascoe and C.W.A. Newey: *Phys. Status Solidi*, 1968, vol. 29, pp. 357-66.
34. C.H. Lloyd and M.H. Loretto: *Phys. Status Solidi*, 1970, vol. 39, pp. 163-70.
35. G.W. Groves and A. Kelly: *Phil. Mag.*, 1963, vol. 89, pp. 877-87.
36. A.H. Cottrell: *Trans. AIME*, 1958, vol. 212, pp. 192-203.
37. R. Petkovic-Luton and M.J. Luton: in *Strength of Metals and Alloys*, ICMSA 7, Montreal, 1985, H.J. McQueen, ed., Pergamon Press, Elmsford, NY, 1986, pp. 743-48.
38. V.C. Nardone, D.E. Matejczyk, and J.K. Tien: *Acta Metall.*, 1984, vol. 32, pp. 1509-17.
39. J.H. Schröder and E. Arzt: *Scripta Metall.*, 1985, vol. 19, pp. 1129-34.
40. C.M. Sellars and R.A. Petkovic-Luton: *Mater. Sci. Eng.*, 1980, vol. 46, pp. 75-87.
41. S.C. Jha and R. Ray: *J. Mater. Sci. Lett.*, 1988, vol. 7, pp. 285-88.
42. S.C. Jha, R. Ray, and D.J. Gaydosh: *Scripta Metall.*, 1989, vol. 23, pp. 805-10.

43. S.C. Jha, R. Ray, and J.D. Whittenberger: *Mater. Sci. Eng. A*, 1989, vol. 119, pp. 103-11.
44. D.J. Srolovitz, M.J. Luton, R. Petkovic-Luton, D.M. Barnett, and W.D. Nix: *Acta Metall.*, 1984, vol. 32, pp. 1079-88.
45. D. Srolovitz, R. Petkovic-Luton, and M.J. Luton: *Scripta Metall.*, 1982, vol. 16, pp. 1401-06.
46. E. Arzt and D.S. Wilkinson: *Acta Metall.*, 1986, vol. 34, pp. 1893-98.
47. E. Arzt and J. Roesler: *Acta Metall.*, 1988, vol. 36, pp. 1053-60.
48. S.H. Hwang: Ph.D. Thesis, Illinois Institute of Technology, Chicago, IL, 1992.
49. E.M. Shulson and D.R. Barker: *Scripta Metall.*, 1983, vol. 17, pp. 519-22.
50. R.R. Bowman, R.D. Noebe, S.V. Raj, and I.E. Locci: *Metall. Trans. A*, 1992, vol. 23A, pp. 1493-1508.
51. M.F. Ashby: in *Oxide Dispersion Strengthening*, Proc. 2nd Bolton Landing Conf., G.S. Ansell, ed., Gordon and Breach, New York, NY, 1968, p. 143.

Creep in Mechanically Alloyed NiAl

S. SUH, M. DOLLAR, and P. NASH
Department of Metallurgical and Materials Engineering
Illinois Institute of Technology
Chicago, IL 60616

ABSTRACT

The creep behavior of mechanically alloyed (MA) NiAl, consolidated by hot extrusion or hot pressing, was examined. Hot extruded MA NiAl exhibited higher creep rates due to the development of a strong <110> texture along the extrusion direction, the presence of somewhat coarser oxides and the lower level of interstitial atoms. In general, minimum creep rates in MA NiAl were on average three orders of magnitude lower than that in their cast counterparts. Improved creep resistance of MA NiAl is postulated to result from the presence of dispersoids and interstitial atoms and, to a limited extent, from its fine grain size. Taking into consideration the temperature and stress ranges in the present study, the measured values of the stress exponent and the activation energies for creep, and the occurrence of the threshold stress below which creep does not occur, one can conclude that creep in the MA NiAl materials is controlled by climb of dislocations over dispersoid.

I. INTRODUCTION

NiAl, an intermetallic compound with the B2 ordered structure is of potential use for aerospace applications (primarily as low density aerofoil material), because of its high melting point, low density, good thermal conductivity and excellent oxidation resistance [1]. However, conventionally processed, polycrystalline NiAl suffers from ambient temperature brittleness [2], low high- temperature strength [1] and inadequate creep resistance [3].

Two processing developments, representing two extremes of microstructural control, have emerged as potential solutions to the problems mentioned above. One is the production of single crystals, pioneered by GE, which clearly has potential for the production of turbine blades, as it is the case in currently produced turbine blades made out of nickel-base, single crystal superalloys. Such processing, however, has limitations both in geometry and microstructure.

An alternative approach is to use grain refinement. Mechanical alloying (MA) of NiAl - a processing technique adopted and modified at the Illinois Institute of Technology [4, 5], used to produce dispersion strengthened fine grained materials, analogous to oxide dispersion strengthened superalloys - belongs to this category. The advantages of this powder metallurgy route are: flexible control of alloy composition and microstructure, possible near net shape processing for complex parts and ease of use for intermetallic matrix composites.

The technique allows us to produce quality powders, which when consolidated have high strength at both ambient and elevated temperatures and good compressive ductility [4]. We have shown the feasibility of producing bulk material by MA followed by consolidation and demonstrated its potential for high temperature structural applications [5]. One of the major issues which needs to be addressed is creep resistance. In this article, results of our recent studies on creep in mechanically alloyed (MA) NiAl materials are presented, discussed and contrasted with the results of analogous studies of their conventionally processed counterparts.

II. EXPERIMENTAL PROCEDURES

II.1. MATERIALS

In the present study, a nominally stoichiometric, NiAl based-material, produced by mechanical alloying of elemental Ni and Al powders and consolidated by either hot extrusion or hot pressing, has been investigated. For comparison with the MA NiAl, a near-stoichiometric, hot extruded cast NiAl has been examined as well. The chemical compositions of the consolidated materials are presented in Table 1.

Table 1. Chemical Composition of Examined Alloys (Atomic Percent)*

Alloy	Ni	Al	C	O	N	H
MA NiAl	48.32	49.74	0.56	0.63	0.12	0.63
Cast	50.1	49.9	0.06	0.007	0.003	0.12

*The content of Ni and Al in cast NiAl sums to 100 pct, since the analysis was conducted separately for metallic and interstitial elements.

II.2. CREEP TESTS

A SATEC M-3 creep machine was used in the present study. The machine is equipped with a tubular furnace with a maximum operating temperature of 1000°C. A K-type thermocouple was connected to the specimen and the test temperature was kept within +/-1.5°C tolerance at all test temperatures. The compression creep fixtures were designed for testing of MA materials. A linear variable differential transformer was used to obtain displacement-voltage responses. The voltage change associated with the sample displacement was recorded every 3 minutes and translated into strain and finally into creep curves. The constant load tests were conducted on 5 mm diameter, 10 mm long cylindrical specimens which had been electrodischarge machined from the consolidated materials, parallel to the directions of hot extrusion or hot pressing.

The apparent activation energy for creep, Q, was determined from the simple Arrhenius-type plot of temperature dependence of creep rate at constant stress:

$$Q = -R\left[\frac{\partial \ln \dot{\varepsilon}}{\partial\left(\frac{1}{T}\right)}\right]_{\sigma} \quad (1)$$

Similarly, the apparent stress exponent, n, was obtained from the plot of minimum creep rate against applied stress at a constant temperature. The exponent n is defined as:

$$n = \left[\frac{\partial \ln \dot{\varepsilon}}{\partial \ln \sigma}\right]_{T} \quad (2)$$

III. RESULTS AND DISCUSSION

III. 1. MICROSTRUCTURE

As exemplified by the optical micrograph of the hot extruded MA NiAl (Fig.1), both hot extruded (HE) and hot pressed (HP) MA materials are fully dense and free from cracks. The optical microstructures reveal also a fairly homogeneous distribution of dispersoids throughout the matrix with average particle size of about 0.1 μm. The particles were identified by X-ray diffraction and energy dispersive spectrometry as aluminum oxide, α-Al_2O_3.

TEM studies of HE and HP MA NiAl revealed fine, equiaxed grains with an average size of about 0.5μm (Fig.2). The other important feature of the microstructu of the MA materials is a bimodal distribution of aluminum oxides. There are two types of oxides: coarse, with diameter of about 100nm (revealed also by optical microscopy), preferentially distributed on grain boundaries and much smaller, with a mean size of about 10nm, dispersed uniformly throughout the grains.

The optical and transmission electron microscopy observations showed that the cast NiAl is a single phase material, fully recrystallized during hot extrusion, with an average grain size of about 50 μm.

III.2. COMPRESSIVE PROPERTIES

The yield strength of the MA NiAl materials exceeds 1200 MPa at room temperature, reaches 1000 MPa at 500°C and drops to about 350 MPa at 800°C. The yield strength of the cast NiAl is only about 300 MPa at room

temperature and decreases to less than 50 MPa at 500°C. The compressive ductility of the MA NiAl materials is significantly higher than that of the cast NiAl (for more on strength and ductility of MA NiAl and cast NiAl, see [4,5]).

III.3. CREEP BEHAVIOR

III.3.1. Creep of MA NiAl

The creep properties of HE and HP MA NiAl were investigated at 800, 850 and 900°C, and at 40, 110 and 180MPa. For HE material, additional tests at a lower stress and temperature (20MPa and 750°C) were carried out. Normalized temperatures and stresses ranged from 0.46 to $0.55T_M$ and from $2\times10^{-4}G$ to $2\times10^{-3}G$, respectively.

Creep curves obtained in the present study are typified by the creep curve for HP MA NiAl deformed at 800°C and 110MPa (Fig.3). Figure 4 illustrates the relationship between creep rate and time derived from Figure 3. As can be seen, the primary creep with a high creep rate is followed by the steady state creep which begins after about 5 - 10 hours. Tertiary creep was not observed, primarily because of crack closure during compression creep testing. Incidentally, the tertiary creep region has rarely been investigated in NiAl-based materials [6] because most testing to date has been in compression [7,8,9].

The steady state creep rates for HP MA NiAl are shown in Table 2. The effects of temperature and stress on the creep rate are illustrated in Figures 5 and 6, respectively. The analysis of the data allowed us to determine the average apparent values of activation energy for creep and stress exponent which equal, 204kJ/mol and 3.5, respectively.

Table 2. The Steady State Creep Rates (s^{-1}) for HP MA NiAl

Stress (MPa)	Temperature (°C) 800	850	900
40	2.19×10^{-9}	5.43×10^{-9}	1.04×10^{-8}
110	4.27×10^{-8}	1.42×10^{-7}	6.97×10^{-7}
180	3.91×10^{-7}	1.26×10^{-6}	1.68×10^{-6}

As mentioned before, the creep performance of HE MA NiAl was also characterized. To observe economy of space, let us just summarize this part of our research and state that the minimum creep rates in HE MA NiAL are always higher (2 - 10 times) than those in HP MA NiAl; the activation energy for creep and the stress exponent were found to be 175kJ/mol and 2, respectively.

The higher creep rates observed in HE MA NiAl may be attributed to:

i) the development of a strong, <110> fiber texture along the extrusion direction [10], and the lack of a measurable texture in HP MA NiAl; the predominant, <110> orientation of grains in hot-extruded MA NiAl is a soft orientation and may be postulated to result in a stronger creep response and higher creep rates, provided dislocation creep predominates which is the case;

ii) the presence of somewhat coarser oxides in HE material; hot extrusion was carried out at higher temperature than hot pressing which leads to a slight, but noticeable, coarsening of dispersoids likely deteriorating creep resistance;

iii) the lower level of interstitial carbon and nitrogen in HE material; during hot pressing coating materials containing carbon and nitrogen were used, increasing the content of these interstitials in the hot-pressed materials, as evidenced in another study [11].

Several other MA NiAl-based materials, with and without ternary additions, were synthesized and processed in our laboratory and their creep properties were investigated. The stress exponent in all the MA materials, including the present alloy, ranged from 2 to 3.8 while the activation energy for creep varied from 175 to 225 kJ/mol. The values of n and Q are indicative of creep mechanisms and their significance is discussed in the following section.

III.3.2. Creep of MA *versus* Cast NiAl

Creep behavior of the stoichiometric, cast NiAl was investigated under the same experimental conditions - characterized earlier - for comparison with the MA NiAl. The steady state creep rates at different

temperatures and stresses are shown in Table 3 and compared with those in HP NiAl. As can be noted there, the creep rate is on average three orders of magnitude lower in MA NiAl than in its cast counterpart tested under the same experimental conditions.

Table 3. The Minimum Creep Rates of HP MA NiAl and Cast NiAl

Stress (MPa)	800°C HP MA NiAl	Cast NiAl
20		9.4×10^{-8}
40	2.19×10^{-9}	1.5×10^{-6}
110	4.27×10^{-8}	1.0×10^{-5}
180	3.91×10^{-7}	

Compressive creep properties of single phase NiAl, both in polycrystalline and single crystal forms, were investigated by many authors [12,13,14,15]. The creep rates measured in these studies at 900°C have been plotted as a function of stress in Fig.7, along with the creep rates for HP MA NiAl. The plot shows that the present material exhibits significantly lower creep rates (on average one to four orders of magnitude) than its single phase counterparts.

Many authors have characterized the creep parameters, the activation energy for creep, Q, and the stress exponent, n, of single phase NiAl. As recently summarized by Nathal [6], the best choice for the activation energy is about 310 kJ/mol and for the stress exponent about 6. This activation energy is reasonably close to the activation energies determined in diffusion experiments which cluster between 150 and 250 kJ/mol [16,17,18]. The relatively high value of the stress exponent is close to the values of n characteristic for pure metal type, or so called Class M, creep (see criteria for classifying dislocation creep behavior, Table 4 [19,20]). In addition, subgrain formation after high temperature deformation of NiAl was observed by many authors (for review see [6]). In sum, strong experimental evidence has been accumulated indicating that dislocation creep is responsible for high temperature creep (700 -1000°C) of single phase NiAl and that the rate of the process is controlled by dislocation climb.

Table 4. Criteria for Classifying Dislocation Creep Behavior

	Class M	Class A
Controlling Mechanism	Climb	Viscous Glide
Stress Exponent	5	3
Activation Energy	Diffusion	Diffusion
Dislocation Structure	Subgrains	Homogeneous

As far as the MA NiAl alloys are concerned, the activation energies for creep (175 - 225 kJ/mol) are clearly within the range of the activation energies determined in diffusion experiments and the stress exponents (2 - 3.8) are significantly lower than for single phase NiAl. This lower value of n may be attributed to the change of the mechanism controlling creep [19].

Values of n close to 3 are characteristic for alloy-type, or so called class A, creep [19,20] (see Table 4). In solid solutions of pure metals, Class A creep is controlled by the movement of dislocations restricted by the drag of solutes, aided by vacancy diffusion [19]. The effects of solute additions on creep rate of NiAl have been summarized by Nathal [6]: the solid solution NiAl alloys exhibit lower creep rates, and values of n near 3 - 4. Thus, the creep mechanism likely changes in the presence of solute atoms from climb controlled in pure NiAl to viscous drag in solution-hardened NiAl, as is the case in solid solutions of pure metals. Such a simple explanation of the low value of n and low creep rates in the present materials cannot be adopted because MA NiAl is strengthened not only by foreign atoms, but also by oxide dispersoids and small grain size [4,5]. The same factors are postulated to contribute to improved creep resistance of MA NiAl and are discussed in the following sections.

III.3.3. The Role of Dispersoids in Controlling Creep

A unique feature of the present MA NiAl is the presence of a bimodal

distribution of aluminum oxide dispersoids. As summarized elsewhere [10], the coarse oxides, residing at grain boundaries, prevent grain growth, affect the progress of recrystallization and play an indirect role in providing the material with a notable room temperature compressive ductility. The fine oxides, dispersed throughout the grains, contribute significantly to the material's high strength at both ambient and elevated temperature. The present materials are not only strong at high temperatures but also microstructurally stable up to 1375°C [21] and these two features are believed to contribute to the much lower creep rates in MA NiAl compared to those in single phase NiAl.

Due to lack of space, a detailed discussion of the role of dispersoids in the present materials will have to be presented elsewhere [22]. In short, however, we can state here that we have gathered TEM evidence indicating that the motion of dislocations during creep deformation is hindered by dispersoids. In addition, our studies have proved that there exists a threshold stress of about 15-20 MPa below which no detectable creep occurs and a model assuming equilibrium climb over non-interacting particles has provided us with the best estimate of the threshold stress [23].

III.3.4. The Role of Grain Size

Dislocation creep mechanisms are generally considered to be independent of grain size. A review of relevant references indicates that, as a first approximation, this is true in NiAl [6]. However, in some cases, creep strength can be somewhat improved by decreasing the grain size [15,24]. It can be speculated that since NiAl is a Class M material - in which subgrain boundaries act as obstacles for dislocations - the improved creep resistance is to be expected when the grain size is finer than the equilibrium subgrain size. Possible, beneficial effects of decreasing grain size are limited to low temperatures and high stresses, where diffusional creep is of secondary importance.

The present MA NiAl materials are notably more creep resistant than their cast counterparts. It is believed to be above all due to the

presence of dispersed particles and solute atoms, but, based on the above comments on the role of grain size, the fine grain size may be postulated to contribute somewhat to the improved creep resistance in MA NiAl. In the present study, creep properties have been investigated at the temperatures 0.5 - 0.6 T_M and the stresses 10^{-3} - $5x10^{-3}$ G, thus clearly within the predominance of the dislocation creep mechanism. The small grain size of about 0.5μm is likely less than a critical subgrain size [6].

III.3.5. More on Creep of MA NiAl

As discussed above, creep of MA NiAl is controlled by diffusion. However, creep does not occur as a result of diffusional flow, but rather is controlled by resistance to dislocation motion dragged above all by dispersoids and aided by vacancy diffusion. It is so because in the present study:

a) creep was investigated in the stress range between 5 x 10^{-4}G and $5x10^{-3}$G (diffusional flow is believed to predominate at < 10^{-4}G [25]);

b) the values of the stress exponent n are low, but much higher than that associated with diffusional flow [19];

c) test temperatures are between 0.5 and 0.6 T_M (diffusion creep is believed to predominate at above 0.7T_M);

d) the alloys exhibit the threshold behavior, due to dislocation - dispersoid interactions.

IV. CONCLUSIONS

1. Creep behavior of MA NiAl, consolidated by hot extrusion or hot pressing, has been examined. Creep tests were carried out at temperatures between 750 and 900°C and over a wide range of stresses between 20 and 180 MPa. The apparent activation energies varied from 175 kJ/mol to 204 kJ/mol, and the values are within the range of activation energies determined in diffusion experiments. The apparent stress exponent ranged from 2 to 3.5.

2. Hot extruded MA NiAl exhibited higher creep rates likely due to the development of a strong <110> texture along the extrusion direction, the presence of somewhat coarser oxides and the lower level of interstitial atoms.

3. Minimum creep rates in MA NiAl were on average three orders of magnitude lower than that in their cast counterpart tested under the same experimental conditions, and significantly lower (1-4 orders of magnitude) than that measured by others in single phase NiAl. Improved creep resistance of NiAl may be postulated to result from the presence of oxide dipersoids and interstitial atoms and, to a limited extent, from its fine grain size.

4. Taking into consideration the temperature and stress ranges in the present study, the measured values of the stress exponent and the activation energies for creep, and the occurrence of the threshold stress below which creep does not occur, one can conclude that creep in the MA NiAl materials is controlled by climb of dislocations over dispersoids.

V. ACKNOWLEDGEMENTS

This research was supported by the Air Force Office of Scientific Research, under the technical direction of Dr. Alan H. Rosenstein (Grant No. 90-0152B).

VI. REFERENCES

1. R. Darolia, *J. Met.*, 43 (1991) #3, 44.
2. I. Baker and P. R. Monroe, *J. Met.*, 40 (1988) #2, 28.
3. G. Sauthoff, in *Proc. of the German Society of Materials Science Conference on Microstructure and Mechanical Properties of Materials*, Bad Nauheim, 1991, p.363.
4. S. Dymek, M. Dollar, P. Nash, and S. J. Hwang, *Mater. Sci. Eng., A152* (1992) 160.
5. M. Dollar, S. Dymek, P. Nash, and S. J. Hwang, *Metall. Trans., 24A*

(1993) 1993.

6. M. V. Nathal, in C. T. Liu (eds), *Ordered Intermetallics*, Kluwer Academic Publisher, Netherlands, 1992, p. 541.
7. J. D. Whittenberger, R. Ray, and S. C. Jha, *Mater. Sci. Eng., A151* (1992) 137.
8. E. Arzt, E. Göhring, and P. Grahle, in I. Baker, R. Darolia, J. D. Whittenberger, and M. H. Yoo (eds) *High Temperature Ordered Intermetallic Alloys V*, MRS Symp. Proc., 288, 1993, p. 861.
9. S. V. Raj and S. C. Farmer, in I. Baker, R. Darolia, J. D. Whittenberger, and M. H. Yoo (eds) *High Temperature Ordered Intermetallic Alloys V*, MRS Symp. Proc., 288, 1993, p. 647.
10. S. Dymek, S. J. Hwang, M. Dollar, J. Kallend, and P. Nash, *Scripta Metall., 27* (1992) 83.
11. M. Dollar, P. Nash, S. Dymek, S. J. Hwang, and S. Suh, *Annual Report, AFOSR-90-0152B*, (1992) p. 67.
12. R. R. Vandervoort, A. K. Muhkerjee, and J. E. Dorn, *Trans. ASM, 59*, (1966) 931.
13. J. Bevk, R. A. Dodd, and P. R. Strutt, *Metall. Trans., 4* (1973) 159.
14. M. Rudy and G. Sauthoff, in C. C. Koch, C. T. Liu, and N. S. Stoloff (eds), *High Temperature Ordered Intermetallic Alloys*, MRS Symp. Proc., 39, (1985) p. 327.
15. J. D. Whittenberger, *J. Mater. Sci., 23*, (1988) 235.
16. G. F. Hancock and B. R. McDonnell, *Phys. Status Solidi, 4*, (1971) 143.
17. A. Lutze-Birk and H. Jacobi, *Scripta Metall., 9*, (1975) 779.
18. S. Shanker and L. L. Siegle, *Metall. Trans., 9A*, (1978) 1467.
19. O. D. Sherby and P. M. Burke, *Prog. Mater. Sci., 13*, (1968) 325.
20. F. A. Mohamed and T. G. Langdon, *Acta Metall., 22*, (1974) 779.
21. S. C. Ur, personal communication, 1994.
22. S. Suh and M. Dollar, "in preparation"
23. M. Dollar, P. Nash, and S. Suh, *Annual Report, AFORS-90-0152B*, (1993) p. 58.
24. D. L. Yaney and W. D. Nix, *J. Mater. Sci., 22*, (1988) 3088.
25. C. M. Sellars and R. Petkovic-Luton, *Mater. Sci. Eng., 46*, (1980) 75.

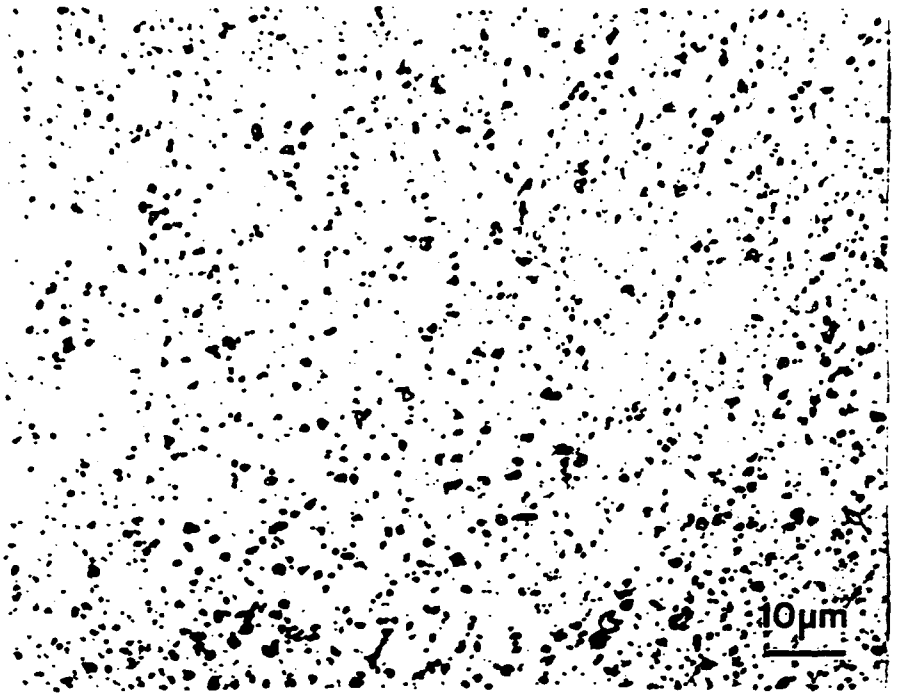

Figure 1. Optical Micrograph of the Hot-Extruded MA NiAl

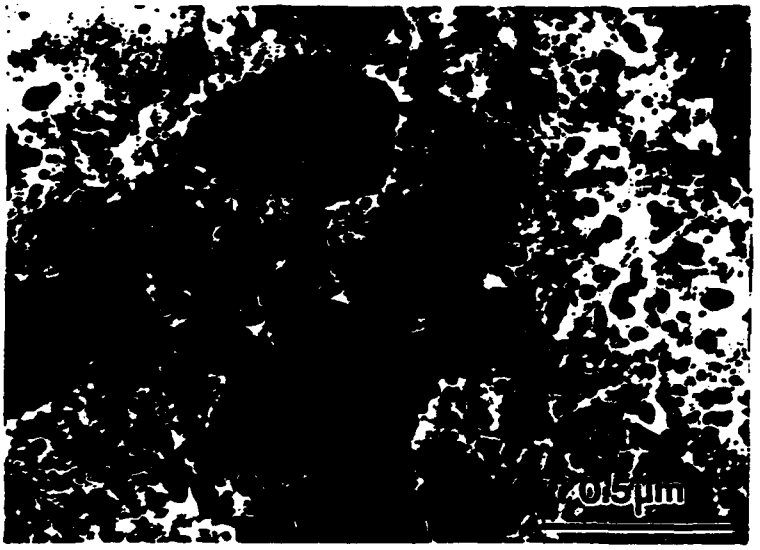

Figure 2. Typical TEM Microstructure of the Hot-Extruded MA NiAl

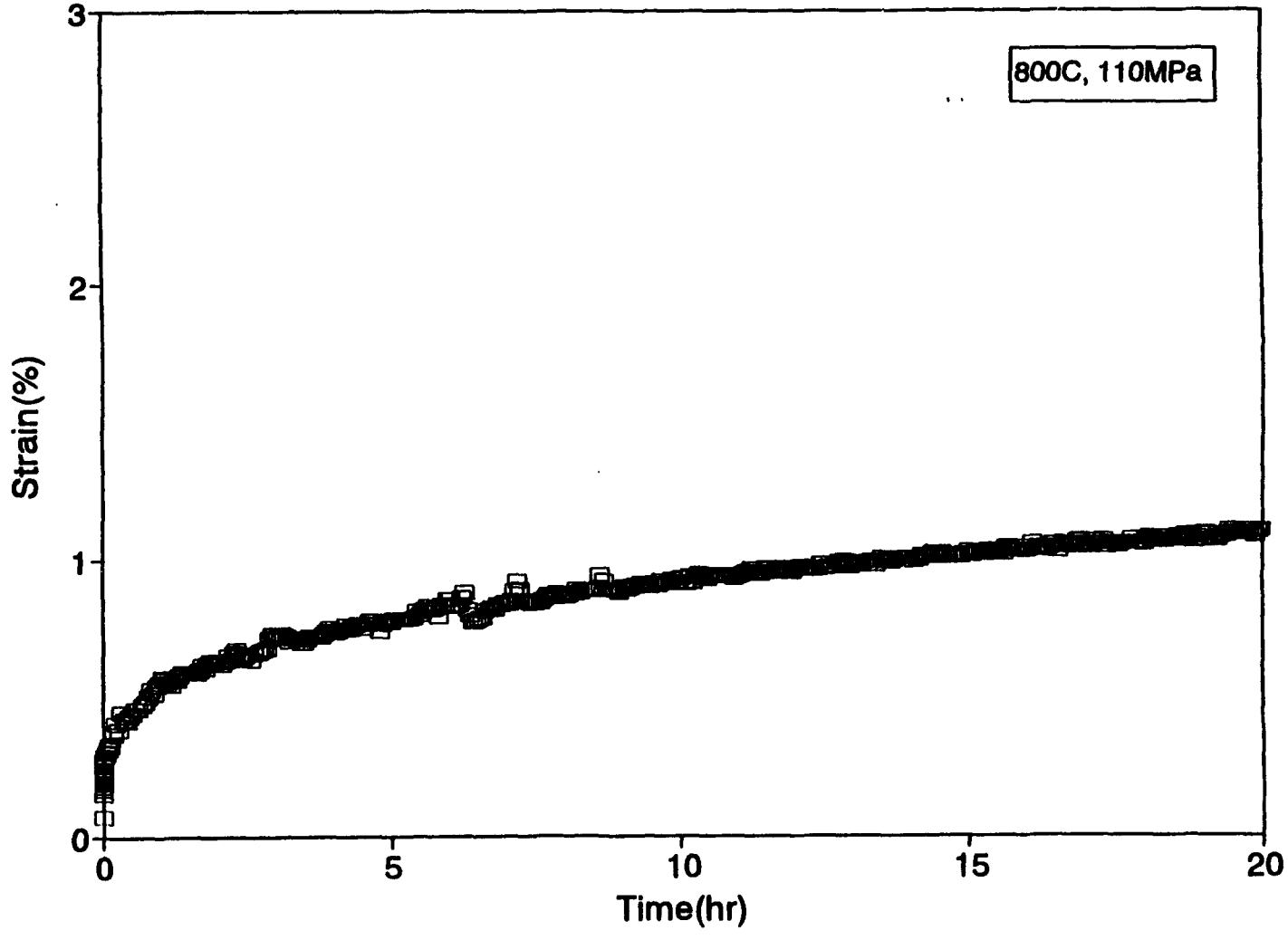

Figure 3. Creep Curve for Hot Pressed MA NiAl Deformed at 800°C and 110MPa

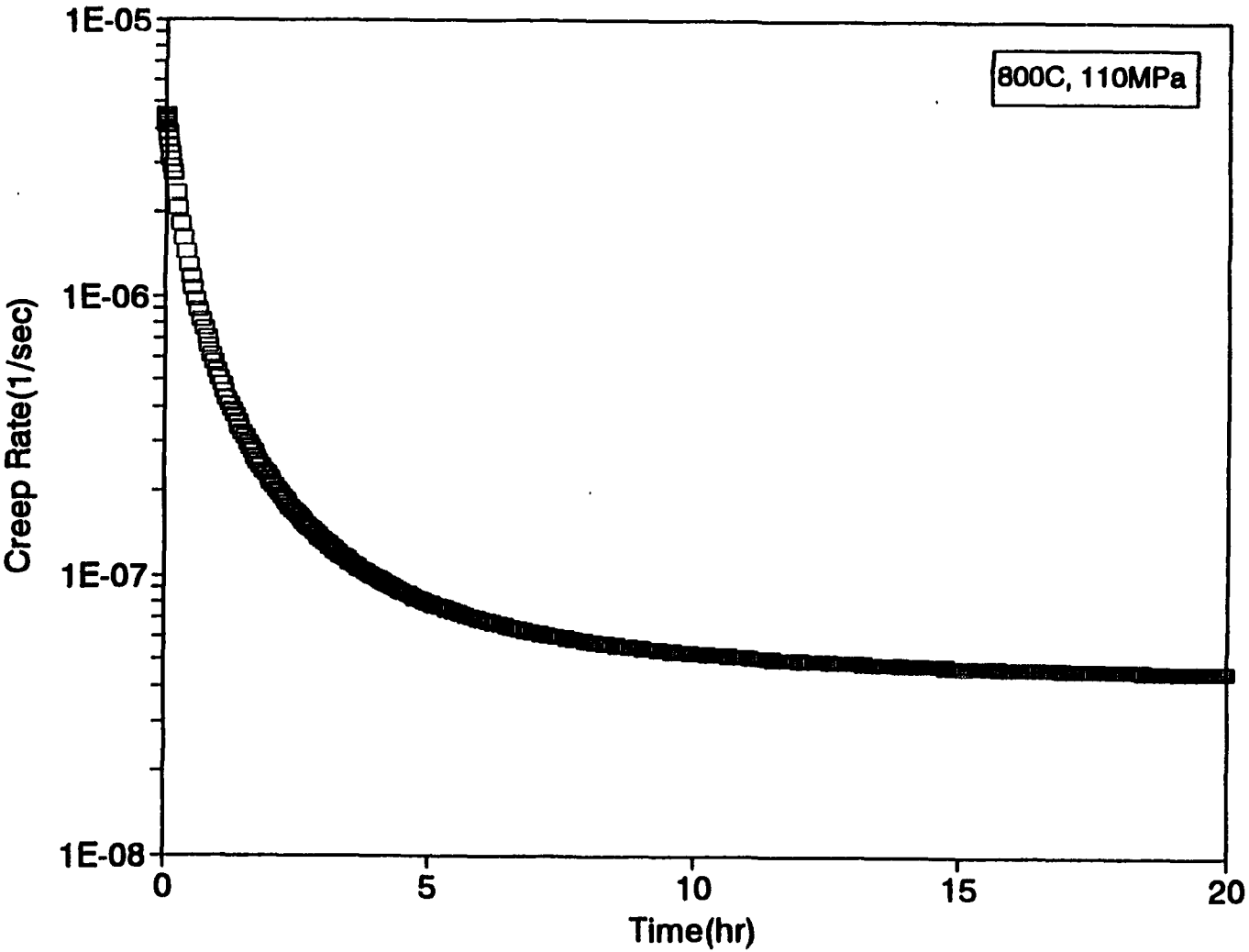

Figure 4. The Creep Rate as a Function of Time for Hot Pressed MA NiAl Deformed at 800°C and 110MPa

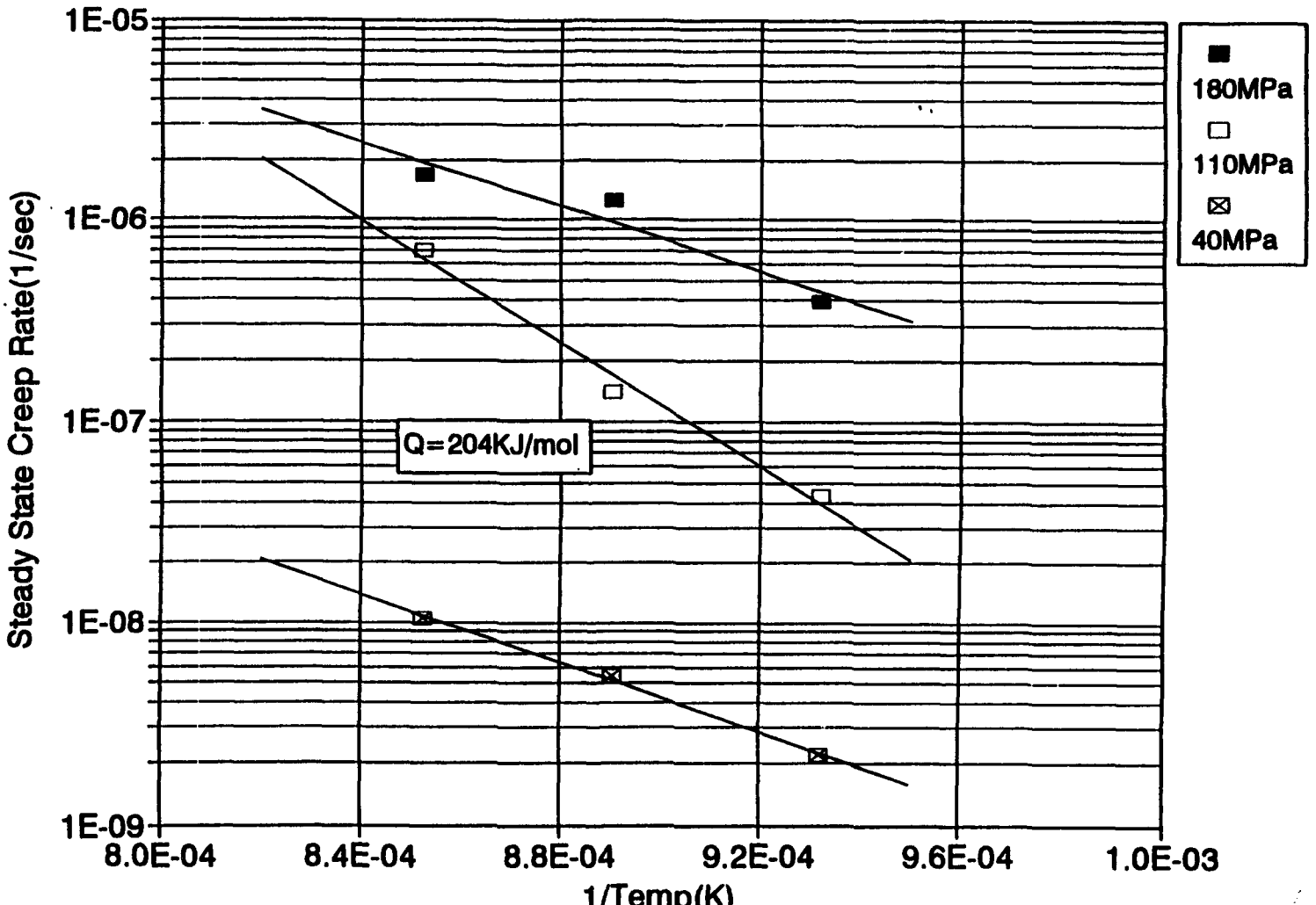

Figure 5. Temperature Dependence of Creep Rate for Hot Pressed MA NiAl

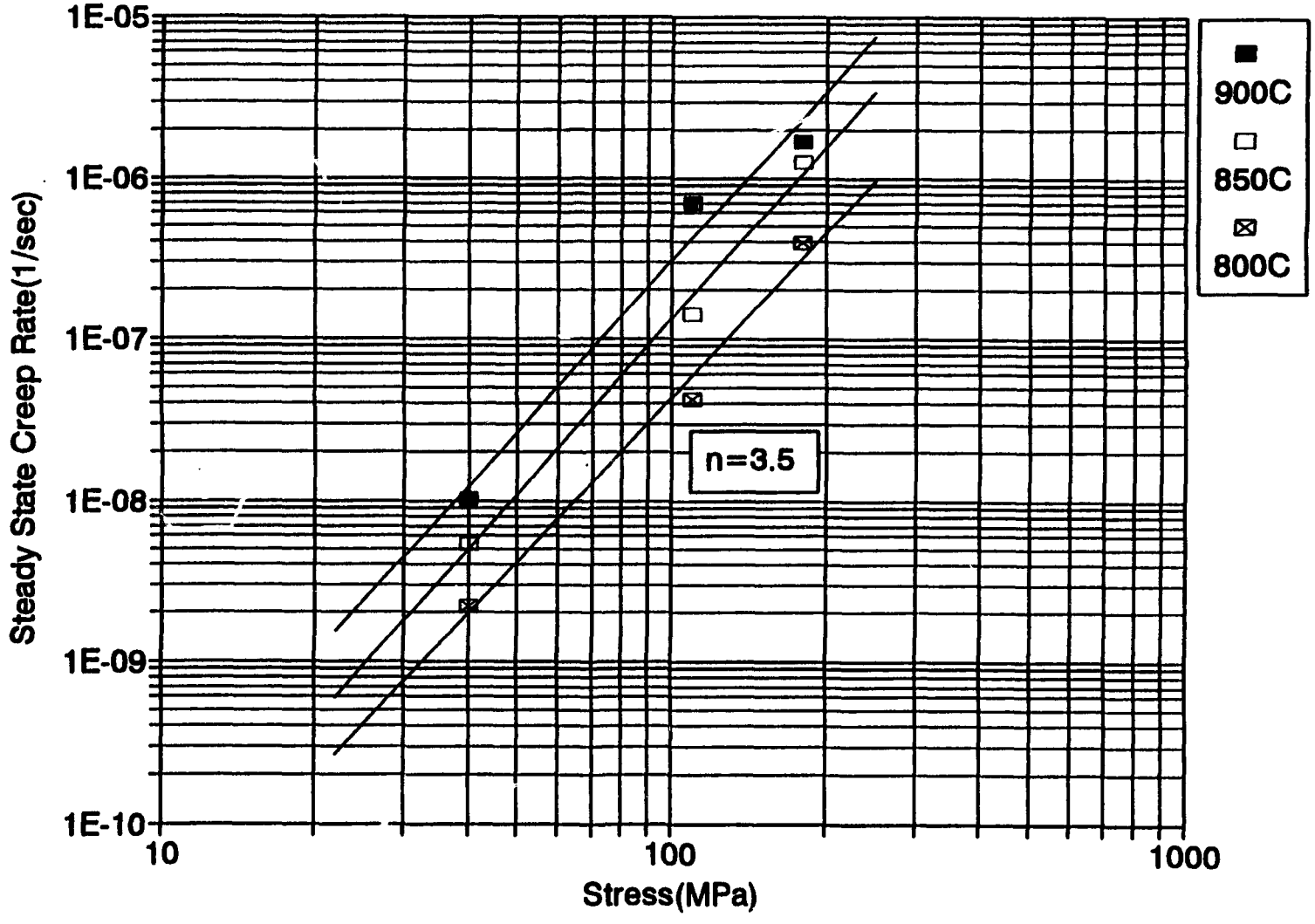

Figure 6. Stress Dependence of Creep Rate for Hot Pressed MA NiAl

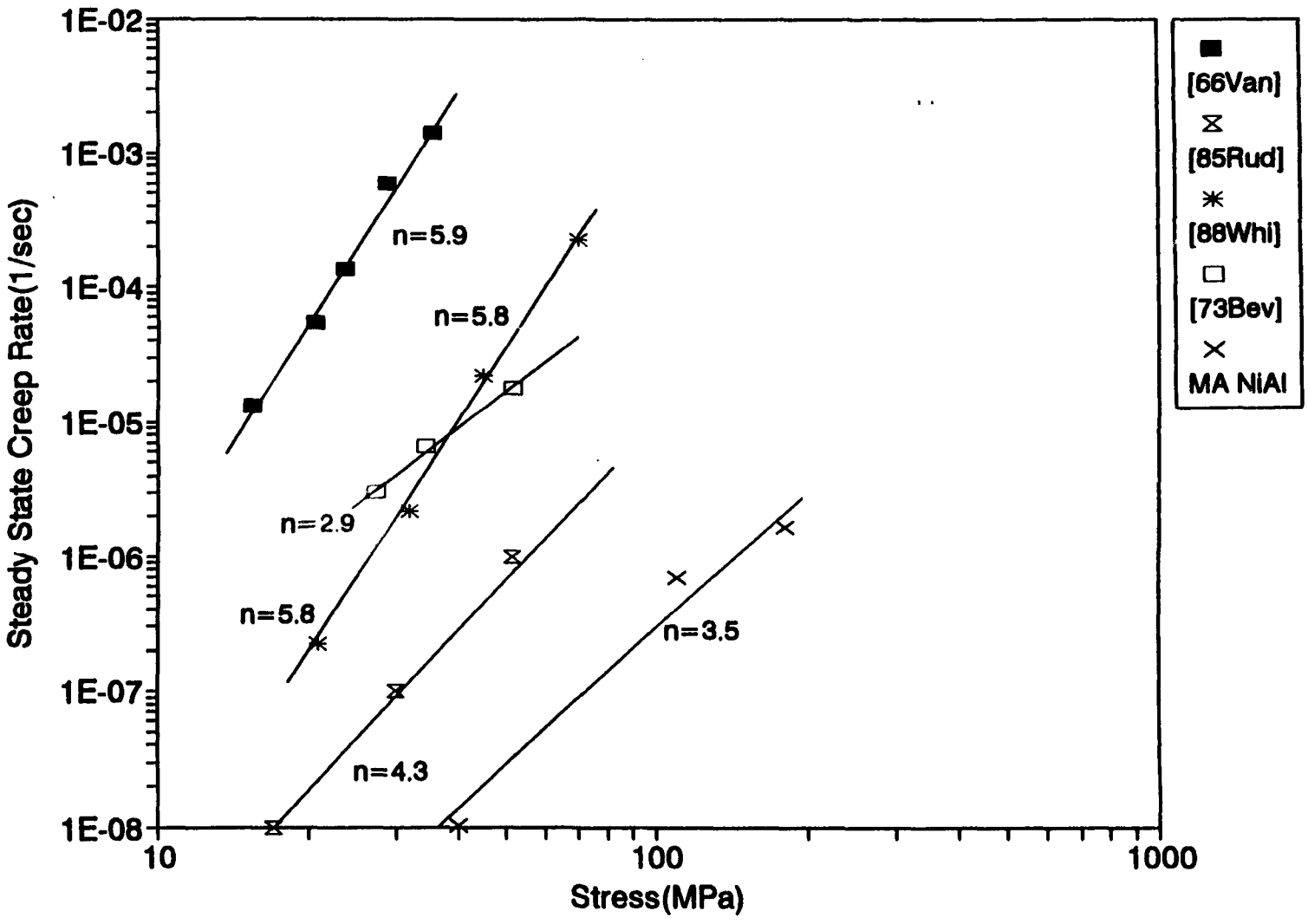

Figure 7. Comparison of Creep Rates for Stoichiometric NiAl and MA NiAl at about 900°C

ON THE THRESHOLD STRESS IN MECHANICALLY ALLOYED NiAl

S. Suh and M. Dollar
Metallurgical and Materials Engineering Department
Illinois Institute of Technology, Chicago Il 60616

Introduction

Intermetallic compounds, such as nickel, iron and titanium aluminides, have emerged as a new class of potential structural materials for high temperature applications such as gas turbine engines. Among others, the NiAl compound is a possible high temperature structural material, because of its low density, high melting temperature, good thermal conductivity and excellent oxidation resistance (1). However, before this material can be of practical use a number of technical problems must be overcome including lack of ductility at room temperature and poor strength at high temperatures.

Our approach has been to use mechanical alloying (MA) followed by hot extrusion to produce dispersion strengthened, fine-grained NiAl-based materials (2), to address both the ambient temperature brittleness and high temperature strength problems. The technique allowed us to process quality powders which, when consolidated, have high strength at both ambient and elevated temperatures and good compressive ductility (3). Recently, we examined creep behavior of mechanically alloyed (MA) NiAl and demonstrated its potential for high temperature structural applications (4). Minimum creep rates in MA NiAl were on average three orders of magnitude lower than that in their cast counterparts. Improved creep resistance of MA NiAl was found to result above all from the presence of dispersoids. In particular, it was found that creep in the MA NiAl materials is controlled by climb of dislocations over the dispersoids.

Virtually all modern theories for dislocation creep in metals and alloys assume that dislocation motion is opposed by back stresses which result from interactions between the moving dislocations and the substructure (5) and that the creep rate is determined by a net stress, equal to the difference between an applied stress and a back stress. The final application of the net stress concept is in the area of dispersion strengthened (DS) materials, which creep behavior is best described in terms of the threshold stress below which creep rate is negligible and which must be overcome in order for dislocations to pass particles (6). Since MA NiAl produced in our laboratory contains a dispersed phase, an attempt has been undertaken to determine whether the material exhibits such threshold behavior.

In this article, threshold behavior in MA NiAl is reported and the physical origin of the threshold stress is discussed. Similarities and differences between creep behavior of MA NiAl and "conventional" DS materials are outlined.

Experimental Procedures and Results

Material and Creep Tests

In the present study, a nominally stoichiometric, NiAl based-material, produced by mechanical alloying of elemental Ni and Al powders and consolidated by hot extrusion, was investigated. The actual chemical composition of the alloy was (at%): 48.32Ni, 49.74Al, 0.56C, 0.63O, 0.12N, 0.63H. The MA NiAl is a dispersion strengthened, equiaxed grain material with an average grain size of about 0.5 μm.

The constant load creep tests were conducted on cylindrical specimens, 5 mm by 10 mm, at temperatures between 750 and 900°C and over a wide range of stresses between 20 and 180 MPa. The steady state creep rates were measured (4) and, based on the data, the apparent activation energy for creep of 175 kJ/mol and the stress exponent equal to 2 were determined.

Determination of The Threshold Stress for Creep

In order to estimate the threshold stress of MA NiAl, a well established procedure, summarized by Purushothaman and Tien (6), was followed. The procedure requires the normalization of stresses by elastic modulus and assumes that the creep rate is determined by a net stress, equal to the difference between an applied stress and the threshold stress. As a result, the conventional power law creep equation given by:

$$\dot{\varepsilon} = A'\sigma^{n} \exp(-\frac{Q_{app}}{RT})$$

can be rewritten as:

$$\dot{\varepsilon} = A[\frac{\sigma_A - \sigma_{th}}{E(T)}]^{n_0} \exp(-\frac{Q}{RT})$$

where σ_A is the applied stress, Q_{app} and Q are apparent and true activation energies for creep, respectively, n and n_o are apparent and true stress exponents, respectively, E(T) is elastic modulus, and A and A' are constants (6).

The threshold stress can be estimated from the linear plot of normalized strain rate against normalized stress:

$$[\frac{\dot{\varepsilon}}{A\exp(-\frac{Q}{RT})}]^{\frac{1}{n_0}} \quad vs \quad \frac{\sigma_A}{E(T)}$$

extrapolated to the zero value of normalized stress.

To construct the plot, the values of n_o, Q and A in the equation had to be determined. First, the true stress exponent n_o was assumed to be equal to the apparent stress exponent n= 2. Then, the true activation energy for creep was calculated from :

$$Q = Q_{app} + \frac{nRT^2}{E(T)} \cdot (\frac{\partial E}{\partial T})$$

Constant A was determined from the actual data (two different stresses and two different strain rates at constant temperature were considered):

$$\dot{\varepsilon}_1^{\frac{1}{n_0}} - \dot{\varepsilon}_2^{\frac{1}{n_0}} = A^{\frac{1}{n_0}} \frac{1}{E(T)} (\sigma_1 - \sigma_2)\exp(-\frac{Q}{n_0 RT})$$

Finally, the following elastic modulus/temperature relationship was used (7):

$$E(GPa) = 249.3 - 0.031(T) + 1\times10^{-5}(T^2)$$

The plot of the normalized strain rate against normalized stress for MA NiAl deformed at 850°C is shown in Figure 1 (the apparent and true activation energies for creep used to construct the plot were 175 and 174 kJ/mol, respectively), and its extrapolation to the zero value of normalized stress provides us with the value of σ_{th}/E at 850°C:

$$\frac{\sigma_{th}}{E(T)} = 7.4\times10^{-5}$$

Hence, the threshold stress determined at 850°C is equal to 17 MPa. The threshold stresses were also determined

at 800 and 900°C; they were found to be 18.9 and 19.4 MPa, respectively.

The determination of the threshold stress using the graphical analysis enabled us to verify whether the assumption that $n \approx n_0$ was justified. In MA NiAl, the true and apparent activation energies are for all practical purposes identical and within the range of the activation energies determined in diffusion experiments (8). As a result, the power law creep equation with the effective stress normalized by elastic modulus can be rewritten as:

$$\dot{\varepsilon} = A'[\frac{\sigma_A - \sigma_{th}}{E(T)}]^{n_0} \exp(-\frac{Q_D}{RT})$$

or:

$$\frac{\dot{\varepsilon}}{D} = B[\frac{\sigma_A - \sigma_{th}}{E(T)}]^{n_0}$$

The true stress exponent n_0 can now be determined from the master plot of diffusion compensated creep rate as a function of modulus corrected effective stress shown in Figure 2. The predicted value of $n_0 = 1.42$ is only somewhat smaller than the apparent stress exponent $n \approx 2$, thus the assumption that $n \approx n_0$ was justified. In order to verify the threshold stress predicted graphically, creep tests of another nominally stoichiometric MA NiAl were conducted at low stresses and at 800°C. The minimum creep rates of 0, 2.5×10^{-10} , and 3.5×10^{-8} s^{-1} were measured at 10, 20, and 40 MPa, respectively. Thus, the graphically predicted value of the threshold stress equal to 19 MPa is in good agreement with the experimentally determined one, since no measurable creep was detected at 10 MPa and the creep rate on the order of only 10^{-10} s^{-1} was measured at 20 MPa.

Discussion

On The Origin of The Threshold Stress in DS Materials

The first attempt to explain the origin of the threshold stress in DS materials was undertaken by Lund and Nix (9) who suggested that creep strength was given by summation of the creep strength of the matrix and the stress for Orowan bowing. Today, however, it is accepted that creep in DS alloys occurs well below the Orowan stress (typically threshold stresses lie between 0.4 and 0.8 of the Orowan stress (10)). Also, the absence of dislocation loops around particles in crept specimens provides another piece of evidence that creep is not controlled by Orowan bowing between particles.

Another mechanism postulated to account for the threshold stress in DS materials involves attractive interaction between dislocations and particles which results in the departure side pinning of dislocation (10, 11). TEM studies have provided ample experimental evidence of dislocations being pinned on dispersoids (12, 13). Weak beam studies of dislocation configurations in the vicinity of particles revealed that, at least in some cases, the dislocations were actually pinned at the departure side of the particles (14). A model, proposed by Arzt and Roesler, assumes partial relaxation of dislocations in the vicinity of the particle-matrix interface and the stress required to detach the dislocation pinned at the departure side is regarded as the threshold stress (10).

The attractive interactions between dislocations and particles are believed to result not only in a threshold stress for creep, necessary for detachment of dislocations captured at attractive particles (11, 15), but also in an increased creep rate at higher stresses and high values of the stress exponent n (10), and rationalize the creep behavior of the DS materials.

In yet another search for an explanation for the creep behavior of DS materials, Roesler and Arzt (16) examined localized dislocation climb over non-attracting particles under equilibrium conditions. The kinetics of the dislocation climb was treated without the usual arbitrary assumption regarding dislocation shape in the vicinity of the particle. The model predicts quantitatively the extent of the climb localization; the localization increases with increasing stress, and, as a result, fewer vacancies are required to support the more localized climb process. This, in turn, leads to a weak creep rate dependence on stress, with the stress exponent $n = 3 - 4$. In the model, a dislocation climbing over a particle untangles its sharp curvature at the point it meets the particle, until climb can

proceed. This lowers the necessary dislocation line length increment and leads to the values of the threshold stress significantly lower than that predicted for attractive interactions between dislocations and particles discussed above. The creep behavior of the DS materials is clearly incompatible with the model.

On The Origin of The Threshold Stress in MA NiAl

As discussed, three kinds of models have been put forward to explain the origin and the magnitude of the threshold stress, i.e., Orowan bowing, detachment of dislocation from attracting particles, and localized climb over non-attracting particles.

The Orowan stress is given by (17):

$$\tau_o = \frac{Gb}{2\pi l}\ln\frac{\bar{x}}{2b}$$

where G is the shear modulus, b is Burger's vector, l is interparticle spacing, and $\bar{x}$ is an average particle diameter. For the present MA NiAl, G is 90.3 GPa (7), b = 0.288 nm (18), $\bar{x}$ = 24.6 nm, and l = 88.4 nm. Consequently, the Orowan stress for MA NiAl was calculated to be 176 MPa, several times higher than the threshold stress of about 20 MPa.

The detachment stress τ_d can be expressed as (11):

$$\tau_d = \tau_o\sqrt{1-k^2}$$

where τ_o is the Orowan stress and k is the relaxation parameter between 0 and 1. Using τ_o=176 MPa in MA NiAl, and k=0.94 (only a partial relaxation, 6%, is needed for detachment mechanism to be the controlling process), the detachment stress of 60 MPa was obtained.

Compared to the Orowan stress, the detachment stress is closer to the actual threshold stress in MA NiAl. However, the difference between these two values is two large for the detachment mechanism to be responsible for the threshold behavior in MA NiAl.

The threshold stress for equilibrium dislocation climb is give by (16):

$$\frac{\tau_{th}}{\tau_o} = \frac{h}{\lambda}$$

where τ_o is the Orowan stress, h is particle height (usually, particle radius), and λ is half the mean interparticle spacing. By substituting h=12.3 nm, and λ=57 nm, the threshold stress for climb of 37 MPa was determined. Thus, the model assuming dislocation climb over non-interacting particles provides us with a better estimate of the threshold stress in MA NiAl than the Orowan bowing and detachment stress models do.

The Creep Behavior of DS materials vs. that of MA NiAl

The creep of DS alloys has been recently reviewed by Raj (19). Creep data compiled by Raj show that the stress exponent for creep varies between 3.5 and 100, and the activation energy exceeds that for diffusion, often up to three times. In general, the stress exponents and activation energies for creep of DS materials tend to be much higher than those for the matrix materials. In most cases, the occurrence of high, apparent values of Q and n was reported to be accompanied by a threshold stress behavior, i.e., the existence of the threshold stress, σ_{th}, below which no detectable creep occurred. Nowadays, it is widespreadly accepted that creep of DS materials is driven not by the full applied stress, σ, but rather by the reduced stress, $\sigma - \sigma_{th}$. The concept of the reduced, effective stress for creep was used to explain the large stress sensitivity (high n values) of DS alloys (13). It was shown that when the creep rates were plotted against the reduced stress rather than against the applied stress (13), the true stress exponent was as low as 4, whereas apparent values of n were as high as 15 - 75. As far as the high activation energy is concerned, Lund and Nix showed that the difference between the apparent activation energy for creep and activation energy for

diffusion was almost entirely accounted for by the contribution of the temperature dependent elastic modulus (20).

In MA NiAl, the threshold stress is much lower and, as a result, the differences between apparent and true values of the stress exponent are insignificant. The temperature effects on elastic modulus, in turn, are marginal and, as a result, the apparent and true values of the activation energy are nearly identical.

Summary

Creep behavior of dispersion strengthened, mechanically alloyed NiAl, consolidated by hot extrusion, was investigated. Apparent activation energy for creep of 175 kJ/mol and apparent stress exponent equal to 2 were determined. The material exhibited threshold behavior, with the threshold stress below which creep rate is negligible of about 20 MPa. The model assuming dislocation climb over non-interacting particles provides us with the best estimate of the threshold stress in MA NiAl. The value, relatively low compared to conventional dispersion strengthened materials, leads to negligible differences between apparent and true stress exponents, in a clear contrast to the DS materials characterized by very high apparent stress exponents.

Acknowledgements

This research was supported by the Air Force Office of Scientific Research, Grant No. 90-0152B.

References

1. R. Darolia, J. Metals, 43, 44 (1991)
2. M. Dollar, S. Dymek, S. J. Hwang, and P. Nash, Met. Trans., 24A, 1993 (1993)
3. S. Dymek, M. Dollar, S. J. Hwang, and P. Nash, Mat. Sci. Eng., A152, 160 (1992)
4. S. Suh, M. Dollar, and P. Nash, Mat. Sci. Eng., accepted for publication.
5. J. C. Gibeling and W. D. Nix, Mat. Sci. Eng., 45, 123 (1980)
6. S. Purushothaman and J. K. Tien, Acta Met., 26, 519 (1978)
7. R. D. Noebe, R. R. Bowman, and M. V. Nathal, "*Review of the Physical and Mechanical Properties and Potential Applications of the B2 Compound NiAl*", NASA Technical Memorandum 105598 (1992)
8. S. Shanker and L. L. Siegle, Met. Trans., 9A. 1467 (1978)
9. R. W. Lund and W. D. Nix, Acta Met., 24, 469 (1976)
10. E. Arzt and J. Roesler, Acta Met., 36, 1053 (1988)
11. E. Arzt and D. S. Wilkinson, Acta Met., 34, 1893 (1986)
12. V. C. Nardon and J. K. Tien, Scripta Met., 17, 467 (1983)
13. V. C. Nardon, D. Matejczyk, and J. K. Tien, Acta Met., 32, 1509 (1984)
14. J. H. Schroeder and E. Arzt, Scripta Met., 19, 1129 (1985)
15. S. C. Jha, R. Ray, and J. D. Whittenberger, Mat. Sci. Eng., A119, 103 (1989)
16. J. Roesler and E. Arzt, Acta Met., 36, 1043 (1988)
17. M. F. Ashby, in: "*Oxide Dispersion Strengthening*", Proc. 2nd Bolton Landing Conf., G. S. Ansell, ed., Gordon and Breach, New York, NY, p.143 (1968)
18. P. Nash, M. F. Singleton, and J. L. Murray, in: "*Phase Diagrams of Binary Nickel Alloys*", P. Nash, ed., ASM International, p.3 (1991)
19. S. V. Raj, NASA Contractor Report 185299 (1991)
20. R. W. Lund and W. D. Nix, Met. Trans., 6A, 1329 (1975)

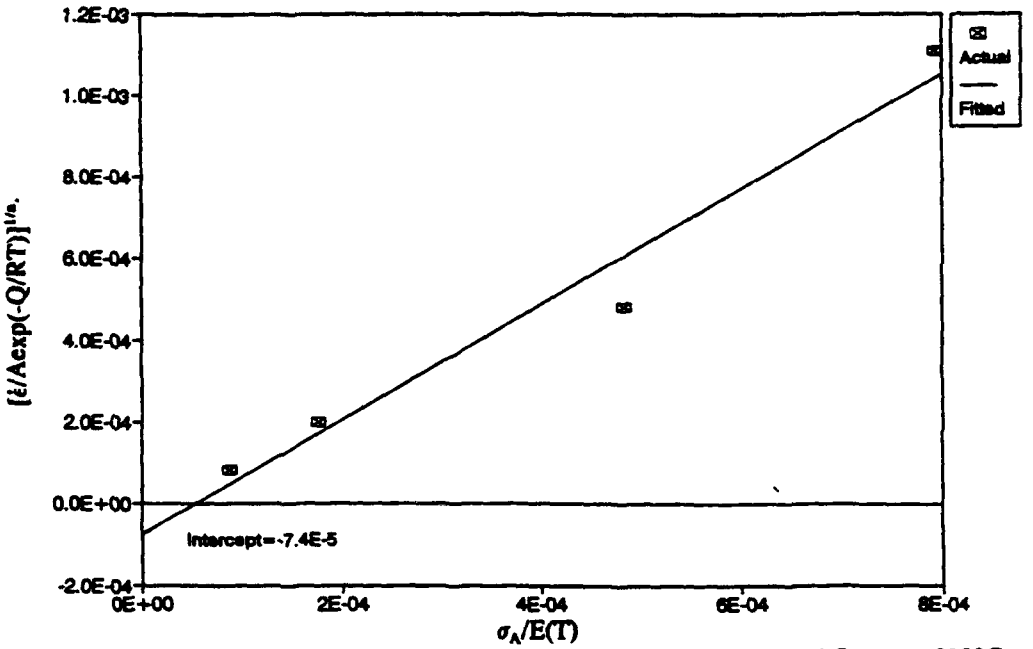

Figure 1. A Construction of Normalized Strain Rate vs. Normalized Stress at 800°C

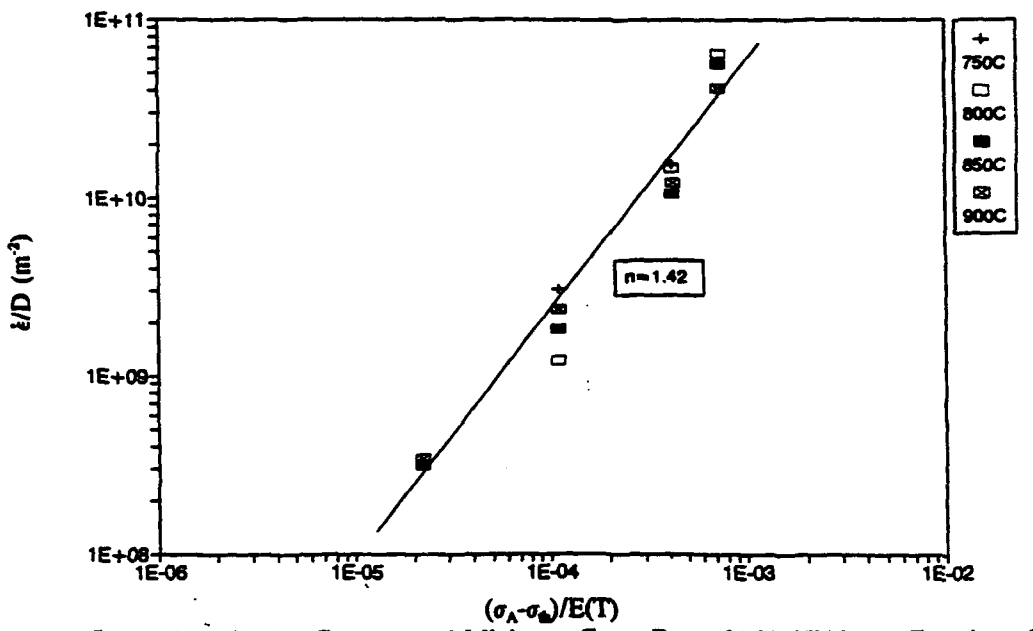

Figure 2. Diffusion Compensated Minimum Creep Rate of MA NiAl as a Function of the Modulus Corrected Effective Stress

XII. APPENDIX III

The Microstructure and Mechanical Properties of Mechanically Alloyed NiAl Based Alloys

BY

SEUNG-JOON HWANG

Submitted in partial fulfillment of the
requirements of the degree of
Doctor of Philosophy
in Metallurgical and Materials Engineering
in the School of Advanced Studies of
Illinois Institute of Technology

Approved_____
Advisor

Chicago, Illinois
May, 1992

CREEP IN MECHANICALLY ALLOYED NiAl-BASED MATERIALS

BY

SUNGJAE SUH

Submitted in partial fulfillment of the
requirements for the degree of
Doctor of Philosophy
in Metallurgical and Materials Engineering
in the Graduate School of the
Illinois Institute of Technology

Approved _____
Advisor

Chicago, Illinois
May, 1994

THE EFFECTS OF CHEMICAL COMPOSITION ON MECHANICAL PROPERTIES OF MECHANICALLY ALLOYED NiAl-BASED ALLOYS

BY

CHU-CHUN CHAO

Submitted in partial fulfillment of the
requirements for the degree of
Master of Science in Metallurgical and Materials Engineering
in the Graduate School of the
Illinois Institute of Technology

Approved _____
Adviser

Chicago, Illinois
May, 1994